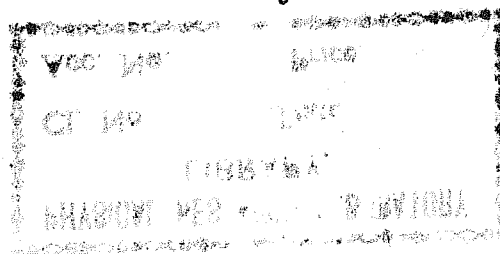


043
CHA

12077

**Studies Concerning the Motion of Charged Particles and the Structure
of Disks in Electromagnetic Fields Surrounding Compact Objects
in the Framework of General Relativity**



**THE LIBRARY
PHYSICAL RESEARCH LABORATORY
VRANGPURA
AHMEDABAD-380 009**

**D. K. CHAKRABORTY
PHYSICAL RESEARCH LABORATORY
AHMEDABAD ***

**A THESIS SUBMITTED FOR THE DEGREE OF
DOCTOR OF PHILOSOPHY
OF THE
RAVISHANKAR UNIVERSITY, RAIPUR**

AUGUST 1982

043



B12077

CONTENTS

Certificate	(i)
Acknowledgement	(ii)
Abstract	(iv)
CHAPTER I	<u>Introduction</u> 1-21
	1. Particle Dynamics 2
	2. Disk Dynamics 5
CHAPTER II	<u>Basic Mathematical Formulations</u> 22-53
	1. Particle Dynamics 22
	2. Disk Dynamics 33
CHAPTER III	<u>Charged Particle Dynamics in an Electromagnetic Field on Kerr Geometry</u> 54-65
	1. Orbits of the Particles as viewed from locally non-rotating frames 55
	2. Motion of the Charged Particles off the Equatorial Plane 60
CHAPTER IV	<u>Structure and Stability of Charged Fluid Disk around Schwarzschild Black Hole</u> 66-87
	1. Steady State Solutions 67
	2. Stability Analysis 81

CHAPTER V	<u>Structure and Stability of Thick Disks around Compact Objects : Newtonian Formulation</u>	88-103
	1. Steady State Solutions	88
	2. Stability Analysis	93
CHAPTER VI	<u>Structure and Stability of Rotating Thick Disks around Compact Objects : General Relativistic Formulation</u>	103-117
References		117-122

CERTIFICATE

Certified:

- (i) that the thesis embodies the work of the candidate himself,
- (ii) that the candidate has worked under me for the period required under para 7 of Ordinance No.16.

Supervisor

A handwritten signature in dark ink, appearing to read 'A.R. Prasanna', written over a horizontal line.

(A.R. Prasanna)

ACKNOWLEDGEMENT

I wish to express my deep appreciation to Prof. A.R. Prasanna for his enthusiasm, competent guidance and encouragement which have contributed immensely to the studies presented here. It is indeed a great pleasure to have worked with him. I thank him very much.

I express my thanks to the University Grants Commission for the award of the Teacher Fellowship under the Faculty Improvement Programme and the Director, Physical Research Laboratory for the hospitality which enabled me to carry out the investigations at PRL.

My sincere thanks are due to Professors C.V. Vishveshwara, J.V. Narlikar, V.L. Ginzburg, R.K. Thakur, R.K. Varma, R. Pratap and K.H. Bhatt for many fruitful discussions which have contributed to the thesis. It is a pleasure to thank Dr. K.S. Rao for the discussions regarding computer programmes.

I have been benefitted by the healthy discussions with my colleagues Manab, Avinash, Ashok, Harish and Rhama. I thank them very much. I thank Ashwin, Ashwini, Rajesh, Ramesh, Surendra, Sushil, Shefali for creating a home like atmosphere away from my home.

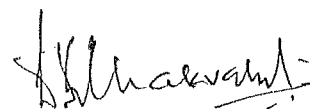
Thanks are also due to Mr. P.S. Shah and the staff, PRL Computer Centre, for a smooth flow of the outputs, and to Swadha, PRL Library, Bhavsar and Vora for preparing the diagrams.

I am indebted to my mother and father and specially to my wife, Maya and daughter, Buna, for bearing with all kinds of hardships during my long period of absence from home. Without their cooperation and forbearance, it would not have been possible for me to carry out this investigation.

My friends Sukumar, Gagan, Nasir, Narendra and Gopal were very much helpful to me during my absence from my home and also during the writing of my thesis. I thank them very much.

I thank Mr. V.T. Viswanathan, Mr. R.R. Singh and Mr. B.R. Soni for carrying out the tasks of the typing and cyclostyling of the manuscript.

Lastly, thanks to everybody who helped me directly or indirectly, academically or otherwise, in producing this thesis.



D.K. Chakraborty

7th July 1982

Abstract

In this thesis we have made a detailed analysis in the frame-work of general relativity, the trajectories of charged particles in electromagnetic field surrounding a Kerr black hole on the equatorial plane as seen from locally non-rotating frames and off the equatorial plane as seen by a far-away observer, as well as the dynamics of pressureless thin charged fluid disk and of structured thick disk around compact objects. We present below a brief summary of the results obtained and the conclusions drawn.

Prasanna and Vishveshwara (1978) studying the trajectories of charged particles on the equatorial plane of a Kerr black hole in an external electromagnetic field have found that the particle gyrates only when it is completely outside the ergosphere, an effect which they attribute to the role of inertial frame dragging. As it is well known this frame dragging arises mainly because of the Boyer-Lindquist coordinates and that if one goes over to a Locally Non-Rotating Frame (LNRF) there is no frame-dragging. It is essential to see whether as a result of this the non-gyration of charged particle also is a Boyer-Lindquist effect which may not exist in LNRF. With this in mind we have considered the orbits of charged particles for the same set of parameters as in the earlier case but as viewed from LNRF. Numerical integration of the corresponding equations of motion clearly show that the particle

gyrates in all cases irrespective of the fact whether the particle is completely inside or completely outside or moves in and out of the ergosphere. This analysis exhibits the fact that for a distant stationary observer (following the global time like killing vector) a charged particle does not gyrate when it is inside the ergosphere whereas in the LNRF the effect of frame dragging has been cancelled out completely. (Prasanna and Chakraborty 1980).

The orbital dynamics on the equatorial plane of a central gravitating source forms a basis for the study of thin disks whereas to understand the structure of thick disks as well as to understand the nature of accretion along the field lines, one requires a study of the motion of the particles along the field lines off the equatorial plane. This aspect of the orbital dynamics we have considered for charged particle motions under the same situations as in the previous case. For this study we first examined the structure of electric and magnetic field lines of the superposed electromagnetic field. The detailed study of the particle orbits in such fields show that the particle bounces between mirror points provided its velocity parallel to the field lines is sufficiently low, otherwise the particle moves continuously towards the central source in the case of dipole field or escapes to infinity in the case of uniform field without showing signs of turning back. In the case of an uniform field, the bending of field lines

near the Kerr black hole and the consequent trapping of the particles clearly indicates how general relativity can modify the phenomena in certain situations (Chakraborty and Prasanna I, 1981).

While considering the dynamics of accretion disks around compact objects we have first developed a fully general relativistic system of dynamical equations governing the equilibrium and perturbations for a non-self-gravitating perfect fluid disk with finite charge density and conductivity, under the influence of the gravitational field of the central source, the self-consistent electromagnetic field and the centrifugal force of the disk. After writing the general dynamical equations in terms of the velocity and field components of a local Lorentz observer, we have studied the structure and stability for three different cases as mentioned below.

We first consider the case of a non-conducting, pressureless infinitesimally thin charged fluid disk confined to the equatorial plane of a Schwarzschild black hole. We determined the matter density when the charge density is constant and the disk is rotating with either rigid or differential rotation, required to maintain the equilibrium under gravitational, centrifugal and electromagnetic forces. The matter density is found to become infinity at the point where centrifugal force becomes equal to the gravitational

force. To avoid such singular points we have considered disks with either the outer edge lying within the singularity point or with the inner edge lying beyond the singularity point, the velocity of disk being necessarily small in the first case.

To study the stability of such disk under radial perturbation we use the normal mode analysis. Taking the time dependence of the perturbed variables as $\exp(i\sigma t)$ we establish an eigenvalue equation of a self-adjoint operator for σ^2 . A sufficient condition for the disk to be unstable will be a particular choice of the parameters such that the eigenvalue is zero, calculated by using a trial function for the eigenfunction itself. We have found that the disks are generally stable. The magnetic field acts as a confining field. We find that depending upon the centrifugal force the matter in the pressureless disk adjusts itself with the help of electric field to such a distribution that the forces balance each other completely and allow the magnetic field to keep the fluid in stable configuration under radial perturbations. It is in fact important to notice that we have several examples of disks which have inner edge well within $6m$ ($m = MG/c^2$) limit and are stable (Prasanna and Chakraborty, 1981).

Next, we have studied the case of a neutral

formulation. Such disks need not be thin and so the structure in the meridional plane is important. For specific density distribution, we determine the steady state velocity and pressure distribution for fluids obeying adiabatic equation of state.

We consider the stability of such fluid disk under axi-symmetric perturbations. It is possible to construct an equation for the square of the frequency (σ^2) of the axi-symmetric oscillations which is symmetric in trial and true Lagrangian displacements which in turn implies a variational principle. We then evaluate σ^2 by choosing trial functions which have adjustable parameters, for the true Lagrangian displacements and extremize σ^2 by adjusting these parameters. Equating this σ^2 to zero we calculate a critical value of adiabatic index γ_c for neutral mode. In all cases that we have considered, critical γ has been found to be less than 4/3 indicating stable configurations. We also find that an ordinary perfect fluid (with $\gamma = 5/3$) disk rotating around central gravitating source is stable under radial pulsations with frequency $\sqrt{MG/r^3}$ (Chakraborty and Prasanna II, 1981).

Finally we have considered the case of a neutral fluid disk with pressure in Schwarzschild geometry. The velocity and pressure distributions have been calculated

for the disk with constant density. Considering the fact that the pressure should be positive within the disk we have found that the inner edge of the disk cannot lie within $4m$ and further if the inner edge lies between $4m$ and $6m$ then the outer edge must lie beyond $2a/(a-4)$ where a is the radius of inner edge in the units of m . There is no restriction on outer edge if the inner edge is at $6m$ or beyond. The stability of such disks are then studied in the same manner as in the corresponding Newtonian case and are found to be generally stable ($\gamma_c < 4/3$). We also find that a pressureless disk collapsing to $\theta = \pi/2$ plane is stable only when its inner edge is beyond $6m$ (a well known result for single particle orbits) with local frequency $\sqrt{\frac{mc^2}{\pi^4} (\pi - 6m)}$ (Chakraborty and Prasanna III, 1981).

CHAPTER I

INTRODUCTION

One of the most important topics of discussions in theoretical astrophysics today deals with the understanding of high energy cosmic sources like quasars, X-ray binaries and the like. Though no definite conclusions exist as to the nature of energy release and transport, it is more or less agreed upon that the main mechanisms have to do with plasma processes in the vicinity of the compact objects (Mestel 1971, Basko and Sunyaev 1976). Bearing this in mind many authors have considered different aspects of plasma processes in astrophysical situations specifically the formation of accretion disks rotating around the compact objects and the resultant luminosity and the spectrum but have mostly restricted to the non-relativistic formulations. As the compact object involved in certain models are black holes it is necessary to consider the mechanisms and processes in a non-flat background. More recently attempts have been made to study the plasma processes on curved background. In a general treatment of a plasma in non-relativistic physics one uses normally a kinetic approach **or** a fluid approach depending upon the scale lengths and densities involved. However either of these two approaches is required only when the collective effects of plasma are important. On the

On the other hand if the density is very low then it may be sufficient to use the single particle approach to get some understanding of the situation. In this chapter we present a historical background of the studies on particle dynamics as well as on disk dynamics alongwith the motivations for our studies.

1. PARTICLE DYNAMICS

To solve the problem of particle trajectories in an electromagnetic field in general relativistic formulation, one should solve the Einstein-Maxwell equations alongwith the covariant Maxwell's equations to obtain the metric potentials g_{ij} and the electromagnetic field components F_{ij} . Finally one should solve the covariant Lorentz equation to get the orbits. The only known class of solutions of Einstein Maxwell's equations which are of astrophysical interest, are the ones from the Kerr-Newman family which represent the geometry outside a black hole of mass M , charge Q , and angular momentum a . The solution reduces to that of Kerr for $Q = 0$, Reissner-Nordstrom for $a = 0$ and Schwarzschild for $Q = 0$, $a = 0$. Carter (1973) was the first to obtain the complete set of first integrals of motion of charged particles in Kerr Newman geometry while Ruffini et al (1973) have worked out the dynamics of charged particles in Kerr-Newman and Reissner-Nordstrom geometries.

A more realistic situation will be the case of compact objects without any net charge, with the electromagnetic field being produced by the external currents. Considering the situations where electromagnetic field energy is very small compared to the rest mass energy of the compact object, several authors have obtained the solutions for a stationary axi-symmetric electromagnetic field around a Schwarzschild black hole (Ginzburg and Ozernoi 1965, Petterson 1974, Bicak and Dvorak 1977) and around a Kerr black hole (Chitre and Vishveshwara 1975, Petterson 1975, King et al 1975). Charged particle dynamics in such electromagnetic field has been extensively studied by Prasanna and Varma (1977) for a Schwarzschild black hole and by Prasanna and Vishveshwara (1978) for a Kerr black hole. A lucid summary of the charged particle dynamics may be found in the article of Prasanna (1980). Some of the plots of the orbits, as obtained by these authors are presented in figures (1-1) to (1-6).

Two general conclusions can be drawn from these orbit plots: (i) that bound stable orbits for charged particles in electromagnetic field exist even very close to the event horizon, and (ii) that the particles execute Larmor gyrations except when they are inside the ergosphere. Both these conclusions have far reaching significance. In case of the disk structures, the inner edge of the disk had

always been conventionally taken to be the last stable, circular orbit (eg. $6m$ for the case of Schwarzschild geometry, $m = MG/c^2$, M being the mass of the black hole) which may not be true in the presence of charges and the electromagnetic field. On the other hand the absence of gyration when the particle goes inside the ergosphere may have its signature on the radiation pattern. The absence of gyration within the ergosphere is, in fact, the reflection of the effect of dragging of inertial frames by the rotating star. If the particle has to gyrate, then during every Larmor circle the angular velocity of the particle will be prograde for one half and retrograde for the other half with respect to the angular velocity of the star. It is well known in the Kerr geometry that the ergosurface is the static limit surface, on and beyond which (i.e. towards the event horizon) no retrograde motion, is possible. Thus the particle can gyrate only outside the ergosurface.

As it is well known that the frame-dragging arises mainly because of the use of Boyer-Lindquist coordinate system used to describe Kerr-geometry and if one goes over to a locally non-rotating frame, this effect would not arise, it is worthwhile to examine the orbits as viewed by locally non-rotating observers. Further, as we could infer

about the possible inner edge of the disk from the studies of particle motion confined to the equatorial plane, it might be possible to infer about the possibilities of having thick disks from the studies of trapped orbits in the meridional plane. Accordingly we consider both these studies of charged particle dynamics in electromagnetic field on Kerr geometry. Chapters 2 and 3 contain the basic mathematical formulations, the methodology and the results of the studies of the charged particles orbits in an electromagnetic field on Kerr geometry as viewed by locally non-rotating observers for the motion confined to equatorial plane and the motion of charged particles off the equatorial plane.

2. DISK DYNAMICS

It is well known that in the case of accretion of matter onto compact objects the accretion is radial or spherically symmetric if either the compact object is at rest with respect to interstellar gas or the incoming matter does not possess angular momentum. Studies regarding such spherically symmetric accretion were made by Bondi (1952), Shvartsman (1971) Shapiro (1973), Cox and Smith (1976), Thorne and Flammang (1980). Detailed accounts of accretion when the compact object is stationary or when it is moving

supersonically with respect to the interstellar gas, may be found in the articles of Zeldovich and Novikov (1971), Novikov and Thorne (1973), and Lightman, Shapiro and Rees (1978).

On the other hand the general picture of the accretion is quite different when (i) a compact object is in orbit about a normal star forming a close binary or (ii) a supermassive black hole resides at the centre of a galaxy. In such cases accretion rate is much higher. For typically observed binary systems that emit X-rays (e.g. Cyg X-1 and Cen X-3) the observations and models suggest that the normal star is dumping gas onto its companion at a rate of $\sim 10^{-9} M_{\odot}/\text{yr}$ which is much higher compared to the typical accretion rate ($\sim 10^{-15} M_{\odot}/\text{yr}$) in the case of an isolated black hole. The second point of difference is that the accreting gas has sufficient angular momentum (specific angular momentum $\tilde{L} \gg 4 mc$) so that instead of falling radially onto the compact object, it forms a rotating disk around it.

Viscosity plays an important role in such accretion disks. It removes angular momentum causing the gas of the disk to spiral gradually onto the compact

object and also it heats the gas causing it to radiate.

The existence of an accretion disk in determination of the emitted radiation is crucial for accretion onto black holes, since there exists no hard surface to decelerate the material and guarantee high efficiency of radiation as in the case of neutron stars.

Thin Disk Models

Models for the disk type accretion around neutron stars and black holes when they form a binary with a normal star as their companion was first considered by Pringle and Rees (1972) and Shakura and Sunyaev (1973). This model and its subsequent modifications by Novikov and Thorne (1973) is termed as standard α -model (Eardley and Lightman 1975). The main problems investigated by these authors are the luminosity and the spectrum of the radiation which are found to depend mainly on the accretion rate.

Earlier Salpeter (1964), Zeldovich (1964), Novikov and Zeldovich (1966) and Shklovsky (1967) had suggested that accretion onto black holes and neutron stars may produce a significant amount of electromagnetic

radiation, while it was demonstrated by Cameron and Mock (1967) that there is a possibility of producing a sizeable flux of X-rays even when the central object is as noncompact a star as a white dwarf. The essential role of the angular momentum of the gas in binary accretion was first emphasized by Prendergast and Burbidge (1968).

The earlier works on accretion disk were based on Newtonian theory of gravitation. However, the corrections due to general relativistic effects are significant specially when the compact object is a black hole and the inner edge of the disk is very near to the event horizon. Thorne (1974) and Novikov and Thorne (1973) have calculated the effects of general relativity on the inner regions of the accretion disks.

While all the above investigations were made on binary accretion, Lynden-Bell (1969) and Lyndel Bell and Rees (1971) have argued that the galaxies might have supermassive black holes ($\sim 10^8 M_{\odot}$) at their centres, as many of the observed forms of activities in galactic nuclei can be interpreted as the effects of accretion of interstellar matter onto a central black hole.

Below, we describe the salient features of α -model of the accretion disk, based primarily on the articles of Shakura and Sunyaev (1976), Lightman, Shapiro and Rees (1978) and Novikov and Thorne (1973). These authors have considered the features like the modes of mass transfer into and out of the disk, the structure of the disk in steady state and the resultant luminosity and the spectrum of the radiation emitted. The gravitational field has been considered to be Newtonian and subsequently general relativistic corrections have been introduced. Mass of the disk is considered to be very small compared to the mass of the central star and therefore the gravitational field produced by the disk is neglected. The gas pressure is considered to be very low as the material forming the disk has sufficient time for cooling during its transfer onto the disk and as such the disk is thin.

Modes of mass transfer, accretion rate

It is conventional to distinguish two modes of mass transfer in case of binary accretion - Roche-lobe overflow and accretion from stellar wind. In a compact star - normal star binary if the surface of the normal star fills the Roche-lobe, it can dump gas onto the compact star continuously through the Lagrangian point L_1 (Figure 1.7). This is likely to be occurring in the H-Z Her-Her X-1

system although perhaps not in other well known X-ray binaries involving more massive stars of the type which are likely to possess strong winds (Van Den Heuvel 1975). However, when the surface of the normal star is inside the Roche-lobe, gas can flow onto the compact object by means of stellar wind only, which blows gas off the star supersonically in all the directions with only that gas blown towards the companion being captured.

At some outer radius r_0 the incoming gas goes into roughly circular orbit. Freshly arriving gas interacts viscously with the gas already in the orbit. Some of the gas gets deposited onto the disk. Other incoming gas is fed angular momentum from the disk by means of viscous stress and thereby gets ejected out of the disk region and back onto the normal star or through the Lagrangian point L_2 into the interstellar space.

The inner edge of the disk r_i is placed very near to the star's surface in case of a white dwarf or a neutron star and consequently the total energy radiated per unit mass of the gas during its passage through the disk is equated to the gravitational binding energy of unit mass when it reaches the inner edge. For a black hole the inner edge is placed at the last stable circular orbit. Thus for a (non-rotating) Schwarzschild black hole $r_i = 6m$. If \dot{M}_d is the accretion rate the total luminosity L of the disk must be

$$L \sim (10^{34} \text{ ergs/sec}) \left(\frac{\dot{M}_d}{10^{-9} M_\odot/\text{yr}} \right) \quad \text{for white dwarf}$$

$$L \sim (10^{37} \text{ ergs/sec}) \left(\frac{\dot{M}_d}{10^{-9} M_\odot/\text{yr}} \right) \quad \text{for neutron star or hole} \quad (1.2.1)$$

In order to match the observed luminosity of $\sim 10^{37}$ ergs/sec for the case of Cyg X-1 a rate of $10^{-9} M_\odot/\text{yr}$ of accretion is needed. This rate is much smaller than the rate ($\sim 10^{-5} M_\odot/\text{yr}$) at which variable stars of the type β -Lyrae are ejecting mass continuously from their atmospheres.

Considering galactic nuclei or quasars as the accreting supermassive holes we need a much higher accretion rate to account for the observed luminosity. For most violent quasars $L \sim 10^{47}$ ergs/sec and so $\dot{M}_d \sim 10 M_\odot/\text{yr}$. For our own galaxy $L \sim 10^{42}$ ergs/sec and therefore $\dot{M}_d \sim 10^{-4} M_\odot/\text{yr}$ which is much smaller than the rate at which all the stars in the galaxy eject mass into the interstellar medium ($\sim 1 M_\odot/\text{yr}$).

Stationary State

The dynamics of the disk is governed by the laws of conservations of mass, angular momentum, energy and vertical momentum, by the nature of viscosity and by the law of radiative transfer from inside of the disk to its lower and upper faces. The gas is assumed to be supported against the gravitational pull of the central compact object mainly by rotation and consequently its velocity in the azimuthal direction is Keplerian. Due to viscous forces, the gas loses its angular momentum and acquires velocity in the radial direction, while in the vertical direction its velocity is assumed to be subsonic

so that the vertical structure is governed by the law of hydrostatic balance. Turbulence and small scale magnetic field contributes to the viscosity and one writes for the case of Keplerian rotation, the integrated viscous-stress as $\tau_{r\phi} = 2\alpha p h$ where p is the pressure, h is the vertical height and α is a constant (and that is why the name α -model). The energy produced due to the friction is transferred to the disk surfaces. The medium is considered as optically thick with the opacity due to Thomson scattering k^{es} and that due to free-free absorption k^{ff} . To discuss the stationary state one also needs an equation of state where one assumes the pressure to be the sum of the gas pressure p_g and the radiation pressure p_r , and an equation connecting the radiation density to the thermodynamical properties of the gas. One can then combine all these equations namely (i) Keplers law, (ii) continuity equation, (iii) momentum equation, (iv) vertical momentum balance, (v) viscosity law, (vi) energy production by friction, (vii) removal of energy by radiation, (viii) equation of state and (ix) equation connecting the radiation density with thermodynamical properties of the gas, to describe density, velocity, temperature and the height as the functions of the radial coordinate r and the parameters \dot{M}_d , M and α .

The entire disk can be divided into three regions

- (a) inner region where $p_r \gg p_g$ and $k^{es} \gg k^{ff}$
- (b) middle region where $p_r \ll p_g$ and $k^{es} \gg k^{ff}$
- (c) outer region where $p_r \ll p_g$ and $k^{es} \ll k^{ff}$

Inner region is the hottest region and most of the radiation is expected to come from this region. The energy production rate Q^+ is zero at r_i , reaches maximum at $r = 49/36 r_i$ and decreases as r^{-3} for large values of r . The total luminosity

$$L = 4\pi \int_{r_i}^{\infty} Q^+ n dr = \frac{1}{2} \dot{M}_d \frac{MG_z}{n_i} \quad (1.2.2)$$

is independent of the nature of the dissipative forces and depends only on the accretion rate \dot{M}_d and the inner radius r_i . In the inner region, radiation pressure dominates over gas pressure and the opacity comes mainly from the Thomson scattering.

Just the opposite happens in the cool outer region: gas pressure dominates over radiation pressure while free-free transition is the main source of opacity. In addition to these, there is an intermediate region also, where scattering is the prime source of opacity, just like the inner region, and gas pressure is much higher than radiation pressure as in the outer region. The boundaries between various regions are determined by equating the quantities which change the sign of inequality during the transition from one region to other.

Instabilities in accretion disk

The original α -model of Novikov and Thorne (1973) was stationary or time-independent model. Lightman I, (1974) on the other hand considered a time dependent model wherein the underlying physics is essentially the same as in

the stationary model but all the variables are allowed to evolve in time. The principal result is a nonlinear "evolution equation" for the surface density $\bar{\epsilon}$ of the disk along with a set of auxiliary equations for determining all the other disk structure variables in terms of the surface density. Besides studying the variability of mass deposition rate as a possible explanation for the observed 35-day cycle of Her X-1 (Pringle 1973, McCray 1973), such time dependent model was used to investigate the stability of the disk (Lightman II, 1974, Lightman and Eardley 1974). Their analysis indicates a secular instability, resulting in a clumping of the disk into rings whenever $\partial \tau_{\text{eq}} / \partial \bar{\epsilon} < 0$ a condition which occurs in the inner portion of the disks with the α -parameter viscosity law, where radiative pressure exceeds thermal gas pressure.

Lightman I, II (1974) used the condition $Q^+ = Q^-$ where Q^- is the rate of removal of energy by radiation, to discuss the stability. It was shown by Shakura and Sunyaev (1976) that the relation $Q^+ = Q^-$ leads to a fixed value of the dynamical viscosity for the inner region of the disk which is much higher than the maximum possible viscosity for a fully ionised gas and radiation. They replaced this law by a more realistic one which takes account of the change of internal energy as a result of work done by pressure forces. They found that disks are unstable when $e_0 = p_r / (p_r + p_g) > 3/5$ for perturbations of wavelengths greater than twice the vertical height.

The instabilities discussed above depends on the relation between Q^+ and Q^- : Q^+ depends on the viscosity law while Q^- is determined by the cooling mechanism. It is therefore worthwhile to examine various cooling mechanisms and viscosity laws which may eventually lead to stable disk configurations. Several attempts were made in these directions. Liang (1977), Liang and Price (1977) and Shakura, Sunyaev and Zilitnkevich (1977) have suggested convection as a source of cooling and Piran (1977) had postulated secondary wind as the stabilizing agency. However, these effects are not sufficient to ensure stability (Piran 1978). It was shown by Piran (1978) that stability of the disk depends more sensitively on the viscosity law and relatively a small variation in viscosity law stabilizes the disk. The trouble is that one does not know as to how to evaluate a modified turbulent or magnetic viscosity.

Discussions of instabilities on gas pressure dominated region, restricting to "pressure equilibrated perturbations" ($\delta p = 0$) was made by Livio and Shaviv (1977). They use Navier-Stokes equations for the motion of the fluid and do not integrate the equations along the vertical directions z . Consequently they allow dynamical variables to depend on z in addition to radial distance r and time t . (In the original α -model, one integrates out the Z -dependence of the variables). The necessary condition for stability against convection is then found to depend on temperature gradient along z and r directions, on entropy as a function

of r and on the dependence of viscous stress on thermodynamical variables.

It may be argued that the instability which occurs in the radiation pressure dominated inner region, may not exist in disks around neutron stars because such inner region may not exist at all in this case. (Lightman 1974 I, II). However, as was shown by Hoshi (1977), Hoshi and Shibazaki (1977) and Shibazaki (1978), the stationary disk around black hole would be very much different from the standard α -model when the effect of pressure gradient force in the equations of motion is taken into account and the formula derived by Ichimaru (1977) for viscous stress is used. Following this Okuda (1980) has discussed the problem of stability of accretion disk around neutron stars by taking into account of the pressure gradient forces in the momentum and energy conservation equations, while keeping the same viscosity law as in the standard α -model. The principle result of this analysis shows that the inner region of the disk is thermally unstable unless the accretion rate is very low.

Thick disks

It was pointed out that the thin disks as described by α -model are not stable in their inner regions and also the various modifications suggested to stabilize the disk are not very satisfactory. Besides, it was realized long back that, in case the accretion rate exceeds the critical value (Supercritical accretion), the inner edge of the

disk will render a thick structure (Shakura and Sunyaev 1973). It now seems that the thin disks (α -model) are inconsistent (Wiita et al 1980) and one should consider thick disks as possible models of the high energy sources.

Investigations on thick fluid disks were started by Fishbone and Moncrief (1976), Abramowicz et al (1978) and Kozłowski et al (1978). Unlike the α -model, the disk considered by these authors has thickness comparable with its radial dimension which reflects the importance of pressure gradient force. The velocity of rotation is then different from being Keplerian. Besides the fluid of the disk is regarded as a perfect fluid (without viscosity), as a result of which one cannot consider the processes of dissipation of energy and the resultant radiation. The main emphasis is on the structure of such disks. In case the heat generation rate is small one can treat the effect of viscosity on the structure and on the heat generation as a perturbation (Kozłowski et al 1978).

Fishbone and Moncrief have (1976) considered stationary and pure azimuthal flow of perfect fluid disk around a Kerr black hole, restricting the discussion to isentropic flow. They have solved the relativistic Euler's equation as derived from the conservation of energy-momentum tensor of perfect fluid and written in the Hamilton-Jacobi

form. The solutions, relating $\ln(h)$ to the components of the metric tensor are obtained by requiring that either $u_\phi u^t$, the angular momentum per unit inertial mass or that $h u_\phi$, the angular momentum per baryon be constant throughout the fluid. Here $u = (u^t, u^r, u^\theta, u^\phi)$ is the four-velocity, h is the enthalpy per baryon. To obtain these solutions the metric is left arbitrary except for the stationary and axisymmetry requirements. It is then possible to impose Einstein's equations upon the metric and thus take the effects of the self-gravitation of the disk into account.

In case of background gravitational field the metric components are specified and therefore $\ln(h)$ can be computed as functions of coordinates. At the boundary of such a disk, pressure is zero and enthalpy is just the rest mass energy per baryon, mc^2 . Thus $\ln(h/mc^2) = 0$ gives the boundary of such a disk.

Following the earlier works of Fishbone and Moncrief (1976) and Abromowicz et al (1978), Paczynski and Wiita (1980), Paczynski (1980) and Wiita et al (1980) have considered thick disks with accretion and have obtained shapes of the disk in stationary state. However, they use a pseudo-Newtonian potential to describe the gravitational field. A fully relativistic treatment has been considered by Jaroszynski et al (1980) while a more general formalism

with wider class of angular momentum distributions in Newtonian framework has been considered by Abramowicz et al (1980). The effect of magnetic field has been recently attempted by Dadhich and Wiita (1981).

Need for a rigorous study of accretion

The original α -model and its subsequent modifications, apart from being unstable, assumes pressure gradient force to be small and as a consequence it is thin and the velocity is Keplerian. If the forces other than gravitational and centrifugal forces are not assumed to be small then they will significantly alter the motion from being geodesic and as such the assumption that the inner edge cannot be closer to the event horizon than the last stable circular orbit may not necessarily remain true. The fact that in the presence of magnetic field we do have bound single particle orbits even very close to the event horizon strengthens our view. The general relativistic corrections are then of more importance.

The thick disk models do consider the pressure gradient force playing significant role. However, the studies made so far, do not describe the behaviour of all the dynamical variables as functions of the coordinates. This, in addition to giving a more complete picture

of such disks can also prove to be useful in discussing the stability of such disks.

All the stability analysis done so far are restricted to local analysis only and have used Newtonian gravitational field (Although recently Kato and Fukue 1980 have discussed radial oscillations of thin gaseous disk around Schwarzschild black hole). In a local analysis the wavelength of the perturbation is assumed to be shorter than the characteristic scale length over which the unperturbed dynamical variables change appreciably. The analysis is therefore valid for short wavelengths only. On the other hand in global analysis one constructs an eigenvalue equation and forms a variational principle to determine the growth rate and then solves it using appropriate boundary conditions. No restrictions on wavelengths is assumed and therefore the conclusion remains valid for all wavelengths of the perturbation.

A rigorous analysis of the structure of the disk by solving equations of motion and then making a global analysis of its stability, in general relativistic frame work is worth attempting. Accordingly we present in Chapter 2 the methodology used to study the stability alongwith the general set of equations governing the motion and linear perturbations of a non-self-gravitating, perfect

fluid disk, including pressure p , charge density ξ and conductivity σ and rotating around a Schwarzschild black hole. We assume an adiabatic flow. These equations are of very general nature. Specialised cases of the general situation as described by these equations, are then considered in Chapters 4, 5 and 6 for $\sigma = 0$, $p = 0$ but $\xi \neq 0$ and for $\xi = 0$, $\sigma = 0$ but $p \neq 0$.

Captions for figures.

Figures (1.1) : Orbits of the particles on equatorial plane
(1.3) : of a Kerr black hole in a dipole field
(Prasanna and Vishveshwara (1978)).

Figures (1.4) : Same as in figures (1.1)- (1.3) for uniform
(1.6) : field.

Figure (1.7) : The equipotentials for the Newtonian + plus-
centrifugal potential in the orbital plane
of a binary system with mass ratio 10:1.
The values of the potential measured in the
units of (total mass of the binary/distance
between their centre of masses) are shown
in the figure (Novikov and Thorne, 1973).

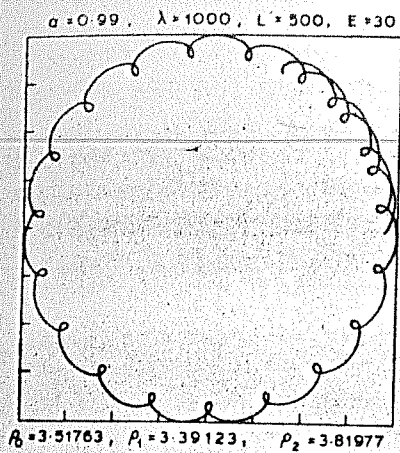


Fig 1.1

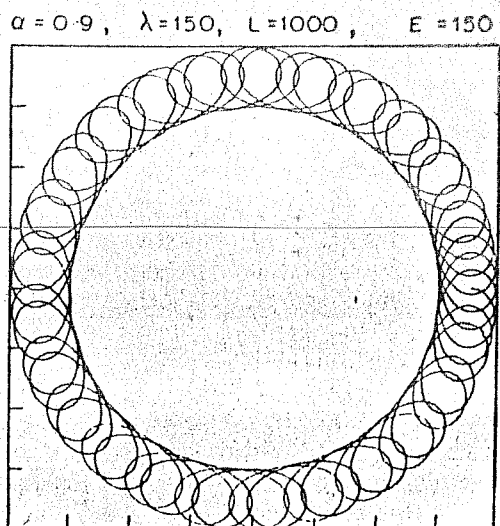


Fig 1.2

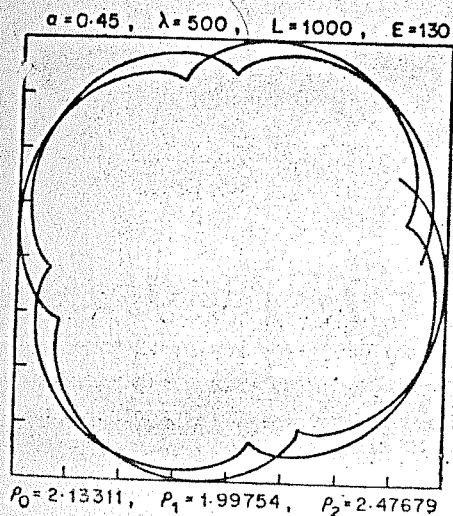


Fig 1.3

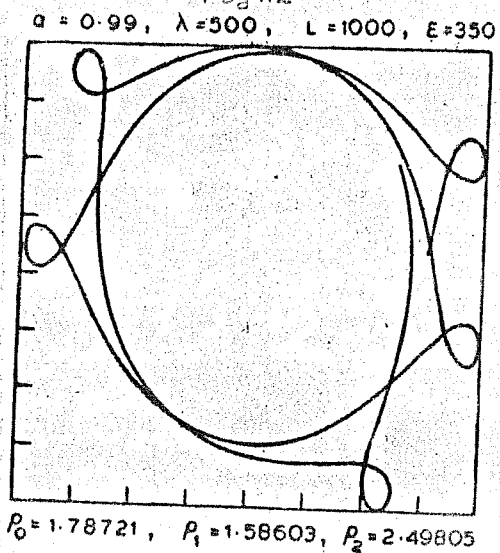


Fig 1.4

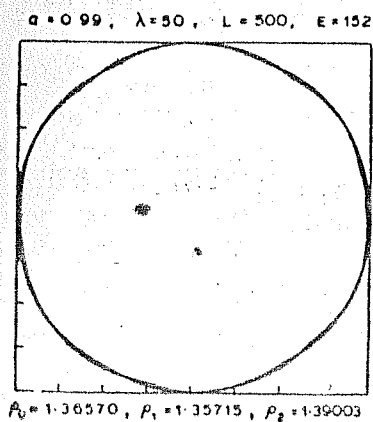
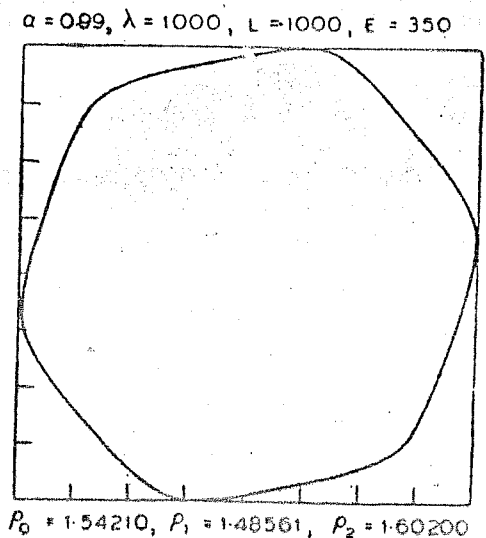


Fig 1.5



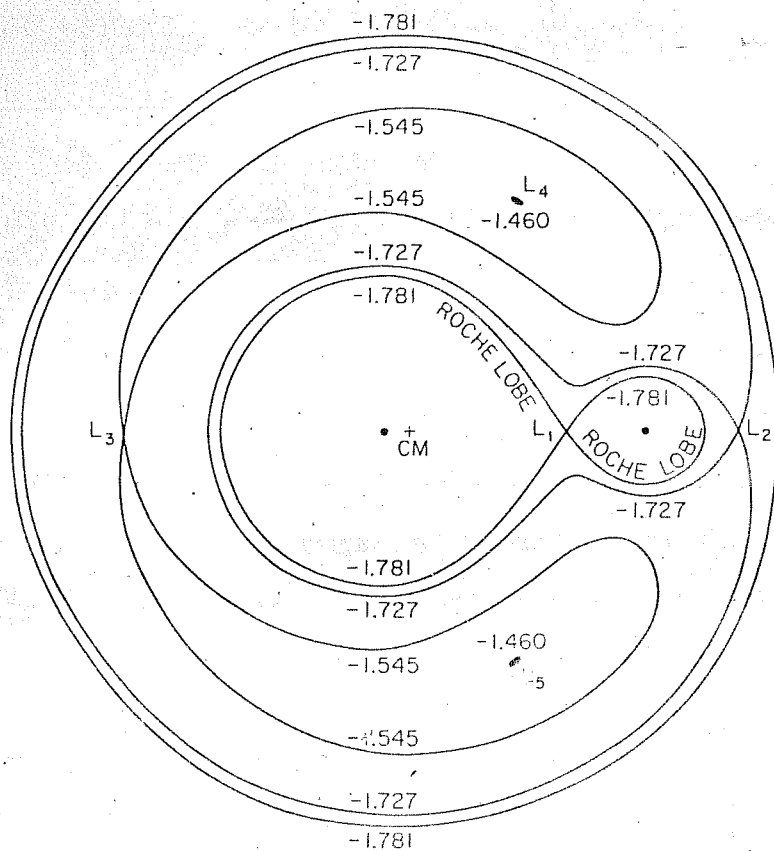


Fig. 1.7

CHAPTER II.

BASIC MATHEMATICAL FORMULATIONS

In this Chapter we present the methodology and the complete set of basic mathematical equations needed for the study of particle as well as disk dynamics.

1. PARTICLE DYNAMICS.

It is well known that the best way to understand the structure of any field is to study the dynamics of test particles in that field. In general relativity, wherein the gravitation is represented by the space-time curvature of the underlying manifold, the structure of the manifold can be completely studied through the geodesics of the manifold which represent the trajectories of test particles in the absence of any other external field (Hawking and Ellis 1972). Alongwith the gravitational field, if there is another field present like an electromagnetic field, then it modifies the gravitational field and therefore the geometry of the space-time, which in turn influences the electromagnetic field and modifies it. Trajectories of a neutral particle are then the geodesics of the modified space-time and thus reveal informations about the interaction of electromagnetic field on the geometry while the orbits of a charged particle deviate from geodesic motion and provide informations about the interaction of the geometry on the electromagnetic field and the vice-versa.

For writing down the equations we shall be using cgs gaussian system of units unless otherwise mentioned. Further we shall adopt the convention that latin indices run from 0 to 3 and greek indices run from 1 to 3, the zeroth component being the time component. Also indices in brackets shall denote the components in the local inertial frame.

The trajectories of a charged particle of charge e and mass M_0 (the word "mass" will always mean the rest mass), in combined electromagnetic and gravitational field are given by the covariant Lorentz equations

$$u^i{}_{;j} u^j = \frac{e}{M_0 c^2} F^i{}_j u^j \quad (2.1.1)$$

where $u^i = dx^i/ds$ is the four velocity of the particle and $F^i{}_j$ is the electromagnetic field tensor with components given by the matrix

$$F_{(i)(j)} = \begin{bmatrix} 0 & -E_1 & -E_2 & -E_3 \\ E_1 & 0 & B_3 & -B_2 \\ E_2 & -B_3 & 0 & B_1 \\ E_3 & B_2 & -B_1 & 0 \end{bmatrix} \quad (2.1.2)$$

where (E_1, E_2, E_3) and (B_1, B_2, B_3) are the components of electric and magnetic fields. c is the velocity of light. The semi-colon denotes the covariant derivative taken with respect to the space-time metric associated with the geometry of the space-time as given by

$$ds^2 = g_{ij} dx^i dx^j \quad (2.1.3)$$

Here g_{ij} are the metric potentials which should be obtained as solutions of the combined set of Einstein - Maxwell equations containing F_{ij} in its source term. F_{ij} also satisfies the covariant Maxwell equations

$$F_{ij,j} = \frac{4\pi}{c} J^i, \quad (2.1.4)$$

$$F_{ij,k} + F_{jk,i} + F_{ki,j} = 0, \quad (2.1.5)$$

J^i being the current density vector.

A self consistent solution of (2.1.4), (2.1.5) and the Einstein Maxwell equation for a given J^i and matter distribution gives us the metric g_{ij} and the electromagnetic field F_{ij} . From g_{ij} we can construct connection coefficients Γ^i_{jk} and finally we can solve (2.1.1) to get the orbits.

In a realistic astrophysical situation involving a neutron star, the electromagnetic field is generated by the currents on its surface while for a black hole it may be due to the current rings in plasma disks surrounding it. In addition to above the interstellar magnetic field may also be present.

With the current and the matter distributions appropriate to the above mentioned situations, we should look for the solutions of Einstein -Maxwell equations which are asymptotically flat and have non-zero dipole moment even in the absence of rotation of the central compact

object. (A charged star produces an induced magnetic dipole moment if it is rotating). These system of equations are formidable to solve in general. However, there are some solutions obtained by perturbation technique under the assumption that the electromagnetic field energy is small compared to the mass-energy of the gravitating source. As a result the electromagnetic field does not affect the back-ground geometry (test field) - the later being solely determined by the central compact object but the background geometry modifies the electromagnetic field (equation 2.1.4)

For the back ground geometry we consider Kerr solution which represents the external field of a rotating black hole of mass M and angular velocity a (in units of c) with metric given by (Misner, Thorne and Wheeler 1973).

$$ds^2 = - \left(1 - \frac{2m\pi}{\Sigma}\right) c^2 dt^2 - \frac{4m\pi a}{\Sigma} \sin^2\theta c dt d\varphi + \frac{\Sigma}{\Delta} dr^2 + \Sigma d\theta^2 + \frac{A}{\Sigma} \sin^2\theta d\varphi^2 \quad (2.1.6)$$

in Boyer Lindquist coordinates (t, r, θ, φ) . In above equation

$$\Sigma = (r^2 + a^2 \cos^2\theta), \quad \Delta = (r^2 + a^2 - 2m\pi), \quad m = MG/c^2, \\ A = (r^2 + a^2)^2 - \Delta a^2 \sin^2\theta \quad (2.1.7)$$

and signature of the metric is +2.

Using the assumption that the electromagnetic field is a test field as mentioned above, several authors

have obtained the solutions for a stationary axisymmetric electromagnetic field around a Kerr black hole (Chitre and Vishveshwara, 1975, Petterson 1975, King et al 1975). We adopt Petterson's solution for the case of dipole magnetic field with zero electrostatic charge, given by

$$A_i = \{A_t, 0, 0, A_\phi\}, \quad (2.1.8)$$

$$A_t = -\frac{3a\mu}{2\beta^2\Sigma} \left[\left\{ r(r-m) + (a^2 - mr)\cos^2\theta \right\} \right. \\ \left. + \frac{1}{2\beta} \ln\left(\frac{r-m+\beta}{r-m-\beta}\right) - (r-m\cos^2\theta) \right], \quad (2.1.9)$$

$$A_\phi = -\frac{3\mu\sin^2\theta}{4\beta^2\Sigma} \left[(r-m)a^2\cos^2\theta + r(r^2 + mr + 2a^2) \right. \\ \left. - \left\{ r(r^3 - 2ma^2 + a^2r) + \Delta a^2\cos^2\theta \right\} \frac{1}{2\beta} \ln\left(\frac{r-m+\beta}{r-m-\beta}\right) \right] \quad (2.1.10)$$

where A_i is the four potential, $\beta = (m^2 - a^2)^{1/2}$, and μ is the dipole moment which is parallel or antiparallel to the rotation axis. The sign of μ has to be taken positive when it is parallel to the rotation axis.

For considering the case of uniform magnetic field we use Wald's (1974) solution for the electromagnetic field obtained by placing a Kerr black hole in an original uniform magnetic field of strength B_0 aligned along the symmetry axis of the black hole. This would give the four potential to be

$$A_t = -aB_0 \left[1 - \frac{mr}{\Sigma} (2 - \sin^2\theta) \right], \quad (2.1.11)$$

$$A_\varphi = \frac{B_0 \sin^2 \theta}{2\Sigma} \left[(r^2 + a^2)^2 - \Delta a^2 \sin^2 \theta - 4ma^2 r \right] \quad (2.1.12)$$

As we are interested in a situation in which both the gravitational and the electromagnetic field are stationary and axi-symmetric, angular momentum l and energy E' are the constants of motion, given by

$$u_\varphi + \frac{e}{M_0 c^2} A_\varphi = \frac{l}{M_0 c}, \quad (2.1.13)$$

$$u_t + \frac{e}{M_0 c^2} A_t = -\frac{E'}{M_0 c^2}. \quad (2.1.14)$$

We use these to write φ - and t - components of the equation of motion. To calculate r - and θ - components of the equation of motion, we use (2.1.1), rewritten as

$$\frac{d^2 x^i}{ds^2} + \Gamma^i_{jk} \frac{dx^j}{ds} \frac{dx^k}{ds} = \frac{e}{M_0 c^2} F^i_j u^j \quad (2.1.15)$$

where

$$F_{ij} = A_{j,i} - A_{i,j}. \quad (2.1.16)$$

The equations of motion appropriate to Kerr back ground geometry can be derived from (2.1.13) to (2.1.15) and are as follows (Prasanna and Vishweshwara 1978).

$$\begin{aligned} \frac{d^2 R}{d\sigma^2} - \frac{[R^2 - a^2 \cos^2 \theta - R a^2 \sin^2 \theta]}{\Sigma \Delta} \left(\frac{dR}{d\sigma} \right)^2 - \frac{R \Delta}{\Sigma} \left(\frac{d\theta}{d\sigma} \right)^2 \\ - \frac{2a^2 \sin \theta \cos \theta}{\Sigma} \left(\frac{dR}{d\sigma} \right) \left(\frac{d\theta}{d\sigma} \right) + \frac{\Delta}{\Sigma^3} (R^2 - a^2 \cos^2 \theta) \left(\frac{d\tau}{d\sigma} \right)^2 \end{aligned}$$

$$\begin{aligned}
& - \frac{2\Delta\alpha\sin^2\theta}{\Sigma^3} (R^2 - \alpha^2\cos^2\theta) \left(\frac{d\varphi}{d\sigma}\right) \left(\frac{d\tau}{d\sigma}\right) \\
& - \frac{\Delta\sin^2\theta}{\Sigma^3} \left\{ R^5 + 2R^3\alpha^2\cos^2\theta - R^2\alpha^2\sin^2\theta + (1-R)\alpha^4\sin^2\theta\cos^2\theta \right. \\
& \left. + R\alpha^4\cos^2\theta \right\} \left(\frac{d\varphi}{d\sigma}\right)^2 = \frac{\Delta}{\Sigma} \left\{ \frac{\partial \bar{A}_\varphi}{\partial R} \frac{d\varphi}{d\sigma} + \frac{\partial A_\tau}{\partial R} \frac{d\tau}{d\sigma} \right\}, \\
& \hspace{15em} (2.1.17)
\end{aligned}$$

$$\begin{aligned}
& \frac{d^2\theta}{d\sigma^2} + \frac{\alpha^2\sin\theta\cos\theta}{\Sigma\Delta} \left(\frac{dR}{d\sigma}\right)^2 + \frac{2R}{\Sigma} \left(\frac{dR}{d\sigma}\right) \left(\frac{d\theta}{d\sigma}\right) \\
& - \frac{\alpha^2\sin\theta\cos\theta}{\Sigma} \left(\frac{d\theta}{d\sigma}\right)^2 - \frac{2R\alpha^2\sin\theta\cos\theta}{\Sigma^3} \left(\frac{d\tau}{d\sigma}\right)^2 \\
& + \frac{4R\alpha(R^2 + \alpha^2)}{\Sigma^3} \sin\theta\cos\theta \left(\frac{d\varphi}{d\sigma}\right) \left(\frac{d\tau}{d\sigma}\right) - \frac{\sin\theta\cos\theta}{\Sigma^3} \left[(R^2 + \alpha^2)^3 \right. \\
& \left. - (R^2 + \alpha^2 + \Sigma)\Delta\alpha^2\sin^2\theta \right] \left(\frac{d\varphi}{d\sigma}\right)^2 = \frac{1}{\Sigma} \left\{ \frac{\partial \bar{A}_\varphi}{\partial \theta} \frac{d\varphi}{d\sigma} + \frac{\partial A_\tau}{\partial \theta} \frac{d\tau}{d\sigma} \right\}, \\
& \hspace{15em} (2.1.18)
\end{aligned}$$

$$\frac{d\varphi}{d\sigma} = \frac{1}{\Delta\Sigma} \left\{ (\Sigma - 2R)(L - \bar{A}_\varphi)/\sin^2\theta + 2R\alpha(E + A_\tau) \right\}, \quad (2.1.19)$$

$$\frac{d\tau}{d\sigma} = \frac{1}{\Delta\Sigma} \left\{ A(E + A_\tau) - 2R\alpha(L - \bar{A}_\varphi) \right\} \quad (2.1.20)$$

wherein

$$R = r/m, \quad \sigma = s/m, \quad \alpha = a/m, \quad \tau = ct/m, \quad E = E'/M_0c^2$$

$$L = \ell/mM_0c, \quad \bar{A}_\varphi = eA_\varphi/mM_0c^2, \quad A_\tau = eA_t/M_0c^2,$$

$$\Delta = R^2 - 2R + \alpha^2, \quad \Sigma = R^2 + \alpha^2\cos^2\theta, \quad (2.1.21)$$

$$A = (R^2 + \alpha^2)^2 - \Delta\alpha^2\sin^2\theta.$$

The four potential A_i , rewritten here in terms of the quantities introduced in (2.1.21), are

case (i) dipolar field

$$A_z = -\frac{3\alpha\lambda}{2\Sigma(1-\alpha^2)} \left[\left\{ R(R-1) + (\alpha^2 - R)\cos^2\theta \right\} \frac{1}{2\sqrt{1-\alpha^2}} \ln \frac{R-1+\sqrt{1-\alpha^2}}{R-1-\sqrt{1-\alpha^2}} - (R - \cos^2\theta) \right], \quad (2.1.22)$$

$$\bar{A}_\varphi = -\frac{3\lambda\sin^2\theta}{4\Sigma(1-\alpha^2)} \left[-\left\{ R(R^3 + \alpha^2 R - 2\alpha^2) + \Delta\alpha^2\cos^2\theta \right\} \frac{1}{2\sqrt{1-\alpha^2}} \ln \frac{R-1+\sqrt{1-\alpha^2}}{R-1-\sqrt{1-\alpha^2}} + (R-1)\alpha^2\cos^2\theta + R(R^2 + R + 2\alpha^2) \right] \quad (2.1.23)$$

with

$$\lambda = e\mu/M_0 c^2 m^2, \quad (2.1.24)$$

case (ii) uniform field

$$A_z = -\alpha\lambda \left[1 - \frac{R}{\Sigma} (2 - \sin^2\theta) \right], \quad (2.1.25)$$

$$\bar{A}_\varphi = \frac{\lambda\sin^2\theta}{2\Sigma} \left[(R^2 + \alpha^2)^2 + \Delta\alpha^2\sin^2\theta - 4\alpha^2 R \right] \quad (2.1.26)$$

with

$$\lambda = eB_0 m/M_0 c^2. \quad (2.1.27)$$

One can then solve (2.1.17) to (2.1.20) alongwith the field components (2.1.22) to (2.1.27) to get the actual orbits. These equations are almost impossible to solve analytically and therefore one resorts to numerical integrations.

If one uses the initial conditions $\theta = \pi/2$ and $u^\theta = 0$, equation (2.1.13) immediately gives $d^2\theta/d\sigma^2 = 0$ or that the particle remains confined to the equatorial plane. To study

such equatorial motion one first studies the effective potential (Bardeen 1972, Prasanna and Vishveshwara 1978).

Using the normalisation condition of four velocity

$$g_{ij} u^i u^j = -1, \quad (2.1.23)$$

the first integrals (2.1.19) and (2.1.20) and that $u^\theta = 0$, one obtains an expression for u^r . The effective potential V_{eff} is the energy calculated from this expression of u^r by putting $u^r = 0$. Plots of the V_{eff} against r gives the turning points r_1 and r_2 for particles with specific choices of initial conditions and other parameters needed to solve the dynamical equations. The particles are then in bound orbits around the Kerr black hole and confined to its equatorial plane.

To obtain the trajectories off the equatorial plane we still take $\theta = \pi/2$ but assume a finite nonzero u^θ as initial condition. The particles are then no longer confined to the equatorial plane and execute motion in 3-dimensional space.

So far we have used Boyer Lindquist coordinate system to describe the metric, electromagnetic field and the dynamical equations governing the motion of the particle. The Boyer Lindquist coordinates which are the natural generalisation of Schwarzschild coordinates are the best for many purposes. However within the ergosphere which is the region between the static limit R_s ,

$$R_s = 1 + \sqrt{1 - a^2 \cos^2 \theta} \quad (2.1.29)$$

and the event horizon

$$R_e = 1 + \sqrt{1 - \alpha^2}, \quad (2.1.30)$$

they are somewhat unphysical, for example a physical observer can not remain at rest with $R, \theta, \varphi = \text{constant}$ but has to rotate in the same sense as the hole itself (inertial frame-dragging). It was shown by Bardeen (1970) that for observers rotating with angular velocity $\omega = -g_{\varphi t}/g_{\varphi\varphi}$ the local geometry is flat. It is then useful to introduce a set of local observers each carrying an orthonormal tetrad of 4-vectors - his locally Minkowskian coordinate basis vectors and describe the physical quantities at each point by their projections on this orthonormal tetrad i.e. their physically measured components in the local observers frame.

For a metric in the standard canonical form

$$ds^2 = -e^{2\nu} c^2 dt^2 + e^{2\psi} (d\varphi - \omega c dt)^2 + e^{2\mu_1} dr^2 + e^{2\mu_2} d\theta^2 \quad (2.1.31)$$

where ν, ψ, μ_1 and μ_2 are functions of r and θ , describing an axisymmetric, stationary and asymptotically flat spacetime, there is a uniquely sensible choice of observers and tetrads: the locally non rotating frames (LNRF) for which the observers world lines are $r = \text{constant}$ $\theta = \text{constant}$ and $\varphi = \omega t + \text{constant}$ where $\omega = -g_{\varphi t}/g_{\varphi\varphi}$. The orthonormal tetrad $\tilde{e}_{(i)}$ carried by such an observer (the set of LNRF basis vectors) at point (t, r, θ, φ) is given by (Bardeen et al 1972)

$$\tilde{e}_{(t)} = \bar{e}^\nu \left(\frac{\partial}{\partial t} + \omega \frac{\partial}{\partial \varphi} \right),$$

$$\tilde{e}_{(r)} = \bar{e}^{\mu_1} \frac{\partial}{\partial r},$$

$$\tilde{e}_{(\theta)} = \bar{e}^{\mu_2} \frac{\partial}{\partial \theta},$$

$$\tilde{e}_{(\varphi)} = \bar{e}^\psi \frac{\partial}{\partial \varphi}.$$

(2.1.32)

The corresponding basis one forms $\tilde{\theta}^{(i)}$ are

$$\tilde{\theta}^{(t)} = e^\nu c dt,$$

$$\tilde{\theta}^{(r)} = e^{\mu_1} dr,$$

$$\tilde{\theta}^{(\theta)} = e^{\mu_2} d\theta,$$

$$\tilde{\theta}^{(\varphi)} = -\omega e^\psi c dt + e^\psi d\varphi$$

(2.1.33)

The transformation relating components in the coordinate basis and frame are carried out through matrices $\|e^i_{(j)}\|$ and its inverse $\|e^{(i)}_j\|$, components of which can be directly read off from (2.1.32), (2.1.33) and the relations

$$\tilde{e}_{(i)} = e^j_{(i)} \frac{\partial}{\partial x^j},$$

$$\tilde{\theta}^{(i)} = e^{(i)}_j dx^j.$$

(2.1.34)

Thus

$$e^i_{(j)} = \begin{bmatrix} e^\nu & 0 & 0 & 0 \\ 0 & e^{\mu_1} & 0 & 0 \\ 0 & 0 & e^{\mu_2} & 0 \\ -\omega e^\psi & 0 & 0 & e^\psi \end{bmatrix} \quad e^i_{(j)} = \begin{bmatrix} \bar{e}^\nu & 0 & 0 & 0 \\ 0 & \bar{e}^{\mu_1} & 0 & 0 \\ 0 & 0 & \bar{e}^{\mu_2} & 0 \\ \omega \bar{e}^\nu & 0 & 0 & \bar{e}^\psi \end{bmatrix} \quad (2.1.35)$$

The essential idea of studying any phenomena in LNRF is to cancel out, as much as possible the frame dragging effect of the hole's rotation.

2. DISK DYNAMICS.

From the studies of particle dynamics we pass on to the study of dynamics of aggregate of particles forming a fluid disk rotating around a compact object. We shall limit our studies to the case of perfect fluid disk only and therefore we cannot study the generation of heat and its transport, because of the neglect of viscosity. Also because of the same reason we do not account for the loss of mass of the disk from its inner edge and its compensation at the outer edge by accretion. We assume that the disk is already formed and in its steady state, radial velocity is zero. We are presently interested in the structure and stability of such 'already formed' disks.

The mass of the disk is negligible compared to that of the central compact object so that the geometry is solely determined by the later. The disk is assumed to be made up of charged as well as neutral fluid and therefore the motion of the disk gives rise to electromagnetic field. The electromagnetic field is regarded as a test field and therefore it does not modify the geometry but the later modifies the electromagnetic field.

The fundamental equations governing the dynamics of the disk are derived from (Prasanna and Chakraborty 1981, Chakraborty and Prasanna III, 1981).

(a) the law of conservation of energy-momentum:

$$T^{ij}_{;j} = 0 \quad (2.2.1)$$

where T^{ij} is the energy momentum tensor given by

$$T^{ij} = p g^{ij} + (p + \rho c^2) u^i u^j + \frac{1}{4\pi} (F^i_m F^{jm} - \frac{1}{4} g^{ij} F_{lm} F^{lm}) \quad (2.2.2)$$

wherein p is the pressure and ρc^2 is the energy density, including rest mass energy, alongwith the Maxwell's equations given by (2.1.4 and 2.1.5) with J^i given by

$$J^i = c \epsilon u^i + \sigma F^{ij} u_j \quad (2.2.3)$$

with ϵ being the charge density and σ the conductivity; and

(b) laws of thermodynamics which include the law of conservation of baryon numbers

$$(n u^i)_{;i} = 0 \quad (2.2.4)$$

wherein n is the number density of baryons and the second law of thermodynamics

$$du + p dV = T ds \quad (2.2.5)$$

where u, V, T and s are internal energy, volume, temperature and entropy. The above set of equations is supplemented by a suitable equation of state to make the system of equations close.

As u^i satisfies the normalisation relationship $u_i u^i = -1$ (equation 2.1.21) and as F_{ij} is antisymmetric, the equation (2.2.1) may be resolved into the equation of continuity

$$e_{,i} u^i + (e + p/c^2) u^i{}_{;i} = -\frac{\sigma}{c^3} F_{ij} F^j{}_k u^i u^k \quad (2.2.6)$$

and the equation

$$(e + p/c^2) u^i{}_{;j} u^j = -\frac{1}{c^2} (g^{ij} + u^i u^j) p_{,j} + \frac{\varepsilon}{c^2} F^i{}_j u^j \\ + \frac{\sigma}{c^3} (F^i{}_j F^j{}_k u^k + u^i F_{jl} F^l{}_k u^j u^k). \quad (2.2.7)$$

Using baryon conservation equation (2.2.4) in continuity equation (2.2.6) we obtain

$$n u^j \left[p \frac{\partial}{\partial x^j} \left(\frac{1}{n} \right) + \frac{\partial}{\partial x^j} \left(\frac{ec^2}{n} \right) \right] = -\frac{\sigma}{c} F_{ij} F^j{}_k u^i u^k. \quad (2.2.8)$$

Further since $1/n$ is the volume per baryon and ec^2/n is the internal energy per baryon, law of thermodynamics yields

$$T d\bar{s} = d\left(\frac{ec^2}{n}\right) + p d\left(\frac{1}{n}\right) \quad (2.2.9)$$

wherein \bar{s} is the entropy per baryon. Equations (2.2.8) and (2.2.9) imply

$$nT u^j \frac{\partial \bar{s}}{\partial x^j} = -\frac{\sigma}{c} F_{ij} F^j{}_k u^i u^k \quad (2.2.10)$$

or that the motion of a perfect fluid with $\sigma = 0$ is adiabatic maintaining the entropy constant along its flow. For a fluid obeying equation of state as given by

$$ec^2 = n M_0 c^2 + \frac{p}{\gamma - 1} \quad (2.2.11)$$

where M_0 is the mass of each baryon and $\gamma = C_p/C_v$ is the ratio of specific heats, equation (2.2.10) reduces to

$$\frac{n^\gamma}{\gamma - 1} u^j \frac{\partial}{\partial x^j} \left(\frac{p}{n^\gamma} \right) = -\frac{\sigma}{c} F_{ij} F^j{}_k u^i u^k. \quad (2.2.12)$$

Equations of momentum conservation can be obtained from (2.2.7) by using its zeroth- component, into its space-

components. The set of momentum equations alongwith the continuity equation (2.2.6) and the Maxwell's equations (2.1.4) and (2.1.5); baryon conservation equation (2.2.4), and the equation (2.2.12) of adiabatic flow now forms the complete set of equations governing the dynamics of the disk, containing all the informations of the original fundamental set of equations (a) and (b) for a fluid obeying equation of state of the type (2.2.11).

In order to compare with corresponding Newtonian equations we introduce 3- velocities v^α such that $u^\alpha = v^\alpha u^0/c$ wherein $u^0 = \frac{dx^0}{ds}$, x^0 being the time coordinate expressed in the length units and write the equations in terms of local Lorentz frame (LLF) components defined by the orthonormal tetrad appropriate to the metric corresponding to the background geometry. The momentum equations as obtained from (2.2.7) then reduce to

$$\begin{aligned}
 & \left(\rho + \frac{p}{c^2}\right)(u^0)^2 \left[\frac{\partial v^\alpha}{\partial t} + v^\beta \frac{\partial v^\alpha}{\partial x^\beta} + c^2 \left(\Gamma^\alpha_{00} - \frac{v^\alpha}{c} \Gamma^0_{00} \right) \right. \\
 & \quad \left. + 2c v^\beta \left(\Gamma^\alpha_{0\beta} - \frac{v^\alpha}{c} \Gamma^0_{0\beta} \right) + v^\beta v^\gamma \left(\Gamma^\alpha_{\beta\gamma} - \frac{v^\alpha}{c} \Gamma^0_{\beta\gamma} \right) \right] \\
 & = - \left(g^{\alpha 0} - g^{00} \frac{v^\alpha}{c} \right) \frac{\partial p}{c \partial t} - \left(g^{\alpha\beta} - g^{0\beta} \frac{v^\alpha}{c} \right) \frac{\partial p}{\partial x^\beta} \\
 & + \epsilon u^0 \left[F^\alpha_0 + \frac{1}{c} F^\alpha_\beta v^\beta - \frac{1}{2} F^0_\beta v^\alpha v^\beta \right] + \frac{u^0 \sigma}{c} \left[\left(F^\alpha_\beta - \frac{v^\alpha}{c} F^0_\beta \right) F^\beta_0 \right. \\
 & \quad \left. + \frac{1}{c} \left(F^\alpha_0 F^0_\beta + F^\alpha_\gamma F^\gamma_\beta - \frac{v^\alpha}{c} F^0_\gamma F^\gamma_\beta \right) v^\beta \right] \quad (2.2.13)
 \end{aligned}$$

while the continuity equation (2.2.6) reduces to

$$\begin{aligned}
& \left(\rho + \frac{p}{c^2} \right) \left[\vartheta^\alpha_{,\alpha} - \Gamma^0_{0\alpha} \vartheta^\alpha + c \Gamma^\alpha_{0\alpha} + \Gamma^\beta_{\alpha\beta} \vartheta^\alpha - \Gamma^0_{\alpha\beta} \frac{\vartheta^\alpha \vartheta^\beta}{c} \right] \\
& + \left(\frac{\partial \rho}{\partial t} + \vartheta^\alpha \frac{\partial \rho}{\partial x^\alpha} \right) - \frac{1}{c^2} \left(\frac{\partial p}{\partial t} + \vartheta^\alpha \frac{\partial p}{\partial x^\alpha} \right) - \frac{1}{c(u^0)^2} \left(g^{00} \frac{\partial p}{c \partial t} + g^{\alpha\alpha} \frac{\partial p}{\partial x^\alpha} \right) \\
& + \frac{1}{u^0 c^2} \left[\varepsilon F^\alpha_0 \vartheta^\alpha + \sigma F^\alpha_\alpha (F^\alpha_0 + \frac{\vartheta^\beta}{c} F^\alpha_\beta) \right] \\
& + \frac{2u^0 \sigma}{c^2} \left[F_{0\alpha} F^\alpha_0 + \frac{2\vartheta^\alpha}{c} F_{0\beta} F^\beta_\alpha \right. \\
& \quad \left. + (F_{\alpha 0} F^\alpha_\beta + F_{\alpha\gamma} F^\gamma_\beta) \frac{\vartheta^\alpha \vartheta^\beta}{c^2} \right] = 0 \quad (2.2.14)
\end{aligned}$$

Baryon conservation equation in terms of ϑ^α is

$$\begin{aligned}
& n \left[\vartheta^\alpha_{,\alpha} - \Gamma^0_{0\alpha} \vartheta^\alpha + c \Gamma^\alpha_{0\alpha} + \Gamma^\beta_{\alpha\beta} \vartheta^\alpha - \Gamma^0_{\alpha\beta} \frac{\vartheta^\alpha \vartheta^\beta}{c} \right] \\
& + \left(\frac{\partial n}{\partial t} + \vartheta^\alpha \frac{\partial n}{\partial x^\alpha} \right) + \left\{ -\frac{1}{c^2} \left(\frac{\partial p}{\partial t} + \vartheta^\alpha \frac{\partial p}{\partial x^\alpha} \right) - \frac{1}{c(u^0)^2} \left(g^{00} \frac{\partial p}{c \partial t} + g^{\alpha\alpha} \frac{\partial p}{\partial x^\alpha} \right) \right. \\
& + \frac{1}{u^0 c^2} \left[\varepsilon F^\alpha_0 \vartheta^\alpha + \sigma F^\alpha_\alpha (F^\alpha_0 + \frac{\vartheta^\beta}{c} F^\alpha_\beta) \right] + \frac{u^0 \sigma}{c^2} \left[F_{0\alpha} F^\alpha_0 \right. \\
& \quad \left. + \frac{2\vartheta^\alpha}{c} F_{0\beta} F^\beta_\alpha + \frac{\vartheta^\alpha \vartheta^\beta}{c^2} (F_{\alpha 0} F^\alpha_\beta + F_{\alpha\gamma} F^\gamma_\beta) \right] \left. \right\} \frac{n}{\left(\rho + \frac{p}{c^2} \right)} = 0 \quad (2.2.15)
\end{aligned}$$

and adiabatic equation in terms of ϑ^α is given by

$$\begin{aligned}
& \frac{n}{r-1} \left[\frac{\partial}{\partial t} \left(\frac{p}{nr} \right) + \vartheta^\alpha \frac{\partial}{\partial x^\alpha} \left(\frac{p}{nr} \right) \right] = -\sigma u^0 \left[F_{0\alpha} F^\alpha_0 \right. \\
& \quad \left. + \frac{2\vartheta^\alpha}{c} F_{0\beta} F^\beta_\alpha + \frac{\vartheta^\alpha \vartheta^\beta}{c^2} (F_{\alpha 0} F^\alpha_\beta + F_{\alpha\gamma} F^\gamma_\beta) \right] \quad (2.2.16)
\end{aligned}$$

with

$$-(u^0)^2 = \left(g_{00} + 2g_{0\alpha} \frac{\vartheta^\alpha}{c} + g_{\alpha\beta} \frac{\vartheta^\alpha \vartheta^\beta}{c^2} \right)^{-1}$$

$$\frac{\vartheta^\alpha}{c} = \frac{\lambda^\alpha_{(B)} \vartheta^{(B)} + c \lambda^0_{(0)}}{\lambda^0_{(B)} \vartheta^{(B)} + c \lambda^0_{(0)}}$$

$$F^i_j = \lambda^i_{(L)} \lambda^{(m)}_j F^{(L)}_{(m)} \quad (2.2.17)$$

For the analysis of disk dynamics we limit ourselves to the case of Schwarzschild background geometry representing the gravitational field of a non-rotating mass M . Hence the metric can be obtained from Kerr metric represented by equation (2.1.6) by putting $a=0$:

$$ds^2 = -\left(1 - \frac{2m}{r}\right) c^2 dt^2 + \left(1 - \frac{2m}{r}\right)^{-1} dr^2 + r^2 (d\theta^2 + \sin^2 \theta d\varphi^2) \quad (2.2.18)$$

The corresponding local Lorentz frame is defined by

$$\begin{aligned} \lambda^{(t)}_t &= \left(1 - \frac{2m}{r}\right)^{\frac{1}{2}}, \quad \lambda^{(r)}_r = \left(1 - \frac{2m}{r}\right)^{-\frac{1}{2}}, \\ \lambda^{(\theta)}_\theta &= r, \quad \lambda^{(\varphi)}_\varphi = r \sin \theta, \quad \lambda^{(i)}_j = 0 \quad \text{if } i \neq j. \end{aligned} \quad (2.2.19)$$

The components of velocity as well as of electromagnetic field are therefore given by

$$\begin{aligned} v^{(r)} &= \left(1 - \frac{2m}{r}\right)^{-\frac{1}{2}} v^r, \quad v^{(\theta)} = r \left(1 - \frac{2m}{r}\right)^{-\frac{1}{2}} v^\theta, \quad v^{(\varphi)} = r \sin \theta \left(1 - \frac{2m}{r}\right)^{-\frac{1}{2}} v^\varphi, \\ F_{(r)(\theta)} &= \frac{1}{r} \left(1 - \frac{2m}{r}\right)^{\frac{1}{2}} F_{r\theta}, \quad F_{(r)(t)} = F_{rt}, \\ F_{(\theta)(\varphi)} &= \frac{1}{r^2 \sin \theta} F_{\theta\varphi}, \quad F_{(\theta)(t)} = \frac{1}{r} \left(1 - \frac{2m}{r}\right)^{-\frac{1}{2}} F_{\theta t}, \\ F_{(\varphi)(r)} &= \frac{1}{r \sin \theta} \left(1 - \frac{2m}{r}\right)^{\frac{1}{2}} F_{\varphi r}, \quad F_{(\varphi)(t)} = \frac{1}{r \sin \theta} \left(1 - \frac{2m}{r}\right)^{-\frac{1}{2}} F_{\varphi t}. \end{aligned} \quad (2.2.20)$$

In the study of charged fluid disk we use charge continuity equation

$$\varepsilon_{,i} u^i + \varepsilon u^i_{,i} = 0 \quad (2.2.21)$$

along with the continuity equation (2.2.6) with $\sigma = 0$ to obtain

$$\left(\rho + \frac{p}{c^2}\right) \left(\frac{\partial}{\partial t} + v^\alpha \frac{\partial}{\partial x^\alpha}\right) \varepsilon = \varepsilon \left(\frac{\partial}{\partial t} + v^\alpha \frac{\partial}{\partial x^\alpha}\right) \rho \quad (2.2.22)$$

which express conservation of both charge as well as of mass, while for the study of neutral fluid disk we use (2.2.14) as the continuity equation. Thus the complete system of equations that govern the dynamics of the disk (charged as well as neutral) is given by (For $\sigma = 0$ case):

the momentum equations

$$\begin{aligned} & \left(\rho + \frac{p}{c^2} \right) \left[\frac{D\vartheta(r)}{Dt} + \frac{mc^2}{r^2} \left(1 - \frac{\vartheta(r)^2}{c^2} \right) - \left(1 - \frac{2m}{r} \right) \left\{ \frac{\vartheta(\theta)^2 + \vartheta(\varphi)^2}{r} \right\} \right] \\ &= - \left(1 - \frac{\vartheta^2}{c^2} \right) \left[\left(1 - \frac{2m}{r} \right) \frac{\partial p}{\partial r} + \frac{\vartheta(r)}{c^2} \frac{\partial p}{\partial t} \right] + \varepsilon \left(1 - \frac{2m}{r} \right)^{\frac{1}{2}} \left(1 - \frac{\vartheta^2}{c^2} \right)^{\frac{1}{2}} \\ & \left[F^{(r)}_{(t)} + \frac{1}{c} \left\{ \vartheta(\theta) F^{(r)}_{(\theta)} - \vartheta(\varphi) F^{(r)}_{(\varphi)} \right\} - \frac{\vartheta(r)}{c^2} \underline{E} \cdot \underline{v} \right], \quad (2.2.23) \end{aligned}$$

$$\begin{aligned} & \left(\rho + \frac{p}{c^2} \right) \left[\frac{D\vartheta(\theta)}{Dt} + \left(1 - \frac{3m}{r} \right) \frac{\vartheta(r)}{r} \frac{\vartheta(\theta)}{r} - \left(1 - \frac{2m}{r} \right)^{\frac{1}{2}} \frac{c \sin \theta}{r} \vartheta(\varphi)^2 \right] \\ &= - \left(1 - \frac{\vartheta^2}{c^2} \right) \left[\left(1 - \frac{2m}{r} \right)^{\frac{1}{2}} \frac{1}{r} \frac{\partial p}{\partial \theta} + \frac{\vartheta(\theta)}{c^2} \frac{\partial p}{\partial t} \right] + \varepsilon \left(1 - \frac{2m}{r} \right)^{\frac{1}{2}} \left(1 - \frac{\vartheta^2}{c^2} \right)^{\frac{1}{2}} \\ & \left[F^{(\theta)}_{(t)} + \frac{1}{c} \left\{ \vartheta(\varphi) F^{(\theta)}_{(\varphi)} - \vartheta(r) F^{(\theta)}_{(r)} \right\} - \frac{\vartheta(\theta)}{c^2} \underline{E} \cdot \underline{v} \right], \quad (2.2.24) \end{aligned}$$

$$\begin{aligned} & \left(\rho + \frac{p}{c^2} \right) \left[\frac{D\vartheta(\varphi)}{Dt} + \left(1 - \frac{3m}{r} \right) \frac{\vartheta(r)}{r} \frac{\vartheta(\varphi)}{r} + \left(1 - \frac{2m}{r} \right)^{\frac{1}{2}} \frac{c \cos \theta}{r} \vartheta(\varphi) \vartheta(\theta) \right] \\ &= - \left(1 - \frac{\vartheta^2}{c^2} \right) \left[\left(1 - \frac{2m}{r} \right)^{\frac{1}{2}} \frac{1}{r \sin \theta} \frac{\partial p}{\partial \varphi} + \frac{\vartheta(\varphi)}{c^2} \frac{\partial p}{\partial t} \right] + \varepsilon \left(1 - \frac{2m}{r} \right)^{\frac{1}{2}} \left(1 - \frac{\vartheta^2}{c^2} \right)^{\frac{1}{2}} \\ & \left[F^{(\varphi)}_{(t)} + \frac{1}{c} \left\{ \vartheta(r) F^{(\varphi)}_{(r)} - \vartheta(\theta) F^{(\varphi)}_{(\theta)} \right\} - \frac{\vartheta(\varphi)}{c^2} \underline{E} \cdot \underline{v} \right], \quad (2.2.25) \end{aligned}$$

the continuity equations

$$\left(\epsilon + \frac{p}{c^2}\right) \frac{D\epsilon}{Dt} = \epsilon \frac{D\epsilon}{Dt}, \quad (2.2.26)$$

$$\begin{aligned} & \left(\epsilon + \frac{p}{c^2}\right) \left[\left(1 - \frac{2m}{r}\right)^{\frac{1}{2}} \left\{ \left(1 - \frac{2m}{r}\right)^{\frac{1}{2}} \frac{1}{r^2} \frac{\partial}{\partial r} (r^2 \vartheta(r)) + \frac{1}{r \sin \theta} \left[\frac{\partial}{\partial \theta} (\sin \theta \vartheta(\theta)) \right. \right. \right. \\ & \quad \left. \left. \left. + \frac{\partial \vartheta(\varphi)}{\partial \varphi} \right] \right\} \right] + \frac{D}{Dt} \left(\epsilon - \frac{p}{c^2}\right) + \frac{1}{c^2} \left(1 - \frac{v^2}{c^2}\right) \frac{\partial p}{\partial t} \\ & + \frac{\epsilon}{c^2} \left(1 - \frac{2m}{r}\right)^{\frac{1}{2}} \left(1 - \frac{v^2}{c^2}\right)^{\frac{1}{2}} \underline{\underline{E}} \cdot \underline{\underline{v}} = 0, \end{aligned} \quad (2.2.27)$$

Maxwell equations

$$\begin{aligned} & \frac{1}{c} \frac{\partial}{\partial t} F_{(\theta)(\varphi)} + \frac{1}{r^2 \sin \theta} \left[\frac{\partial}{\partial \theta} \left\{ r \sin \theta \left(1 - \frac{2m}{r}\right)^{\frac{1}{2}} F_{(\varphi)(t)} \right\} \right. \\ & \quad \left. - \frac{\partial}{\partial \varphi} \left\{ r \left(1 - \frac{2m}{r}\right)^{\frac{1}{2}} F_{(\theta)(t)} \right\} \right] = 0, \end{aligned} \quad (2.2.28)$$

$$\begin{aligned} & \frac{1}{c} \frac{\partial}{\partial t} F_{(\varphi)(r)} + \frac{1}{r \sin \theta} \left(1 - \frac{2m}{r}\right)^{\frac{1}{2}} \left[\frac{\partial}{\partial \varphi} F_{(r)(t)} \right. \\ & \quad \left. - \frac{\partial}{\partial r} \left\{ r \sin \theta \left(1 - \frac{2m}{r}\right)^{\frac{1}{2}} F_{(\varphi)(t)} \right\} \right] = 0, \end{aligned} \quad (2.2.29)$$

$$\begin{aligned} & \frac{1}{c} \frac{\partial}{\partial t} F_{(r)(\theta)} + \frac{1}{r} \left(1 - \frac{2m}{r}\right)^{\frac{1}{2}} \left[\frac{\partial}{\partial r} \left\{ r \left(1 - \frac{2m}{r}\right)^{\frac{1}{2}} F_{(\theta)(t)} \right\} \right. \\ & \quad \left. - \frac{\partial}{\partial \theta} F_{(r)(t)} \right] = 0, \end{aligned} \quad (2.2.30)$$

$$\begin{aligned} & \frac{\partial}{\partial r} \left\{ r^2 \sin \theta F_{(\theta)(\varphi)} \right\} + \frac{\partial}{\partial \theta} \left\{ r \sin \theta \left(1 - \frac{2m}{r}\right)^{\frac{1}{2}} F_{(\varphi)(r)} \right\} \\ & + \frac{\partial}{\partial \varphi} \left\{ r \left(1 - \frac{2m}{r}\right)^{\frac{1}{2}} F_{(r)(\theta)} \right\} = 0, \end{aligned} \quad (2.2.31)$$

$$\begin{aligned} & -\frac{1}{c} \frac{\partial}{\partial t} F_{(r)(t)} + \frac{1}{r^2 \sin \theta} \left[\frac{\partial}{\partial \theta} \left\{ r \sin \theta \left(1 - \frac{2m}{r}\right)^{\frac{1}{2}} F_{(r)(\theta)} \right\} \right. \\ & \quad \left. - \frac{\partial}{\partial r} \left\{ r \left(1 - \frac{2m}{r}\right)^{\frac{1}{2}} F_{(\varphi)(r)} \right\} \right] = \frac{4\pi\epsilon}{c} \left(1 - \frac{2m}{r}\right)^{\frac{1}{2}} \left(1 - \frac{v^2}{c^2}\right)^{\frac{1}{2}} \vartheta(r), \end{aligned} \quad (2.2.32)$$

$$-\frac{1}{c} \frac{\partial}{\partial t} F_{(\theta)}(t) + \frac{1}{r \sin \theta} \left(1 - \frac{2m}{r}\right)^{\frac{L}{2}} \left[\frac{\partial}{\partial \varphi} F_{(\theta)}(\varphi) - \frac{\partial}{\partial r} \left\{ r \sin \theta \left(1 - \frac{2m}{r}\right)^{\frac{L}{2}} F_{(r)}(\theta) \right\} \right] = \frac{4\pi \varepsilon}{c} \left(1 - \frac{2m}{r}\right)^{\frac{L}{2}} \left(1 - \frac{v^2}{c^2}\right)^{-\frac{L}{2}} \vartheta^{(\theta)}, \quad (2.2.33)$$

$$-\frac{1}{c} \frac{\partial}{\partial t} F_{(\varphi)}(t) + \frac{1}{r} \left(1 - \frac{2m}{r}\right)^{\frac{L}{2}} \left[\frac{\partial}{\partial r} \left\{ r \left(1 - \frac{2m}{r}\right)^{\frac{L}{2}} F_{(\varphi)}(r) \right\} - \frac{\partial}{\partial \theta} F_{(\theta)}(\varphi) \right] = \frac{4\pi \varepsilon}{c} \left(1 - \frac{2m}{r}\right)^{\frac{L}{2}} \left(1 - \frac{v^2}{c^2}\right)^{-\frac{L}{2}} \vartheta^{(\varphi)}, \quad (2.2.34)$$

$$\frac{1}{r^2 \sin \theta} \left[\frac{\partial}{\partial r} \left\{ r^2 \sin \theta F_{(r)}(t) \right\} + \frac{\partial}{\partial \theta} \left\{ r \sin \theta \left(1 - \frac{2m}{r}\right)^{-\frac{L}{2}} F_{(\theta)}(t) \right\} + \frac{\partial}{\partial \varphi} \left\{ r \left(1 - \frac{2m}{r}\right)^{-\frac{L}{2}} F_{(\varphi)}(t) \right\} \right] = 4\pi \varepsilon \left(1 - \frac{2m}{r}\right)^{-\frac{L}{2}} \left(1 - \frac{v^2}{c^2}\right)^{-\frac{L}{2}}, \quad (2.2.35)$$

the baryon conservation equation

$$\begin{aligned} & \eta \left[\left(1 - \frac{2m}{r}\right)^{\frac{L}{2}} \left\{ \left(1 - \frac{2m}{r}\right)^{\frac{L}{2}} \frac{1}{r^2} \frac{\partial}{\partial r} (r^2 \vartheta^{(r)}) + \frac{1}{r \sin \theta} \left[\frac{\partial}{\partial \theta} (\sin \theta \vartheta^{(\theta)}) + \frac{\partial \vartheta^{(\varphi)}}{\partial \varphi} \right] \right\} + \frac{D\eta}{Dt} - \frac{\eta}{c^2 (p + b/c^2)} \left[\frac{Dp}{Dt} - \left(1 - \frac{v^2}{c^2}\right) \frac{\partial p}{\partial t} \right. \right. \\ & \quad \left. \left. - \varepsilon \left(1 - \frac{2m}{r}\right)^{\frac{L}{2}} \left(1 - \frac{v^2}{c^2}\right)^{\frac{L}{2}} \underline{E} \cdot \underline{\vartheta} \right] \right] = 0 \end{aligned} \quad (2.2.36)$$

and the adiabatic equation

$$\frac{D}{Dt} (p \eta^{-\gamma}) = 0, \quad (2.2.37)$$

wherein

$$v^2 = (v^{(r)})^2 + (v^{(\theta)})^2 + (v^{(\varphi)})^2, \quad (2.2.38)$$

$$\underline{E} \cdot \underline{\vartheta} = F_{(r)}(t) \vartheta^{(r)} + F_{(\theta)}(t) \vartheta^{(\theta)} + F_{(\varphi)}(t) \vartheta^{(\varphi)}, \quad (2.2.39)$$

and

$$\frac{D}{Dt} = \frac{\partial}{\partial t} + \left(1 - \frac{2m}{r}\right)^{\frac{1}{2}} \left\{ \left(1 - \frac{2m}{r}\right)^{\frac{1}{2}} \vartheta(r) \frac{\partial}{\partial r} + \frac{\vartheta(\theta)}{r} \frac{\partial}{\partial \theta} + \frac{\vartheta(\varphi)}{r \sin \theta} \frac{\partial}{\partial \varphi} \right\}. \quad (2.2.40)$$

In order to consider the stability of the fluid flow around the black hole, we consider perturbations in all the physical variables as given by

$$\rho = \rho_0 + \delta\rho, \quad p = p_0 + \delta p, \quad \varepsilon = \varepsilon_0 + \delta\varepsilon, \quad n = n_0 + \delta n,$$

$$\vartheta(x) = \vartheta_0(x) + \delta\vartheta(x),$$

$$F(i,j) = F_0(i,j) + \delta F(i,j) \quad (2.2.41)$$

wherein subscript '0' refers to the steady state parameters and δ denotes small variations in the corresponding dynamical variables. Introducing these expressions in the general equations (2.2.23) to (2.2.37) and retaining only the linear terms in the perturbations, we get the following linearised set of equations governing the perturbations:

$$\begin{aligned} & \left(\rho_0 + \frac{p_0}{c^2} \right) \left[\frac{\partial}{\partial t} \delta\vartheta(r) + \frac{D}{Dx} \delta\vartheta(r) + \left(\delta \frac{D}{Dx} \right) \vartheta_0(r) \right. \\ & \quad \left. - \frac{2}{r} \left(1 - \frac{2m}{r} \right) \left\{ \vartheta_0(\theta) \delta\vartheta(\theta) + \vartheta_0(\varphi) \delta\vartheta(\varphi) \right\} - \frac{2m}{r^2} \vartheta_0(r) \delta\vartheta(r) \right] \\ & + \left(\delta\rho + \frac{\delta p}{c^2} \right) \left[\frac{D}{Dx} \vartheta_0(r) - \frac{1}{r} \left(1 - \frac{2m}{r} \right) (\vartheta_0(\theta)^2 + \vartheta_0(\varphi)^2) + \frac{m c^2}{r^2} \left(1 - \frac{\vartheta_0(r)^2}{c^2} \right) \right] \end{aligned}$$

$$\begin{aligned}
&= -\left(1 - \frac{v_0^2}{c^2}\right) \left[\left(1 - \frac{2m}{\kappa}\right) \frac{\partial}{\partial \kappa} \delta p + \frac{v_0^{(\kappa)}}{c^2} \frac{\partial}{\partial t} \delta p \right] + \frac{2v_0 \delta v}{c^2} \left(1 - \frac{2m}{\kappa}\right) \frac{\partial p_0}{\partial \kappa} \\
&+ \left(1 - \frac{2m}{\kappa}\right)^{\frac{1}{2}} \left[F_0(\kappa)(t) + \frac{1}{c} \left\{ v_0^{(\theta)} F_0(\kappa)(\theta) - v_0^{(\varphi)} F_0(\varphi)(\kappa) \right\} - \frac{v_0^{(\kappa)}}{c^2} \underline{E}_0 \cdot \underline{v}_0 \right] \\
&\left[\left\{ \delta v_{+\frac{1}{2}} \right\} \varepsilon_0 + \delta \varepsilon \left(1 - \frac{v_0^2}{c^2}\right)^{\frac{1}{2}} \right] + \varepsilon_0 \left(1 - \frac{2m}{\kappa}\right)^{\frac{1}{2}} \left(1 - \frac{v_0^2}{c^2}\right)^{\frac{1}{2}} \left[\delta F(\kappa)(t) \right. \\
&+ \frac{1}{c} \left\{ v_0^{(\theta)} \delta F(\kappa)(\theta) + \delta v^{(\theta)} F_0(\kappa)(\theta) - v_0^{(\varphi)} \delta F(\varphi)(\kappa) - \delta v^{(\varphi)} F_0(\varphi)(\kappa) \right\} \\
&\left. - \frac{v_0^{(\kappa)}}{c^2} \delta(\underline{E} \cdot \underline{v}) - \frac{\delta v^{(\kappa)}}{c^2} \underline{E}_0 \cdot \underline{v}_0 \right], \tag{2.2.42}
\end{aligned}$$

$$\begin{aligned}
&\left(p_0 + \frac{p_0}{c^2}\right) \left[\frac{\partial}{\partial t} \delta v(\theta) + \frac{D}{Dx} \delta v(\theta) + \left(\delta \frac{D}{Dx}\right) v_0^{(\theta)} \right. \\
&\left. - \frac{2}{\kappa} \left(1 - \frac{2m}{\kappa}\right)^{\frac{1}{2}} \cot \theta v_0^{(\varphi)} \delta v^{(\varphi)} + \left(1 - \frac{3m}{\kappa}\right) \frac{1}{\kappa} (v_0^{(\kappa)} \delta v(\theta) + \delta v^{(\kappa)} v_0^{(\theta)}) \right] \\
&+ \left(\delta p + \frac{\delta p}{c^2}\right) \left[\frac{D}{Dx} v_0^{(\theta)} - \frac{v_0^{(\varphi)^2}}{\kappa} \left(1 - \frac{2m}{\kappa}\right)^{\frac{1}{2}} \cot \theta + \left(1 - \frac{3m}{\kappa}\right) \frac{v_0^{(\kappa)} v_0^{(\theta)}}{\kappa} \right] \\
&= -\left(1 - \frac{v_0^2}{c^2}\right) \left[\left(1 - \frac{2m}{\kappa}\right) \frac{1}{\kappa} \frac{\partial}{\partial \theta} \delta p + \frac{v_0^{(\theta)}}{c^2} \frac{\partial}{\partial t} \delta p \right] + \frac{2v_0 \delta v}{\kappa c^2} \left(1 - \frac{2m}{\kappa}\right)^{\frac{1}{2}} \frac{\partial p_0}{\partial \theta} \\
&+ \left(1 - \frac{2m}{\kappa}\right)^{\frac{1}{2}} \left[F_0(\theta)(t) + \frac{1}{c} \left\{ v_0^{(\varphi)} F_0(\theta)(\varphi) - v_0^{(\kappa)} F_0(\kappa)(\theta) \right\} - \frac{v_0^{(\theta)}}{c^2} \underline{E}_0 \cdot \underline{v}_0 \right] \\
&\left[\left\{ \delta v_{+\frac{1}{2}} \right\} \varepsilon_0 + \delta \varepsilon \left(1 - \frac{v_0^2}{c^2}\right)^{\frac{1}{2}} \right] + \varepsilon_0 \left(1 - \frac{2m}{\kappa}\right)^{\frac{1}{2}} \left(1 - \frac{v_0^2}{c^2}\right)^{\frac{1}{2}} \left[\delta F(\theta)(t) \right. \\
&+ \frac{1}{c} \left\{ v_0^{(\varphi)} \delta F(\theta)(\varphi) + \delta v^{(\varphi)} F_0(\theta)(\varphi) - v_0^{(\kappa)} \delta F(\kappa)(\theta) - \delta v^{(\kappa)} F_0(\kappa)(\theta) \right\} \\
&\left. - \frac{v_0^{(\theta)}}{c^2} \delta(\underline{E} \cdot \underline{v}) - \frac{\delta v^{(\theta)}}{c^2} \underline{E}_0 \cdot \underline{v}_0 \right], \tag{2.2.43}
\end{aligned}$$

$$\left(p_0 + \frac{p_0}{c^2}\right) \left[\frac{\partial}{\partial t} \delta \vartheta(\varphi) + \frac{D}{Dx} \delta \vartheta(\varphi) + \left(\delta \frac{D}{Dx}\right) \vartheta_0(\varphi) \right]$$

$$\left(+ \frac{1}{\hbar} \left(1 - \frac{2m}{\hbar}\right)^{\frac{L}{2}} \cot \theta \left(\vartheta_0^{(\vartheta)} \delta \vartheta(\varphi) + \delta \vartheta^{(\vartheta)} \vartheta_0^{(\varphi)} \right) + \left(1 - \frac{3m}{\hbar}\right) \frac{1}{\hbar} \left(\vartheta_0^{(\vartheta)} \delta \vartheta(\varphi) \right. \right.$$

$$\left. + \delta \vartheta^{(\vartheta)} \vartheta_0^{(\varphi)} \right) \left] + \left(\delta p + \frac{\delta p}{c^2} \right) \left[\frac{D}{Dx} \vartheta_0^{(\varphi)} + \frac{\vartheta_0^{(\vartheta)} \vartheta_0^{(\varphi)}}{\hbar} \left(1 - \frac{2m}{\hbar}\right)^{\frac{L}{2}} \cot \theta \right.$$

$$\left. + \left(1 - \frac{3m}{\hbar}\right) \frac{\vartheta_0^{(\vartheta)} \vartheta_0^{(\varphi)}}{\hbar} \right] = - \left(1 - \frac{\vartheta_0^L}{c^2}\right) \left[\frac{1}{\hbar \sin \theta} \left(1 - \frac{2m}{\hbar}\right)^{\frac{L}{2}} \frac{\partial}{\partial \varphi} \delta p \right.$$

$$\left. + \frac{\vartheta_0^{(\varphi)}}{c^2} \frac{\partial}{\partial t} \delta p \right] + \frac{2 \vartheta_0 \delta \vartheta}{\hbar c^2 \sin \theta} \left(1 - \frac{2m}{\hbar}\right)^{\frac{L}{2}} \frac{\partial p_0}{\partial \varphi}$$

$$+ \left(1 - \frac{2m}{\hbar}\right)^{\frac{L}{2}} \left[F_{0(\varphi)(t)} + \frac{1}{c} \left\{ \vartheta_0^{(\vartheta)} F_{0(\varphi)(\vartheta)} - \vartheta_0^{(\vartheta)} F_{0(\vartheta)(\varphi)} \right\} - \frac{\vartheta_0^{(\varphi)}}{c^2} \underline{\underline{E_0 \cdot \underline{v}_0}} \right]$$

$$\left[\left\{ \delta \vartheta_{\pm \frac{L}{2}} \right\} \underline{\underline{E_0}} + \delta \varepsilon \left(1 - \frac{\vartheta_0^L}{c^2}\right)^{\frac{L}{2}} \right] + \varepsilon_0 \left(1 - \frac{2m}{\hbar}\right)^{\frac{L}{2}} \left(1 - \frac{\vartheta_0^L}{c^2}\right)^{\frac{L}{2}} \left[\delta F_{(\varphi)(t)} \right.$$

$$+ \frac{1}{c} \left\{ \vartheta_0^{(\vartheta)} \delta F_{(\varphi)(\vartheta)} + \delta \vartheta^{(\vartheta)} F_{0(\varphi)(\vartheta)} - \vartheta_0^{(\vartheta)} \delta F_{(\vartheta)(\varphi)} - \delta \vartheta^{(\vartheta)} F_{0(\vartheta)(\varphi)} \right\}$$

$$- \frac{\vartheta_0^{(\varphi)}}{c^2} \delta \left(\underline{\underline{E_0 \cdot \underline{v}_0}} \right) - \frac{\delta \vartheta^{(\varphi)}}{c^2} \underline{\underline{E_0 \cdot \underline{v}_0}} \Big],$$

(2.2.44)

$$\left(p_0 + \frac{p_0}{c^2}\right) \left[\frac{\partial}{\partial t} \delta \varepsilon + \frac{D}{Dx} \delta \varepsilon + \left(\delta \frac{D}{Dx}\right) \varepsilon_0 \right] + \left(\delta p + \frac{\delta p}{c^2}\right) \frac{D \varepsilon_0}{Dx}$$

$$= \varepsilon_0 \left[\frac{\partial}{\partial t} \delta p + \frac{D}{Dx} \delta p + \left(\delta \frac{D}{Dx}\right) p_0 \right] + \delta \varepsilon \frac{D p_0}{Dx}, \quad (2.2.45)$$

$$\left(p_0 + \frac{p_0}{c^2}\right) \left[\left(1 - \frac{2m}{\hbar}\right)^{\frac{L}{2}} \left\{ \left(1 - \frac{2m}{\hbar}\right)^{\frac{L}{2}} \frac{1}{\hbar^2} \frac{\partial}{\partial \hbar} (\hbar^2 \delta \vartheta^{(\vartheta)}) \right. \right.$$

$$\left. + \frac{1}{\hbar \sin \theta} \left[\frac{\partial}{\partial \theta} (\sin \theta \delta \vartheta^{(\vartheta)}) + \frac{\partial}{\partial \varphi} \delta \vartheta^{(\varphi)} \right] \right\} \right]$$

$$\begin{aligned}
& + (\delta E + \frac{\delta p}{c^2}) \left[\left(1 - \frac{2m}{r}\right)^{\frac{1}{2}} \left\{ \left(1 - \frac{2m}{r}\right)^{\frac{1}{2}} \frac{1}{r^2} \frac{\partial}{\partial r} (r^2 \vartheta_0'(r)) \right. \right. \\
& \left. \left. + \frac{1}{r \sin \theta} \left[\frac{\partial}{\partial \theta} (\sin \theta \vartheta_0'(\theta)) + \frac{\partial}{\partial \varphi} \vartheta_0'(\varphi) \right] \right\} \right] + \frac{\partial}{\partial t} (\delta E - \frac{\delta p}{c^2}) \\
& + \frac{\partial}{\partial x} (\delta p - \frac{\delta p}{c^2}) + (\delta \frac{\partial}{\partial x}) (p_0 - \frac{p_0}{c^2}) + \frac{1}{c^2} (1 - \frac{\vartheta_0^2}{c^2}) \frac{\partial}{\partial t} \delta p \\
& + (1 - \frac{2m}{r})^{\frac{1}{2}} E_0 \cdot \vartheta_0 \left[\left\{ \delta \vartheta_{+L} \right\}_0 + \delta E (1 - \frac{\vartheta_0^2}{c^2})^{\frac{1}{2}} \right] \\
& + \frac{E_0}{c^2} (1 - \frac{2m}{r})^{\frac{1}{2}} (1 - \frac{\vartheta_0^2}{c^2})^{\frac{1}{2}} \delta (E \cdot \vartheta), \tag{2.2.46}
\end{aligned}$$

$$\begin{aligned}
& \frac{1}{c} \frac{\partial}{\partial t} \delta F_{(\varphi)(0)} + \frac{1}{r^2 \sin \theta} \left[\frac{\partial}{\partial \theta} \left\{ r \sin \theta (1 - \frac{2m}{r})^{\frac{1}{2}} \delta F_{(\varphi)}(t) \right\} \right. \\
& \left. - \frac{\partial}{\partial \varphi} \left\{ r (1 - \frac{2m}{r})^{\frac{1}{2}} \delta F_{(\theta)}(t) \right\} \right] = 0, \tag{2.2.47}
\end{aligned}$$

$$\begin{aligned}
& \frac{1}{c} \frac{\partial}{\partial t} \delta F_{(\varphi)}(r) + \frac{1}{r \sin \theta} (1 - \frac{2m}{r})^{\frac{1}{2}} \left[\frac{\partial}{\partial \varphi} \delta F_{(r)}(t) \right. \\
& \left. - \frac{\partial}{\partial r} \left\{ r \sin \theta (1 - \frac{2m}{r})^{\frac{1}{2}} \delta F_{(\varphi)}(t) \right\} \right] = 0, \tag{2.2.48}
\end{aligned}$$

$$\begin{aligned}
& \frac{1}{c} \frac{\partial}{\partial t} \delta F_{(r)}(\theta) + \frac{1}{r} (1 - \frac{2m}{r})^{\frac{1}{2}} \left[\frac{\partial}{\partial r} \left\{ r (1 - \frac{2m}{r})^{\frac{1}{2}} \delta F_{(\theta)}(t) \right\} \right. \\
& \left. - \frac{\partial}{\partial \theta} \delta F_{(r)}(t) \right] = 0, \tag{2.2.49}
\end{aligned}$$

$$\begin{aligned}
& \frac{\partial}{\partial r} \left[r^2 \sin \theta \delta F_{(\theta)(\varphi)} \right] + \frac{\partial}{\partial \theta} \left[r \sin \theta (1 - \frac{2m}{r})^{\frac{1}{2}} \delta F_{(\varphi)}(r) \right] \\
& + \frac{\partial}{\partial \varphi} \left[r (1 - \frac{2m}{r})^{\frac{1}{2}} \delta F_{(r)}(\theta) \right] = 0, \tag{2.2.50}
\end{aligned}$$

$$- \frac{1}{c} \frac{\partial}{\partial t} \delta F_{(r)}(t) + \frac{1}{r^2 \sin \theta} \left[\frac{\partial}{\partial \theta} \left\{ r \sin \theta (1 - \frac{2m}{r})^{\frac{1}{2}} \delta F_{(r)}(t) \right\} \right.$$

$$\begin{aligned}
-\frac{\partial}{\partial \varphi} \left\{ \kappa \left(1 - \frac{2m}{\kappa}\right)^{\frac{L}{2}} \delta F_{(\varphi)(\kappa)} \right\} &= \frac{4\pi}{c} \left(1 - \frac{2m}{\kappa}\right)^{\frac{L}{2}} \left[\varepsilon_0 \varphi_0^{(2)} \left\{ \delta \varphi_{\frac{L}{2}} \right\} \right. \\
&\quad \left. + \left(1 - \frac{\varphi_0^2}{c^2}\right)^{-\frac{L}{2}} (\varepsilon_0 \delta \varphi^{(2)} + \delta \varepsilon \varphi_0^{(2)}) \right], \quad (2.2.51)
\end{aligned}$$

$$\begin{aligned}
-\frac{1}{c} \frac{\partial}{\partial t} \delta F_{(\theta)(t)} + \frac{1}{\kappa \sin \theta} \left(1 - \frac{2m}{\kappa}\right)^{\frac{L}{2}} \left[\frac{\partial}{\partial \varphi} \delta F_{(\theta)(\varphi)} \right. \\
\left. - \frac{\partial}{\partial \kappa} \left\{ \kappa \sin \theta \left(1 - \frac{2m}{\kappa}\right)^{\frac{L}{2}} \delta F_{(\kappa)(\theta)} \right\} \right] &= \frac{4\pi}{c} \left(1 - \frac{2m}{\kappa}\right)^{\frac{L}{2}} \left[\varepsilon_0 \varphi_0^{(\theta)} \left\{ \delta \varphi_{\frac{L}{2}} \right\} \right. \\
&\quad \left. + \left(1 - \frac{\varphi_0^2}{c^2}\right)^{-\frac{L}{2}} (\varepsilon_0 \delta \varphi^{(\theta)} + \delta \varepsilon \varphi_0^{(\theta)}) \right], \quad (2.2.52)
\end{aligned}$$

$$\begin{aligned}
-\frac{1}{c} \frac{\partial}{\partial t} \delta F_{(\varphi)(t)} + \frac{1}{\kappa} \left(1 - \frac{2m}{\kappa}\right)^{\frac{L}{2}} \left[\frac{\partial}{\partial \kappa} \left\{ \kappa \left(1 - \frac{2m}{\kappa}\right)^{\frac{L}{2}} \delta F_{(\kappa)(\varphi)} \right\} \right. \\
\left. - \frac{\partial}{\partial \theta} \delta F_{(\theta)(\varphi)} \right] &= \frac{4\pi}{c} \left(1 - \frac{2m}{\kappa}\right)^{\frac{L}{2}} \left[\varepsilon_0 \varphi_0^{(\varphi)} \left\{ \delta \varphi_{\frac{L}{2}} \right\} \right. \\
&\quad \left. + \left(1 - \frac{\varphi_0^2}{c^2}\right)^{-\frac{L}{2}} (\varepsilon_0 \delta \varphi^{(\varphi)} + \delta \varepsilon \varphi_0^{(\varphi)}) \right], \quad (2.2.53)
\end{aligned}$$

$$\begin{aligned}
\frac{1}{\kappa^2 \sin \theta} \left[\frac{\partial}{\partial \kappa} \left\{ \kappa^2 \sin \theta \delta F_{(\kappa)(t)} \right\} + \frac{\partial}{\partial \theta} \left\{ \kappa \sin \theta \left(1 - \frac{2m}{\kappa}\right)^{\frac{L}{2}} \delta F_{(\theta)(t)} \right\} \right. \\
\left. + \frac{\partial}{\partial \varphi} \left\{ \kappa \left(1 - \frac{2m}{\kappa}\right)^{\frac{L}{2}} \delta F_{(\varphi)(t)} \right\} \right] &= 4\pi \left(1 - \frac{2m}{\kappa}\right)^{\frac{L}{2}} \left[\varepsilon_0 \left\{ \delta \varphi_{\frac{L}{2}} \right\} \right. \\
&\quad \left. + \left(1 - \frac{\varphi_0^2}{c^2}\right)^{-\frac{L}{2}} \delta \varepsilon \right], \quad (2.2.54)
\end{aligned}$$

$$\begin{aligned}
n_0 \left(e_0 + \frac{p_0}{c^2} \right) \left[\left(1 - \frac{2m}{\kappa}\right)^{\frac{L}{2}} \left\{ \left(1 - \frac{2m}{\kappa}\right)^{\frac{L}{2}} \frac{1}{\kappa^2} \frac{\partial}{\partial \kappa} (\kappa^2 \delta \varphi^{(2)}) \right. \right. \\
\left. \left. + \frac{1}{\kappa \sin \theta} \left[\frac{\partial}{\partial \theta} (\sin \theta \delta \varphi^{(\theta)}) + \frac{\partial}{\partial \varphi} \delta \varphi^{(\varphi)} \right] \right\} \right] \\
+ \left[n_0 \left(\delta e + \frac{\delta p}{c^2} \right) + \delta n \left(e_0 + \frac{p_0}{c^2} \right) \right] \left[\left(1 - \frac{2m}{\kappa}\right)^{\frac{L}{2}} \left\{ \left(1 - \frac{2m}{\kappa}\right)^{\frac{L}{2}} \frac{1}{\kappa^2} \frac{\partial}{\partial \kappa} (\kappa^2 \varphi_0^{(2)}) \right. \right.
\end{aligned}$$

$$\begin{aligned}
& + \frac{1}{2 \sin \theta} \left[\frac{\partial}{\partial \theta} (\sin \theta \vartheta_0^{(\theta)}) + \frac{\partial}{\partial \varphi} \vartheta_0^{(\varphi)} \right] \Big\} \\
& + (e_0 + \frac{b_0}{c^2}) \left[\frac{\partial}{\partial t} \delta n + \frac{D}{Dx} \delta n + (\delta \frac{D}{Dx}) n_0 \right] + (\delta e + \frac{\delta b}{c^2}) \frac{D n_0}{Dx} \\
& - \frac{n_0}{c^2} \left[\frac{\partial}{\partial t} \delta p + \frac{D}{Dx} \delta p + (\delta \frac{D}{Dx}) p_0 \right] - \frac{\delta n}{c^2} \frac{D}{Dx} p_0 \\
& + \frac{n_0}{c^2} (1 - \frac{v_0^2}{c^2}) \frac{\partial}{\partial t} \delta p + \frac{\epsilon_0 n_0}{c^2} (1 - \frac{2m}{\hbar})^{\frac{1}{2}} (1 - \frac{v_0^2}{c^2})^{\frac{1}{2}} \delta(\vec{E} \cdot \vec{\vartheta}) \\
& + (1 - \frac{2m}{\hbar})^{\frac{1}{2}} \vec{E}_0 \cdot \vec{\vartheta}_0 \left[\vec{E}_0 \cdot \left\{ \frac{\delta \vartheta}{\partial t} + \frac{\delta \vartheta}{\partial x} \right\} n_0 + (1 - \frac{v_0^2}{c^2})^{\frac{1}{2}} (\vec{E}_0 \delta n + n_0 \delta E) \right] = 0, \quad (2.2.55)
\end{aligned}$$

$$\begin{aligned}
& \frac{D}{Dt} (n_0^{-r} \delta p - r p_0 n_0^{-r-1} \delta n) + \frac{D}{Dx} (n_0^{-r} \delta p - r p_0 n_0^{-r-1} \delta n) \\
& + (\delta \frac{D}{Dx}) (p_0 n_0^{-r}) = 0 \quad (2.2.56)
\end{aligned}$$

where we have used the notations

$$v_0^2 = (v_0^{(x)})^2 + (v_0^{(\theta)})^2 + (v_0^{(\varphi)})^2,$$

$$\vartheta_0 \delta \vartheta = \vartheta_0^{(x)} \delta \vartheta^{(x)} + \vartheta_0^{(\theta)} \delta \vartheta^{(\theta)} + \vartheta_0^{(\varphi)} \delta \vartheta^{(\varphi)},$$

$$\vec{E}_0 \cdot \vec{\vartheta}_0 = F_{0(x)}(t) \vartheta_0^{(x)} + F_{0(\theta)}(t) \vartheta_0^{(\theta)} + F_{0(\varphi)}(t) \vartheta_0^{(\varphi)}$$

$$\begin{aligned}
\delta(\vec{E} \cdot \vec{\vartheta}) &= F_{0(x)}(t) \delta \vartheta^{(x)} + \delta F_{(x)}(t) \vartheta_0^{(x)} + F_{0(\theta)}(t) \delta \vartheta^{(\theta)} + \delta F_{(\theta)}(t) \vartheta_0^{(\theta)} \\
&+ F_{0(\varphi)}(t) \delta \vartheta^{(\varphi)} + \delta F_{(\varphi)}(t) \vartheta_0^{(\varphi)},
\end{aligned}$$

$$\frac{D}{Dx} = (1 - \frac{2m}{\hbar})^{\frac{1}{2}} \left\{ (1 - \frac{2m}{\hbar})^{\frac{1}{2}} \vartheta_0^{(x)} \frac{\partial}{\partial x} + \frac{\vartheta_0^{(\theta)}}{\hbar} \frac{\partial}{\partial \theta} + \frac{\vartheta_0^{(\varphi)}}{\hbar \sin \theta} \frac{\partial}{\partial \varphi} \right\},$$

$$(\delta \frac{D}{Dx}) = (1 - \frac{2m}{\hbar})^{\frac{1}{2}} \left\{ (1 - \frac{2m}{\hbar})^{\frac{1}{2}} \delta \vartheta^{(x)} \frac{\partial}{\partial x} + \frac{\delta \vartheta^{(\theta)}}{\hbar} \frac{\partial}{\partial \theta} + \frac{\delta \vartheta^{(\varphi)}}{\hbar \sin \theta} \frac{\partial}{\partial \varphi} \right\},$$

$$\left\{ \delta \vartheta_{\pm \frac{1}{2}} \right\} = \left\{ \left(1 - \frac{(\vartheta_0^2 + 2\vartheta_0 \delta \vartheta)}{c^2} \right)^{\pm \frac{1}{2}} - \left(1 - \frac{\vartheta_0^2}{c^2} \right)^{\pm \frac{1}{2}} \right\}$$

$$\left\{ \delta \vartheta_{\pm \frac{1}{2}} \right\} = \left\{ \left(1 - \frac{(\vartheta_0^2 + 2\vartheta_0 \delta \vartheta)}{c^2} \right)^{-\frac{1}{2}} - \left(1 - \frac{\vartheta_0^2}{c^2} \right)^{-\frac{1}{2}} \right\} \quad (2.2.57)$$

To discuss the stability as governed by the above set of equations, we use the normal mode analysis and the variational principle technique as developed by Chandrasekhar (1964) and Chandrasekhar and Friedman (I, II, 1972).

The variational principle:

It is useful to distinguish between Eulerian changes (denoted by δ) and Lagrangian changes (denoted by Δ) of dynamical variables under perturbation. Eulerian changes are the changes in dynamical variables at a fixed point in space while the Lagrangian changes describe changes in dynamical variables as we move along with the fluid element. These two are related by

$$\Delta = \delta + \xi^\alpha \frac{\partial}{\partial x^\alpha} \quad (2.2.58)$$

where $\delta \vartheta^\alpha = \xi^\alpha_{,0}$. ξ^α is called the Lagrangian displacement.

In case of radial oscillations of thin disk we have only ξ^r , the radial component of the Lagrangian displacement, non-zero. We consider in normal mode

$$\xi^r(r, t) = \xi^r(r) e^{i\sigma t} \quad (2.2.59)$$

and construct an eigen value equation for the amplitude $\xi^r(r)$ of a Hermitian operator with σ^2 as its eigen value (Arfken, 1970)

$$\sigma^2 W(r) \xi = - \frac{d}{dr} \left(P \frac{d\xi}{dr} \right) + Q(r) \xi, \quad (2.2.60)$$

called "pulsation equation". Here P , Q and W are functions of r . W is called the weight function. ξ is subjected to boundary conditions. Using the boundary conditions

$$P \xi \frac{d\xi}{dr} \Big|_{r=a} = P \xi \frac{d\xi}{dr} \Big|_{r=b} = 0 \quad (2.2.61)$$

the operator on the right hand side of (2.2.60) is Hermitian. (Actually condition (2.2.61) is slightly more restrictive than is required to make the operator Hermitian, but nevertheless we find this condition more suitable for our purpose). As such the usual properties of Hermitian operator follow namely the eigen functions form a complete set with the eigen values being all real and orthogonal.

A variational base for determining σ^2 is formed by multiplying (2.2.60) by ξ and integrating over the range (a, b) of r . We thus obtain

$$\sigma^2 \int_a^b W \xi^2 dr = \int_a^b P \left(\frac{d\xi}{dr} \right)^2 dr + \int_a^b Q \xi^2 dr. \quad (2.2.62)$$

As the eigen functions form a complete set, any given function which satisfies the same boundary conditions as the true eigen function ξ but otherwise completely arbitrary ("trial function"), can be expanded in terms of the eigen function. It can be shown that if we calculate σ^2 as given by (2.2.62), using a trial function for ξ we get the upper bound of the lowest eigen value (refer, for example, Schiff, 1955). Because eigen values σ^2 are all real, a sufficient condition for the onset of

dynamical instability is that σ^2 , evaluated by the manner indicated above, is zero.

The situation is more complicated in the case of axisymmetric thick disks. Dynamical variables are functions of η and θ . In an axisymmetric perturbation we have ξ^η and ξ^θ both non-zero. We then distinguish two classes of the equations governing the perturbation: initial value equations and dynamical equations. Initial value equations are those, that are first order in time derivatives. Dynamical equations are those that are second order in time derivatives. Initial value equations can be directly integrated with respect to time when they are expressed in terms of a Lagrangian displacement. In contrast, dynamical equations lead to an eigen value problem that determines the normal modes of oscillation of the system. Using the relation of the type (2.2.5b) both for ξ^η and ξ^θ in the dynamical equations one obtains the pulsation equations of the form

$$\sigma^2 P \xi^\eta = L(\eta, \theta, \frac{\partial}{\partial \eta}, \frac{\partial}{\partial \theta}, \delta y, \xi^\eta, \xi^\theta), \quad (2.2.63)$$

$$\sigma^2 P \xi^\theta = M(\eta, \theta, \frac{\partial}{\partial \eta}, \frac{\partial}{\partial \theta}, \delta y, \xi^\eta, \xi^\theta) \quad (2.2.64)$$

where P is some function of η and θ and L and M are operators involving functions of η and θ , derivatives of ξ^η, ξ^θ and other dynamical variables y . Using initial value equations, functions involving δy can be expressed in terms of ξ^η and ξ^θ . (2.2.63) and (2.2.64) are the eigen

value equations which should be solved consistently with the initial value equations with proper boundary conditions chosen according to the physical requirements. If p denotes the pressure, the boundary condition can be chosen such that Δp vanishes at the boundary of the disk.

To evaluate σ^2 one takes trial displacements $\bar{\xi}^r$ and $\bar{\xi}^\theta$, evaluate variations δy by putting these trial displacements in initial value equations, multiply (2.2.63) by $\bar{\xi}^r$ and (2.2.64) by $\bar{\xi}^\theta$, add them and integrate over the range of r and θ . One then gets

$$\begin{aligned} \sigma^2 \iint P (\bar{\xi}^r \xi^r + \bar{\xi}^\theta \xi^\theta) r^2 \sin \theta dr d\theta \\ = \iint (\bar{\xi}^r L + \bar{\xi}^\theta M) r^2 \sin \theta dr d\theta. \end{aligned} \quad (2.2.65)$$

One finds that the left hand side is manifestly symmetric in the barred and unbarred quantities. One then manipulates the right hand side of the above equation and brings it into a similar manifestly symmetric form. To achieve this one has to perform numerous integrations by parts and substitutions from the initial value equations. The final result is an equation of the form

$$\begin{aligned} \sigma^2 \iint P (\bar{\xi}^r \xi^r + \bar{\xi}^\theta \xi^\theta) r^2 \sin \theta dr d\theta \\ = \iint N_1 r^2 \sin \theta dr d\theta \end{aligned} \quad (2.2.66)$$

where N_1 is symmetric in barred and unbarred variables. Identifying the barred and unbarred variables in (2.6.66) the resultant equation

$$\begin{aligned} \sigma^2 \iint P((\xi^r)^2 + (\xi^\theta)^2) r^2 \sin\theta dr d\theta \\ = \iint N_2 r^2 \sin\theta dr d\theta \end{aligned} \quad (2.2.67)$$

can then be shown to imply a variational principle in the following sense: suppose one evaluates σ^2 from the equation (2.2.67) successively with the aid of two trial displacements ξ^α and $\xi^\alpha + \delta\xi^\alpha$ ($\alpha = r, \theta$) and the associated variations δy and $\delta y + \delta^2 y$, one finds an increment $\delta\sigma^2$ as a result of variations in trial functions. Writing the expression for $\delta\sigma^2$ and demanding it to be zero, can be shown to be equivalent to solving the original dynamical equations (2.2.63) and (2.2.64). In the following discussion we shall show this in our calculations for stability of thick fluid disk where the form of N_1 is explicitly known.

In particular we are interested in the neutral mode of deformation. A sufficient condition for neutral mode of deformation is that if for some ξ^α and associated variations consistent with the initial value equations the quantity on the right hand side of (2.2.67) and its first variation vanish simultaneously.

In this chapter we have developed a general set of equation of motion of a particle in Kerr background geometry

and equations of motion and stability of a fluid disk with possible charges in Schwarzschild geometry. We have also outlined the methodology for the study of dynamics of particles and dynamics and stability of disks. In the following chapters we use these formalisms to study few cases of particle as well as disk dynamics.

CHAPTER III

CHARGED PARTICLE DYNAMICS IN AN ELECTROMAGNETIC FIELD ON KERR GEOMETRY

It was mentioned in Chapter I that the charged particles in an electromagnetic field on Kerr background geometry execute Larmor motion (gyration) in their bound orbits only when they are completely outside the ergosphere. This is due to inertial frame dragging which precludes completely any retrograde motion within the ergosphere. But it is well known that this frame dragging arises mainly because of the Boyer-Lindquist coordinates and that if one goes over to a locally non-rotating frame (LNRF) as defined by Bardeen (1970) and Bardeen et al (1972) there is no frame dragging. It is essential to see whether as a result of this, the non-gyration of the charged particle is also a coordinate effect which does not exist in LNRF. Accordingly we proceed to study the orbits as viewed from LNRF for the same set of parameters as in the earlier case (Prasanna and Chakraborty, 1980).

Further as we could infer about the possible inner edge of the disks from the studies of orbital dynamics confined to the equatorial plane the study of charged particle motion off the equatorial plane may possibly reveal some indications regarding the thickness of stable thick disks. It is therefore worthwhile to take up this problem

also and study the trapping of particles due to magnetic field in meridional plane (Chakraborty and Prasanna I, 1981).

1. ORBITS OF THE PARTICLES AS VIEWED FROM LOCALLY NON-ROTATING FRAMES:

The general set of equations describing the motion of the particle when viewed from LNRF can be obtained by transforming the dynamical variables from coordinate basis to LNRF. The transformation matrix can be obtained from (2.1.34), after writing the metric of the space-time in canonical form and comparing it with (2.1.30). The metric for Kerr geometry (equation 2.1.6) in canonical form is given by (Breuer 1975)

$$ds^2 = -\frac{\Sigma \Delta}{A} c^2 dt^2 + \frac{\Sigma}{\Delta} dr^2 + \Sigma d\theta^2 + \frac{A \sin^2 \theta}{\Sigma} \left(d\phi - \frac{2mar}{A} c dt \right)^2 \quad (3.1.1)$$

Comparison of (3.1.1) with (2.1.20) yields

$$e^{2\nu} = \frac{\Sigma \Delta}{A}, \quad e^{2\mu_1} = \frac{\Sigma}{\Delta}, \quad e^{2\mu_2} = \Sigma, \\ e^{2\psi} = \frac{A \sin^2 \theta}{\Sigma}, \quad \omega = \frac{2mar}{A} \quad (3.1.2)$$

and therefore the transformation matrix $\|e^{(i)}_j\|$ as given by (2.1.34) appropriate to Kerr geometry becomes

$$e^{(i)}_j = \begin{bmatrix} (\Sigma \Delta / A)^{\frac{1}{2}} & 0 & 0 & 0 \\ 0 & (\Sigma / \Delta)^{\frac{1}{2}} & 0 & 0 \\ 0 & 0 & \Sigma^{\frac{1}{2}} & 0 \\ -\frac{2mar}{(\Sigma A)^{\frac{1}{2}}} \sin \theta & 0 & 0 & \left(\frac{A}{\Sigma} \right)^{\frac{1}{2}} \sin \theta \end{bmatrix} \quad (3.1.3)$$

The laws of transformations for four velocity u^i , field components F^i_j and Γ^i_{jk} are

$$u^{(i)} = e^{(i)}_j u^j, \quad (3.1.4)$$

$$F^{(i)}_j = e^{(i)}_k e^l_j F^k_l, \quad (3.1.5)$$

$$\Gamma^{(c)}_{(a)(b)} = \Gamma^i_{jk} e^{(a)}_i e^j_{(a)} e^k_{(b)} + e^{(c)}_{(a),d} e^{(c)}_i e^d_{(b)} \quad (3.1.6)$$

wherein $e^i_{(j)}$ is the inverse matrix of $e^{(i)}_j$. Using these transformations we can transform equations of motion (2.1.17) to (2.1.20) in LNRF. We shall limit ourselves to the equatorial orbits only and therefore we use the initial conditions $u^\theta = 0$, $\theta = \pi/2$. We then have

$$\begin{aligned} \frac{du^{(r)}}{d\sigma} = & \frac{1}{B} \left\{ \Delta^{\frac{1}{2}} \left(1 - \frac{\alpha^2}{R^2} \right) (u^{(\varphi)})^2 + \frac{2\alpha}{R} \left(3 + \frac{\alpha^2}{R^2} \right) u^{(\varphi)} u^{(t)} \right. \\ & \left. - \frac{1}{R^3} \Delta^{\frac{1}{2}} \left[(R^2 + \alpha^2)^2 - 4\alpha^2 R \right] (u^{(t)})^2 \right\} \\ & + \frac{1}{RB^{\frac{1}{2}}} \left\{ \Delta^{\frac{1}{2}} \bar{A}_{\varphi,R} u^{(\varphi)} + \frac{2\alpha}{R} \bar{A}_{\varphi,R} u^{(t)} + B u^{(t)} A_{t,R} \right\} \quad (3.1.7) \end{aligned}$$

$$u^{(\varphi)} = (L - \bar{A}_\varphi) / B^{\frac{1}{2}}, \quad (3.1.8)$$

$$u^{(t)} = \frac{1}{(B\Delta)^{\frac{1}{2}}} \left[B(E + A_t) - \frac{2\alpha}{R} (L - \bar{A}_\varphi) \right], \quad (3.1.9)$$

wherein the field component A_i are given by (2.1.22) to (2.1.27) by putting $\theta = \pi/2$ and

$$B = R^2 + \alpha^2 + 2\alpha^2/R$$

We find that the above equations of motion and of fields contain coordinate R but are independent of

coordinates φ and τ . To examine the nature of the orbit of the particle when viewed from LNRF, we determine the local velocities $u^{(\tau)}$ and $u^{(\varphi)}$ at each 'instant' σ as might be measured by an observer stationary at the location of the particle at that instant. From the observations of such local observers, each measuring the local velocity of the particle as it flies past them, we can work out the nature of the orbit. In case the particle gyrates, then with increasing σ we have the regions where $u^{(\varphi)}$ changes sign whereas $u^{(\tau)}$ keeps the same sign. With a further increase in σ we have a region where $u^{(\varphi)}$ continues to maintain the same sign as it had at the end of the first region but $u^{(\tau)}$ changes sign. This pattern of sign change is repeated continuously in $u^{(\tau)}$ and $u^{(\varphi)}$ alternatively in successive regions obtained with increasing σ .

If we now use a coordinate system $(R, \bar{\varphi}, \bar{\tau})$ such that

$$\frac{dR}{d\sigma} = u^{(\tau)}, \quad \frac{d\bar{\varphi}}{d\sigma} = u^{(\varphi)}, \quad \frac{d\bar{\tau}}{d\sigma} = u^{(t)} \quad (3.1.10)$$

then, since

$$u^{(\tau)} = \frac{R}{\Delta^{\frac{1}{2}}} u^{\tau} \quad (3.1.11)$$

and further since $R/\Delta^{\frac{1}{2}}$ is positive, the coordinates $(R, \bar{\varphi})$ will carry the signature of the patterns of signs of $u^{(\tau)}$ and

$u^{(\varphi)}$; an increase (decrease) in R or $\bar{\varphi}$ with σ will imply positive (Negative) $u^{(\tau)}$ or $u^{(\varphi)}$ (Table 3.1). At this stage we note that the introduction of coordinates $\bar{\varphi}$ and $\bar{\tau}$ is possible because the equations governing the motion and the

fields are independent of φ and τ . Accordingly the equations of motion are

$$\begin{aligned} \frac{d^2 R}{d\sigma^2} = & \frac{\Delta^{\frac{L}{2}}}{R} \left\{ \frac{1}{B} \left[\Delta^{\frac{L}{2}} \left(1 - \frac{\alpha^2}{R^3} \right) \left(\frac{d\bar{\varphi}}{d\sigma} \right)^2 + \frac{2\alpha}{R} \left(3 + \frac{\alpha^2}{R^3} \right) \frac{d\bar{\varphi}}{d\sigma} \frac{d\bar{\tau}}{d\sigma} \right. \right. \\ & \left. \left. - \frac{1}{R^3 \Delta^{\frac{L}{2}}} \left\{ (R^2 + \alpha^2)^2 - 4\alpha^2 R \right\} \left(\frac{d\bar{\tau}}{d\sigma} \right)^2 \right] + \frac{1}{R B^{\frac{L}{2}}} \left[\Delta^{\frac{L}{2}} \bar{A}_{\varphi, R} \frac{d\bar{\varphi}}{d\sigma} \right. \right. \\ & \left. \left. + \frac{2\alpha}{R} \bar{A}_{\varphi, R} \frac{d\bar{\tau}}{d\sigma} + B A_{\tau, R} \frac{d\bar{\tau}}{d\sigma} \right] - \frac{1}{\Delta^{\frac{L}{2}}} \left[1 - \frac{R(R-U)}{\Delta} \right] \left(\frac{dR}{d\sigma} \right)^2 \right\}, \quad (3.1.12) \end{aligned}$$

$$\frac{d\bar{\varphi}}{d\sigma} = (L - \bar{A}_{\varphi}) / B^{\frac{L}{2}}, \quad (3.1.13)$$

$$\frac{d\bar{\tau}}{d\sigma} = \frac{1}{(B\Delta)^{\frac{L}{2}}} \left[B(E + A_{\tau}) - \frac{2\alpha}{R} (L - \bar{A}_{\varphi}) \right]. \quad (3.1.14)$$

Using the normalisation relationship

$$n_{(i)(j)} u^{(i)} u^{(j)} = -1 \quad (3.1.15)$$

and the first integrals (3.1.13) and (3.1.14) we obtain

$$\begin{aligned} (u^{(2)})^2 = & \frac{1}{\Delta} \left\{ (R^2 + \alpha^2 + \frac{2\alpha^2}{R})(E + A_{\tau})^2 - (1 - \frac{2}{R})(L - \bar{A}_{\varphi})^2 \right. \\ & \left. - \frac{4\alpha}{R}(E + A_{\tau})(L - \bar{A}_{\varphi}) - \Delta \right\} \quad (3.1.16) \end{aligned}$$

wherein we have used the condition $u^{(0)} = 0$. The effective potential is obtained from above by putting $u^{(2)} = 0$

$$V_{\text{eff}} = E_{\text{min}} = -A_{\tau} + K/R_1$$

$$K = 2\alpha(L - \bar{A}_{\varphi}) + \Delta^{\frac{L}{2}} \left\{ R^2 (L - \bar{A}_{\varphi})^2 + R R_1 \right\}^{\frac{L}{2}}$$

$$R_1 = R^3 + \alpha^2 R + 2\alpha^2 \quad (3.1.17)$$

The effective potential is the same as obtained by Prasanna and Vishveshwara (1973) while studying the particle orbits in coordinate

basis. This is simply because of the relationship $u^{(r)} = \Delta^{\frac{1}{2}} u^r / R$. The turning points, therefore, remains unchanged.

We integrate the set of equations (3.1.12) to (3.1.14) numerically with appropriate A_z and \bar{A}_φ for the two cases of dipolar and uniform fields and use the same set of parameters α, λ, L and E as was used by Prasanna and Vishveshwara. To fix up initial conditions (denoted by subscripts '0') we choose $\varphi_0 = 0$ and R_0 the point which is well within the potential well of the corresponding V_{eff} . For such φ_0 and R_0 initial $u_0^{(r)}$ is calculated from (3.1.16).

Table (3.1) gives the values of $u^{(r)}$, $u^{(\varphi)}$, R and $\bar{\varphi}$ as σ increases for dipolar field which clearly indicates how the signature of the signs of $u^{(r)}$ and $u^{(\varphi)}$ is carried over to the coordinate system $(R, \bar{\varphi})$ and establishes, the gyrating nature of the orbit. The orbits themselves are shown in figures (3.1) to (3.6). As may be seen from these plots, the gyration exists in all cases irrespective of the fact whether the particle is completely outside (figures 3.1 and 3.4) or completely inside (figures 3.2 and 3.5) or moves in and out of the ergosphere (figures 3.3 and 3.6). We now analyse the consequence of the condition that $d\bar{\varphi}/d\sigma$ has to go through zero for some $R=R_g$, a condition which is necessary for the particle to gyrate. The above condition implies that $L = (\bar{A}_\varphi)_{R_g}$ and therefore

$$\left(\frac{dR}{d\sigma} \right)_{R_g} = \left[\frac{\Delta^{\frac{1}{2}}}{R} \left\{ -1 + \frac{B}{\Delta} (E + A_z)^2 \right\}^{\frac{1}{2}} \right]_{R_g} \quad (3.1.18)$$

which can be made real irrespective of what R_g is. We note

that the same condition gave a constraint that $R_g > 2$, for the orbits studied in coordinate basis (Prasanna and Vishveshwara, 1978).

Results and discussions.

We have analysed the orbits of charged particles in electromagnetic field on the equatorial plane of Kerr black hole as viewed from LNRF. The orbits are then found to be gyrating irrespective of whether they are in or out of the ergosphere. But for a distant stationary observer (following the global time like Killing vector) the charged particle does not gyrate when it is inside the ergosphere because of the frame dragging effect which in turn is due to the angular momentum of the black hole. This implies that in LNRF the effect of frame dragging has been cancelled out completely at least in regard to the motion of charged particle around Kerr black hole. The analysis as seen from LNRF may be considered similar to the case of analysis of a co-moving observer on the surface of a collapsing sphere who would cross the event horizon in finite time where as for the distant observer this would happen only asymptotically as $t \rightarrow \infty$.

2. MOTION OF THE CHARGED PARTICLES OFF THE EQUATORIAL PLANE:

So far we have confined ourselves to the motion of the particles on the equatorial plane only. If the initial velocity in θ -direction is not zero or if the initial position is not at $\theta = \pi/2$ or both, then the resultant motion is in three dimensional space. Motion off the equatorial plane in the case of the charged particle in magnetic field on Schwarzschild back ground geometry has been studied by Prasanna and Varma (1977). In the θ - ϕ plane

the particle follows the magnetic field lines and as well as gyrates about the field lines. As the field was a dipolar field, particle finds stronger magnetic field as it moves further away from the equatorial plane. For suitable choice of initial condition and field strength it gets reflected from the mirror points. The location of the mirror point depends upon the initial velocity parallel to the field lines, if all the other parameters are kept constant.

To study the motion of the charged particles off the equatorial plane of a Kerr black hole we (Chakraborty and Prasanna I, 1981) first study the structure of the electromagnetic field in a more detailed way. Starting from the expressions (2.1.22) to (2.1.27) we first calculate the electromagnetic field tensor F_{ij} using (2.1.16) and finally using the transformation law (3.1.5) we obtained the components of the electric field $(E_r, E_\theta, E_\varphi)$ and of the magnetic field $(B_r, B_\theta, B_\varphi)$ in LNRF as given by

$$\bar{E}_r = \frac{A^{\frac{1}{2}}}{\Sigma} A_{\tau, R} + \frac{2\alpha R}{\Sigma A^{\frac{1}{2}}} \bar{A}_{\varphi, R}$$

$$\bar{E}_\theta = \left(\frac{A}{\Delta}\right)^{\frac{1}{2}} \frac{1}{\Sigma} A_{\tau, \theta} + \frac{2\alpha R}{(\Delta A)^{\frac{1}{2}} \Sigma} \bar{A}_{\varphi, \theta}$$

$$\bar{E}_\varphi = 0$$

$$\bar{B}_r = \frac{1}{A^{\frac{1}{2}} \sin \theta} \bar{A}_{\varphi, \theta}$$

$$\bar{B}_\theta = -\left(\frac{\Delta}{A}\right)^{\frac{1}{2}} \frac{\bar{A}_{\varphi, R}}{\sin \theta}$$

$$\bar{B}_\varphi = 0$$

(3.2.1).

where $\bar{E}_\alpha = m E_\alpha$ and $\bar{B}_\alpha = m B_\alpha$.

We plot the lines of force defined by

$$ds_\alpha = K B_\alpha, \quad (3.2.2)$$

for the magnetic field and

$$ds_\alpha = K E_\alpha \quad (3.2.3)$$

for the electric field, K being a constant. For selected values of α and λ , the plots of lines of force are presented in figures (3.7) for the case of the dipolar field and in (3.11) for the case of the uniform field.

We also calculate the components of 3-velocity parallel and perpendicular to the magnetic field lines. The components of four velocity in LNRF are

$$\begin{aligned} u^{(r)} &= (\Sigma/\Delta)^{\frac{1}{2}} \frac{dr}{d\sigma}, \\ u^{(\theta)} &= \Sigma^{\frac{1}{2}} \frac{d\theta}{d\sigma}, \\ u^{(\varphi)} &= \left(\frac{A}{\Sigma}\right)^{\frac{1}{2}} \sin\theta \frac{d\theta}{d\sigma} - \frac{2\alpha R}{(A\Sigma)^{\frac{1}{2}}} \sin\theta \frac{d\tau}{d\sigma}, \\ u^{(t)} &= \left(\frac{\Sigma\Delta}{A}\right)^{\frac{1}{2}} \frac{d\tau}{d\sigma} \end{aligned} \quad (3.2.4)$$

and the components of 3-velocity v^α are then (in LNRF)

$$v^{(r)} = \frac{c u^{(r)}}{u^{(t)}}, \quad v^{(\theta)} = \frac{c u^{(\theta)}}{u^{(t)}}, \quad v^{(\varphi)} = \frac{c u^{(\varphi)}}{u^{(t)}} \quad (3.2.5)$$

Defining the angle z between \bar{B}_r and the lines of force by

$$\tan z = \bar{B}_\theta / \bar{B}_r$$

we find the parallel and perpendicular components $v_{||}$ and v_\perp

$$U_{||} = U^{(r)} \cos z + U^{(\theta)} \sin z, \quad (3.2.6)$$

$$U_{\perp} = \left\{ (U^{(\phi)})^2 + (U^{(r)} \sin z - U^{(\phi)} \cos z)^2 \right\}^{\frac{1}{2}}. \quad (3.2.7)$$

Actual orbits of the particles are obtained by integrating numerically the equations of motion (2.1.17) to (2.1.20) along with the field components (2.1.22) to (2.1.27). Along with its trajectory we also calculate $U_{||}$ and U_{\perp} . To fix up the initial conditions we note that when $\theta = \pi/2$ and $U^{\theta} = 0$

$$(U^{(r)})^2 \equiv (U^{(r)})^2_{0, \pi/2} = \frac{\Delta}{R^2} (U^{(r)})^2 \quad (3.2.8)$$

wherein $U^{(r)}$ is the same as obtained in (3.1.16). In (3.2.8) putting $U^{\theta} = 0$ we can obtain effective potential V_{eff} for the motion of particle studied in coordinate basis and confined to $\theta = \pi/2$ plane. For a selected value E of energy V_{eff} curve gives the turning points R_1 and R_2 such that for any R satisfying $R_1 < R < R_2$, $U^{(r)}$ as calculated from the equation (3.2.8) is real. Now if we take $\theta = \pi/2$ but $U^{\theta} \neq 0$, the normalisation condition for the four velocity yields

$$(U^{(r)})^2 = (U^{(r)})^2_{0, \pi/2} - \Delta (U^{\theta})^2 \quad (3.2.9)$$

Now since Δ is positive for any R outside the event horizon, $U^{(r)}$ as given by (3.2.9) is real, for the same E as above and for R satisfying $R_1 < R < R_2$, when

$$0 < \Delta (U^{\theta})^2 < (U^{(r)})^2_{0, \pi/2} \quad (3.2.10)$$

This sets the upper bound for U^{θ} . We fix up the initial positions $\phi_0 = 0$, $\theta_0 = \pi/2$, $R_1 < R_0 < R_2$ and calculate the

maximum allowed value of u^θ at the initial position, as given by the inequality (3.2.10). Using any value of u^θ between the maximum and zero as its initial value we calculate initial u^r by using (3.2.9). Among the number of cases that we studied, we present a few cases through tables and plots. Tables (3.2) to (3.5) show the values of $R, \theta, \phi, \psi_{||}$ and B , where B is the net magnetic field, along the trajectory of the particle and figures (3.3) to (3.10) and (3.12) to (3.14) show the plots of the orbits on the $(r - \theta)$ plane, for different choices of α, λ, E, L and the initial $\psi_{||} (= \psi_{||0})$ for dipole as well as for uniform magnetic field. It is seen from these tables and the plots that the particles follow more or less the magnetic field lines and are trapped between mirror points if $\psi_{||0}$ is sufficiently low. In case $\psi_{||0}$ is high, they continue to move towards the event horizon for the case of dipole field whereas they escape to infinity for the case of uniform field without showing any signs of reflection. The sign of $\psi_{||}$ changes on each reflection.

Results and discussions.

We have presented above a study of charged particle orbits off the equatorial plane of a Kerr black hole in uniform and dipole magnetic field. The effect of curvature of the underlying space time on the field lines are very apparent in the case of uniform field. The magnetic field lines which would have been straight, parallel and equally spaced in a flat space time, are now curved in the vicinity of the Kerr black hole,

showing very clearly the effect of geometry on the field structure. Depending upon the field strength and the initial conditions, the particles get trapped if $v_{||0}$ is low or else they continue to follow the field lines without any reflection, both for dipole as well as uniform magnetic field.

Trapping of the particles in dipolar field is not unusual in the sense that even in flat space time, the charged particles are trapped in a dipole field. The bending of field lines, in case of an uniform field on Kerr geometry is purely a general relativistic effect. The trapping of the particles in such situations are therefore more interesting. We found a number of cases of trapped orbits in meridional plane in case of an uniform field, some of which are presented through the respective tables and figures. The initial value of the parallel velocity is very small compared to what we have in the case of a dipolar field, in order to have trapped orbits. This gives rise to the possibility of having thick disk around black holes immersed in the galactic magnetic field of the order of $10^{-5} G$. The coupling parameter λ , for protons, appropriate to such case is

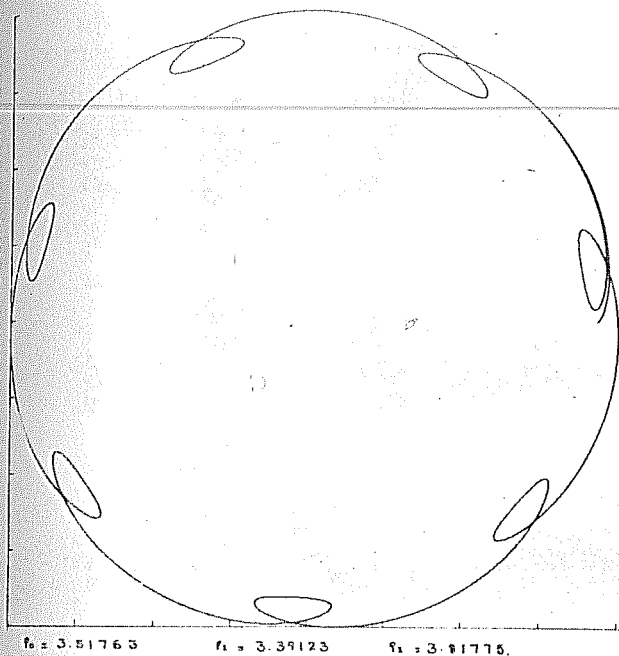
$$\lambda \approx 5.0 \times 10^{-7} M/M_0$$

For a supermassive black hole of mass $\sim 10^8 M_0$, $\lambda \approx 50$. The cases presented through the tables and the plots for $\lambda = 50$ corresponds to such a physically realistic situation.

Captions for Figures and Tables.

- Figures (3.1)- : Orbits of the particle as seen by LNRF observers
(3.3) : in the case of dipole field.
- Figures (3.4)- : Same as above in the case of uniform
(3.6) : field.
- Figure (3.7) : Lines of force for magnetic and electric
field for dipole field for $\alpha = .99$, $\lambda = 300$
- Figures (3.8)- : Orbits of the particle off the equatorial
(3.10) : plane following the magnetic field lines for
dipole field for $\alpha = .99$, $\lambda = 300$, $E = 5$, $L = 100$, $R_c = 4.559$
and different ψ_{110}
- Figure (3.11): Same as figure (3.7) for uniform field.
- Figures (3.12)- : Same as figures (3.8)- (3.10) for the case
(3.14) : of uniform field.
- Table (3.1): Velocities $u^{(2)}$ and $u^{(\phi)}$ showing its signature
on coordinates $(R, \bar{\phi})$.
- Tables (3.2)- : Orbits of the particle in $(R - \theta)$ plane
(3.3) : giving the values of $R, \theta, \phi, \psi_{11}$ and B
for dipole field.
- Tables (3.4)- : Same as tables (3.2)-(3.3) for the case of
(3.5) : uniform field.

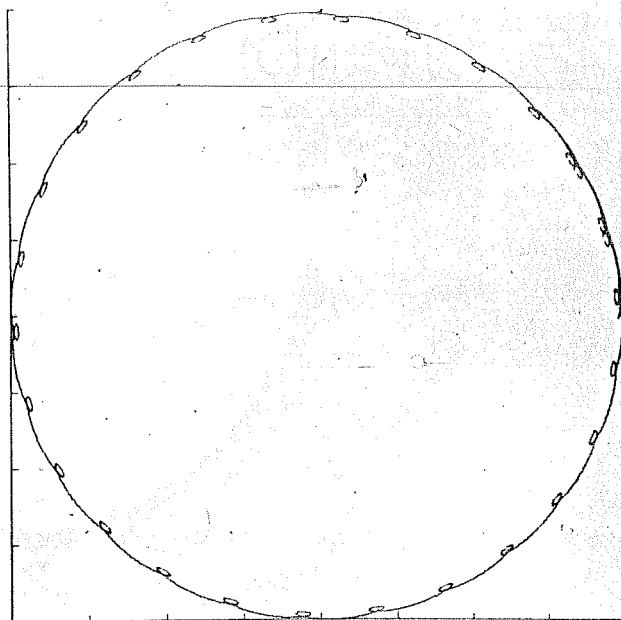
$\alpha = 0.99$ $\lambda = 1000$ $L = 500$ $E = 30$



$f_0 = 3.51763$ $f_1 = 3.39123$ $f_2 = 3.91775$

Fig. 3.1

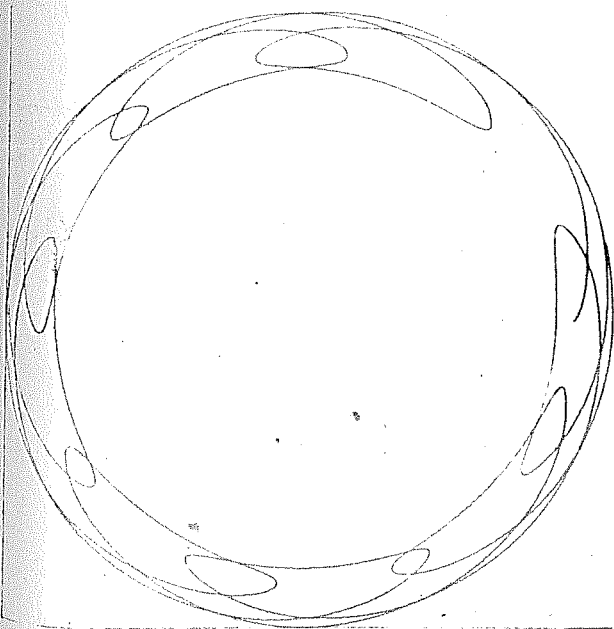
$\alpha = 0.99$ $\lambda = 50$ $L = 500$ $E = 152$



$f_0 = 1.36570$ $f_1 = 1.35715$ $f_2 = 1.39003$

Fig. 3.2

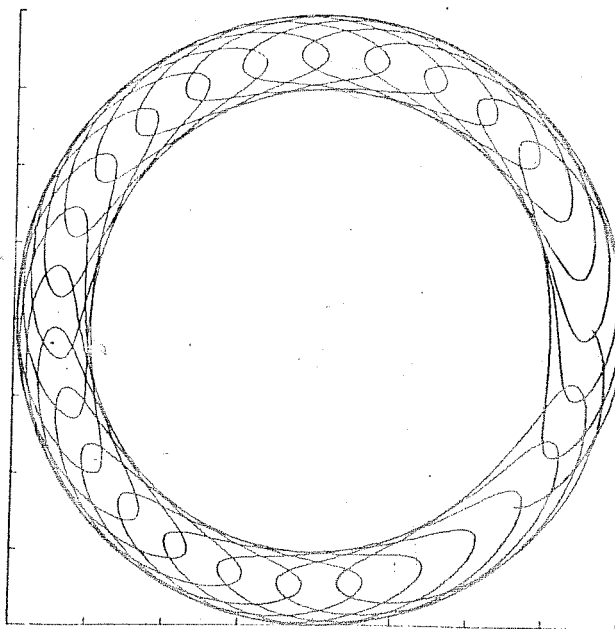
$\alpha = 0.45$ $\lambda = 500$ $L = 1000$ $E = 130$



$f_0 = 2.13311$ $f_1 = 1.99764$ $f_2 = 2.47679$

Fig. 3.3

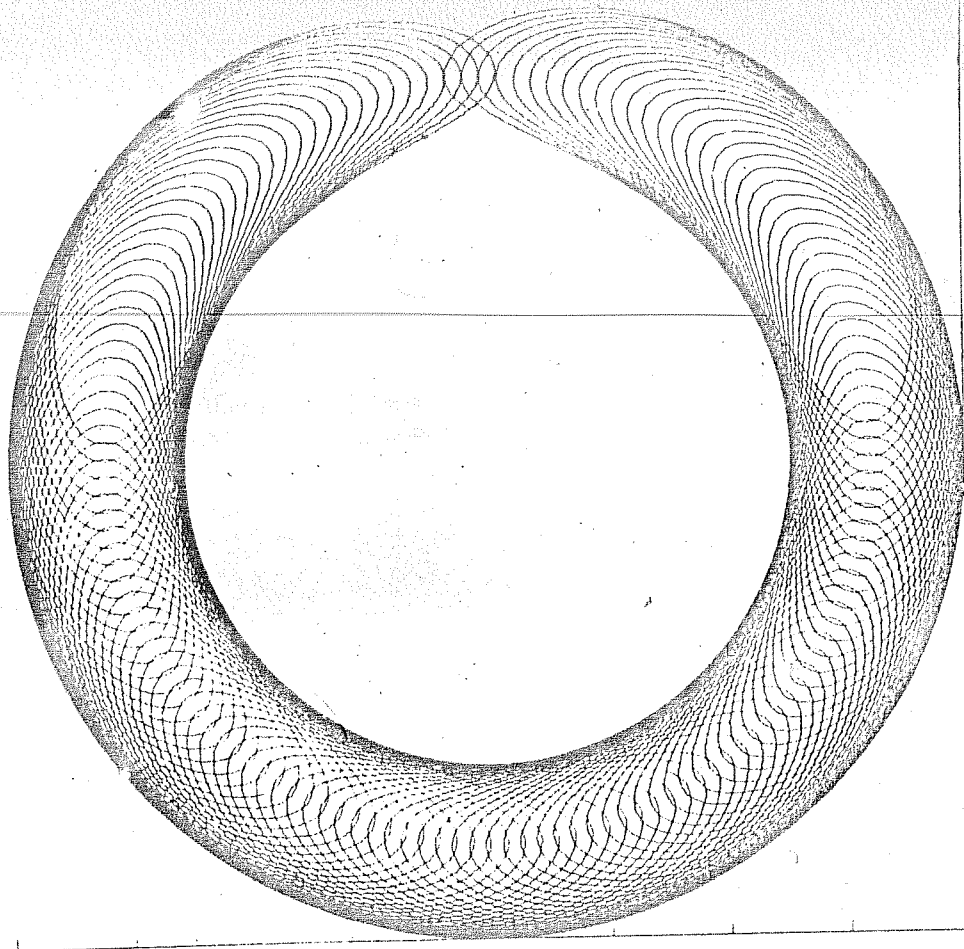
$\alpha = 0.9$ $\lambda = 150$ $L = 1000$ $E = 150$



$f_0 = 3.65400$ $f_1 = 3.13043$ $f_2 = 4.18248$

Fig. 3.4

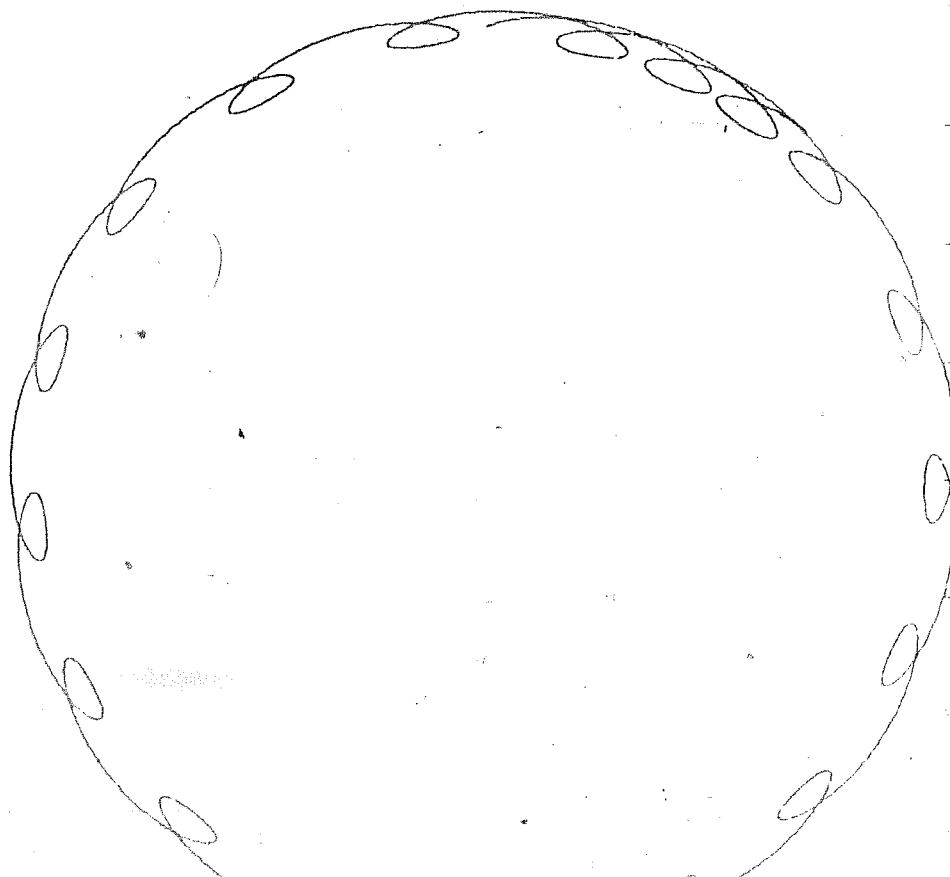
$\alpha = 0.99$ $\lambda = 500$ $L = 1000$ $E = 350$



$\rho_0 = 1.78721$ $\rho_1 = 1.58603$ $\rho_2 = 2.49805$

Fig. 3.6

$\alpha = 0.99$ $\lambda = 1000$ $L = 1000$ $E = 350$



$\rho_0 = 1.54210$ $\rho_1 = 1.48561$ $\rho_2 = 1.60200$

Fig. 3.5

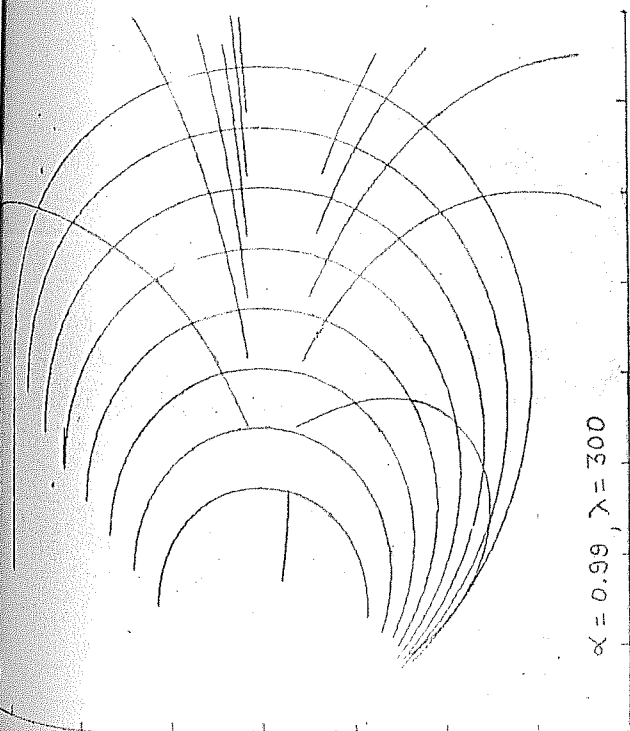


Fig. 3.7

$V_{II} = 0.76$

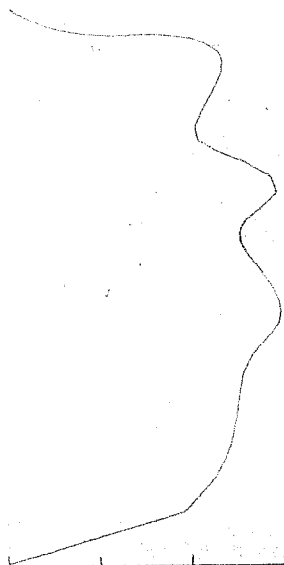


Fig. 3.8

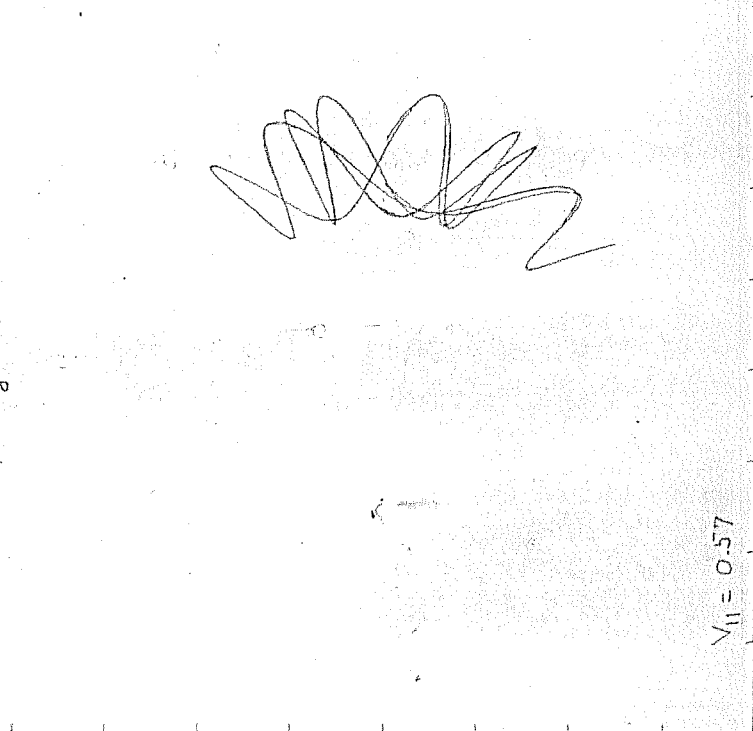


Fig. 3.9

$V_{II} = 0.38$

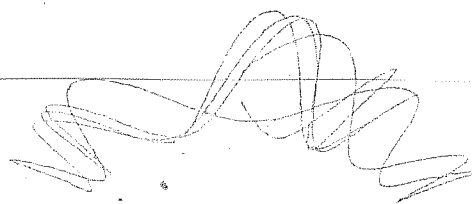
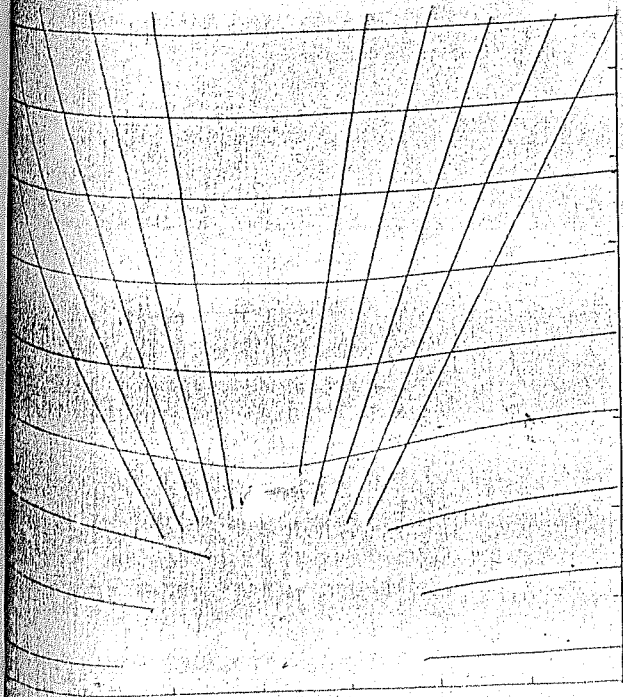


Fig. 3.10



$\alpha = 0.99, \lambda = 50$

Fig 3.11



$L = 748.0, R_0 = 5.272, V_{II} = 0.076$

Fig 3.12



$L = 316.0, R_0 = 3.272, V_{II} = 0.167$



$L = 316.0, R_0 = 3.272, V_{II} = 0.083$

TABLE 3.1

$\alpha = .99$, $\lambda = 1000$, $L = 1000$, $E = 3.5$, Uniform field.

$u^{(n)}$	R	$u^{(\varphi)}$	$\bar{\varphi}$
52.14	1.56	-36.82	-0.03
31.53	1.59	-64.57	-0.13
- 3.96	1.60	-72.09	-0.27
- 37.52	1.59	-59.01	-0.41
- 53.66	1.55	-29.00	-0.50
- 47.80	1.51	1.99	-0.53
- 26.01	1.49	24.03	-0.50
2.68	1.49	31.10	-0.44
30.64	1.50	21.30	-0.39
50.27	1.52	- 3.23	-0.37
52.44	1.56	-35.09	-0.41
32.43	1.59	-63.82	-0.51
- 2.77	1.60	-73.06	-0.65
- 36.67	1.59	-60.56	-0.79
- 53.50	1.55	-30.05	-0.88
- 43.27	1.52	1.08	-0.91
- 26.85	1.49	23.75	-0.88

TABLE 3.2

 $\alpha = .45, \lambda = 300, L = 100, E = 5, U_{10} = 0.78, R_e = 1.893$

R	θ	ϕ	U_{11}	θ
4.56	1.57	0.0	0.78	5.49
4.31	1.70	-0.016	0.92	6.82
4.26	1.84	-0.047	0.84	7.51
4.32	2.00	-0.005	0.63	7.70
4.25	2.10	0.15	0.50	8.69
3.88	2.11	0.31	0.49	12.24
3.48	2.11	0.22	0.54	18.62
3.51	2.31	0.29	0.40	19.84
3.22	2.27	0.46	0.46	27.55
3.08	2.26	0.39	0.53	32.86
3.04	2.34	0.33	0.54	35.59
3.01	2.45	0.43	0.54	38.79
2.82	2.44	0.61	0.65	51.11
2.58	2.48	0.51	0.79	77.19
2.34	2.65	0.78	0.89	131.0
2.22	2.64	0.85	0.93	182.4
2.11	2.63	0.89	0.96	251.8

TABLE 3.3

 $\alpha = .45, \quad \lambda = 300, \quad L = 100, \quad E = 5, \quad \vartheta_{He} = 0.19 \quad R_e = 1.393$

R	θ	φ	ϑ_{II}	B
4.56	1.57	0.0	0.19	5.49
4.31	1.68	- 0.21	0.21	6.82
4.97	1.75	- 0.15	0.03	4.11
5.31	1.78	- 0.04	- 0.04	3.31
5.14	1.67	0.52	- 0.33	3.57
4.15	1.42	0.54	- 0.75	7.96
4.31	1.11	0.38	- 0.14	7.96
4.24	1.13	0.76	- 0.14	8.37
4.19	1.46	1.13	- 0.79	7.56
5.25	1.77	1.24	0.26	3.41
5.12	1.82	1.70	0.01	3.80
4.54	1.74	1.83	-0.15	5.74
5.39	1.54	1.76	-0.12	2.99
5.62	1.50	2.37	-0.01	2.60
4.42	1.54	2.60	0.09	6.10
4.09	1.57	2.45	0.13	8.24
5.33	1.62	2.50	0.02	3.11
5.87	1.63	2.86	-0.03	2.23
5.03	1.58	3.31	-0.13	3.83

TABLE 3.4

 $\alpha = .45, \lambda = 50, L = 1000, E = 25.0, \vartheta_{110} = 0.27, R_e = 1.893$

R	θ	ϕ	ϑ_{11}	β
6.31	1.57	0.0	-0.27	41.38
6.34	1.60	0.055	-0.27	41.43
6.38	1.61	0.007	-0.27	41.34
6.21	1.63	0.035	-0.27	41.75
6.47	1.74	0.064	-0.27	41.86
6.36	1.78	0.063	-0.27	41.85
6.56	1.80	0.024	-0.27	42.13
6.76	1.87	0.045	-0.26	42.75
6.74	1.95	0.088	-0.25	43.14
6.85	1.96	0.085	-0.25	44.34
6.89	2.02	0.084	-0.24	43.78
7.09	2.04	0.094	-0.23	44.08
7.30	2.07	0.052	-0.20	44.45
7.55	2.13	0.101	-0.15	44.99

TABLE 3.5

 $\alpha = .45, \lambda = 50, L = 1000, E = 25.0, U_{10} = 0.18, Re = 1.893$

R	θ	ϕ	U_{11}	B
6.31	1.57	0.0	-0.16	41.33
6.45	1.65	0.054	-0.13	41.64
6.44	1.77	0.079	-0.13	41.80
6.46	1.86	0.074	-0.17	42.34
6.70	1.93	0.046	-0.16	42.93
6.91	2.03	0.075	-0.11	43.83
7.01	2.07	0.097	-0.06	44.17
7.09	2.08	0.103	-0.6x10	44.33
7.09	2.08	0.126	0.3x10	44.33
7.02	2.05	0.109	0.077	44.09
7.01	1.97	0.146	0.14	43.56
6.66	1.88	0.132	0.17	42.70
6.32	1.77	0.159	0.18	41.73
6.36	1.63	0.217	0.13	41.49
6.33	1.57	0.225	0.13	41.41

CHAPTER IV.

STRUCTURE AND STABILITY OF CHARGED FLUID DISKS AROUND A SCHWARZSCHILD BLACK HOLE.

In this chapter we present our analysis of the structure and stability of charged fluid disk around a Schwarzschild black hole (Prasanna and Chakraborty 1981). It was mentioned in Chapter 1 that even a weak magnetic field associated with the Schwarzschild geometry results in a stable orbit for charged particle even very close to the event horizon ($r \simeq 2.1 r_g$). This made us consider the structure and stability of disks in a more detailed way in general relativistic formulation; for if the inner edge could get so close to the event horizon then the general relativistic effects would not be negligible. Further we solve the entire system of fluid equations and Maxwell equations self consistently on a curved background such that the disk is under the influence of the gravitational field of the black hole and the electromagnetic field produced by its own motion. The effect of geometry in the electromagnetic field is taken through solving Maxwell equations on the curved background so that the coupling between the fields is well taken care of. As far as we know such a formulation has not been treated in the earlier literature and thus a detailed discussion even for simpler cases would possibly provide guidelines for treatment of more complicated problems.

The general set of assumptions and a complete set of equations describing the dynamical behaviour of the disk are

already presented in Chapter 2. For the case of charged fluid disk the momentum equations (2.2.23) to (2.2.25), the continuity equation (2.2.26) and the Maxwell equations (2.2.28) to (2.2.35) alongwith the corresponding equations describing perturbations are sufficient to study the structure and stability of charged fluid disks.

1. STEADY STATE SOLUTIONS.

We restrict ourselves to the case of an axisymmetric disk implying thereby that all physical parameters are independent of azimuthal coordinate ϕ and further that $\vartheta_0(\eta) = 0$, $\vartheta_0(\theta) = 0$ and $\vartheta_0(\phi) = \vartheta_0$. The equations governing the steady state motion then reduce to

$$\left(\rho_0 + \frac{p_0}{c^2}\right) \left\{ \frac{m c^2}{r^2} - \left(1 - \frac{2m}{r}\right) \frac{\vartheta_0^2}{r} \right\} = - \left(1 - \frac{\vartheta_0^2}{c^2}\right) \left(1 - \frac{2m}{r}\right) \frac{\partial p_0}{\partial r} + \epsilon_0 \left(1 - \frac{2m}{r}\right)^{\frac{1}{2}} \left(1 - \frac{\vartheta_0^2}{c^2}\right)^{\frac{1}{2}} \left[F_0(\eta)(t) - \frac{\vartheta_0}{c} F_0(\phi)(\eta) \right], \quad (4.1.1)$$

$$-\left(\rho_0 + \frac{p_0}{c^2}\right) \frac{\cot \theta}{r} \vartheta_0^2 = - \left(1 - \frac{\vartheta_0^2}{c^2}\right) \frac{1}{r} \frac{\partial p_0}{\partial \theta} + \epsilon_0 \left(1 - \frac{\vartheta_0^2}{c^2}\right)^{\frac{1}{2}} \left[F_0(\theta)(t) + \frac{\vartheta_0}{c} F_0(\theta)(\phi) \right], \quad (4.1.2)$$

$$\epsilon_0 \left(1 - \frac{2m}{r}\right)^{\frac{1}{2}} \left(1 - \frac{\vartheta_0^2}{c^2}\right)^{\frac{3}{2}} F_0(\phi)(t) = 0, \quad (4.1.3)$$

$$\frac{\partial}{\partial r} \left[r \left(1 - \frac{2m}{r}\right)^{\frac{1}{2}} F_0(\theta)(t) \right] - \frac{\partial}{\partial \theta} F_0(\eta)(t) = 0, \quad (4.1.4)$$

$$\frac{\partial}{\partial r} \left[r \left(1 - \frac{2m}{r}\right)^{\frac{1}{2}} F_0(\phi)(t) \right] = 0, \quad (4.1.5)$$

$$\frac{\partial}{\partial \theta} [\sin \theta F_0(\varphi)(t)] = 0, \quad (4.1.6)$$

$$\frac{\partial}{\partial r} [r^2 \sin \theta F_0(\theta)(\varphi)] + \frac{\partial}{\partial \theta} [r \sin \theta (1 - \frac{2m}{r})^{-\frac{1}{2}} F_0(\varphi)(r)] = 0, \quad (4.1.7)$$

$$\frac{\partial}{\partial \theta} [\sin \theta F_0(r)(\theta)] = 0, \quad (4.1.8)$$

$$\frac{\partial}{\partial r} [r (1 - \frac{2m}{r})^{\frac{1}{2}} F_0(r)(\theta)] = 0, \quad (4.1.9)$$

$$\begin{aligned} & \therefore \frac{1}{r} \left[\frac{\partial}{\partial r} \left\{ r (1 - \frac{2m}{r})^{\frac{1}{2}} F_0(\varphi)(r) \right\} - \frac{\partial}{\partial \theta} F_0(\theta)(\varphi) \right] \\ & \quad = \frac{4\pi \epsilon_0}{c} (1 - \frac{v_0^2}{c^2})^{-\frac{1}{2}} v_0, \end{aligned} \quad (4.1.10)$$

$$\begin{aligned} & \frac{1}{r} \frac{\partial}{\partial r} [r^2 F_0(r)(t)] + \frac{1}{\sin \theta} \frac{\partial}{\partial \theta} [\sin \theta (1 - \frac{2m}{r})^{-\frac{1}{2}} F_0(\theta)(t)] \\ & \quad = 4\pi \epsilon_0 r (1 - \frac{2m}{r})^{-\frac{1}{2}} (1 - v_0^2/c^2)^{-\frac{1}{2}} \end{aligned} \quad (4.1.11)$$

The continuity equation is identically satisfied. Our aim is to solve this set of equations self consistently and then consider the corresponding perturbation equations. Equation (4.1.3) directly implies that the toroidal electric field

$F_\varphi(t)$, is identically zero, which is consistent with two of the Maxwell's equations (4.1.5) and (4.1.6). Similarly we find that the toroidal magnetic field is not coupled with any of the physical parameters of the system and hence without loss of generality it is taken to be zero consistent with equations (4.1.8) and (4.1.9). This reduces our system of equations to six equations connecting six variables which are thus completely determined.

Presently we shall consider two special cases:

Case 1. Differential rotation: u^φ and ϵ_0 are constant, where

ϵ_0 is the charge density as seen by the comoving observer.

Case 2. Rigid rotation: u^φ/u^0 and b are constant, where

$b = (1 - \frac{2m}{r})^{-\frac{1}{2}} (1 - \frac{v^2}{c^2})^{-\frac{1}{2}}$ is the charge density as seen by the observer at infinity.

Case 1. Differential Rotation.

Since $u^\varphi = \text{constant}$, $u^\varphi = \Omega/c$ with $\Omega = \text{constant}$, the azimuthal component of 3-velocity in local Lorentz frame would be $v_\theta = r \Omega \sin \theta (1 + \frac{r^2 \Omega^2 \sin^2 \theta}{c^2})^{-\frac{1}{2}}$. The equations (4.1.7) and (4.1.10) involving magnetic field components become similar to the ones considered by Ginzburg and Ozernoi (1965) except for the source term in (4.1.10). Adopting the same procedure as used by these authors we assume the magnetic field components to have the form

$$F_{\phi(\theta)(\varphi)} = B_r = (2\mu \cos \theta / r^3) f(r)$$

and

$$F_{\phi(\varphi)(r)} = B_\theta = (\mu \sin \theta / r^3) g(r) \quad (4.1.12)$$

with μ the dipole moment, and 'f' and 'g' giving the contributions to the field components from the curvature of the background geometry. Substituting these in equations (4.1.7) and (4.1.10) we get the equations for f and g to be

$$\frac{d}{dr} \left(\frac{f}{r} \right) + \frac{g}{r^2} \left(1 - \frac{2m}{r} \right)^{-\frac{1}{2}} = 0 \quad (4.1.13)$$

and

$$\frac{d}{dr} \left[\frac{g}{r} \left(1 - \frac{2m}{r} \right)^{-\frac{1}{2}} \right] + \frac{2f}{r^3} = \frac{4\pi \Omega \epsilon_0}{c} r^2 \quad (4.1.14)$$

Hence

$$f = C_1 f_1 + C_2 f_2 - \frac{2\pi}{5} \frac{\Omega \varepsilon_0 r^5}{\mu c} h_1,$$

where

$$f_1 = \frac{r^3}{m^3} \left[\ln \left(1 - \frac{2m}{r} \right) + \frac{2m}{r} \left(1 + \frac{m}{r} \right) \right],$$

$$f_2 = r^3 / 2m^3$$

and

$$h_1 = 1 + \frac{4m}{r} + \frac{8m^2}{r^2} \ln \left(\frac{r}{2m} - 1 \right); \quad (4.1.15)$$

$$g = -C_1 g_1 - C_2 g_2 + \frac{8\pi}{5} \frac{\Omega \varepsilon_0 r^5}{\mu c} h_2,$$

where

$$g_1 = \frac{2r^2}{m^2} \left[\frac{r}{m} \ln \left(1 - \frac{2m}{r} \right) + \left(1 - \frac{2m}{r} \right)^{-1} + 1 \right] \left(1 - \frac{2m}{r} \right)^{\frac{1}{2}},$$

$$g_2 = (r^3/m^3) \left(1 - \frac{2m}{r} \right)^{\frac{1}{2}},$$

and

$$h_2 = \left[1 + \frac{3m}{r} + \frac{4m^2}{r^2} \ln \left(\frac{r}{2m} - 1 \right) + \frac{m}{r} \left(\frac{r}{2m} - 1 \right)^{-1} \right] \left(1 - \frac{2m}{r} \right)^{\frac{1}{2}}. \quad (4.1.16)$$

C_1 and C_2 are the constants of integration. In order to determine these constants of integration we expect the field to be continuous at inner and outer boundaries r_a and r_b .

In order to solve for electrical fields we now consider the fact that Maxwell's equations should be solved consistently with the fluid equations. In view of this we solve for the components of electric field from momentum equations (4.1.1) and (4.1.2) getting

$$F_{0(r)}(t) = E_r = \left(1 + \frac{r^2 \Omega^2}{c^2} \sin^2 \theta\right)^{-\frac{1}{2}} \left[\left(\epsilon_0 + \frac{p_0}{c^2}\right) \frac{c^2}{\epsilon_0 r} \left\{ \frac{m}{r} - \left(1 - \frac{3m}{r}\right) \frac{r^2 \Omega^2}{c^2} \sin^2 \theta \right\} \left(1 - \frac{2m}{r}\right)^{-\frac{1}{2}} + \frac{1}{\epsilon_0} \left(1 - \frac{2m}{r}\right)^{\frac{1}{2}} \frac{\partial p_0}{\partial r} + \frac{r \Omega}{c} \sin \theta \frac{\mu \sin \theta}{r^3} g \right], \quad (4.1.17)$$

$$F_{0(\theta)}(t) = E_\theta = \left(1 + \frac{r^2 \Omega^2}{c^2} \sin^2 \theta\right)^{-\frac{1}{2}} \left[-\left(\epsilon_0 + \frac{p_0}{c^2}\right) \frac{c^2}{\epsilon_0 r} \times \frac{r^2 \Omega^2}{c^2} \sin \theta \cos \theta + \frac{1}{r \epsilon_0} \frac{\partial p_0}{\partial \theta} - \frac{r \Omega}{c} \sin \theta \frac{2 \mu \cos \theta}{r^3} f \right], \quad (4.1.18)$$

Using these expressions for the electric field in (4.1.4) and (4.1.11) we get the constraint equations for ρ_0 and p_0 as follows:

$$\begin{aligned} R \frac{\partial}{\partial R} \left[\left(1 + R^2 \omega^2 \sin^2 \theta\right)^{-\frac{1}{2}} \left(1 - \frac{2}{R}\right)^{\frac{1}{2}} \left\{ \left(\epsilon_0 + \frac{p_0}{c^2}\right) R^2 \omega^2 \sin \theta \cos \theta + \omega \sin \theta \cos \theta \left[\frac{2\alpha}{R} (C_1 f_1 + C_2 f_2) - \frac{4\pi}{5} \omega R^4 h_1 \beta \right] - \frac{1}{c^2} \frac{\partial p_0}{\partial \theta} \right\} \right] \\ + \frac{\partial}{\partial \theta} \left[\left(1 + R^2 \omega^2 \sin^2 \theta\right)^{-\frac{1}{2}} \left\{ \left(\epsilon_0 + \frac{p_0}{c^2}\right) \left[\frac{1}{R} - \left(1 - \frac{3}{R}\right) R^2 \omega^2 \sin^2 \theta \right] \times \left(1 - \frac{2}{R}\right)^{-\frac{1}{2}} + \omega \sin^2 \theta \left[\frac{\alpha}{R} (-C_1 g_1 - C_2 g_2) + \frac{8\pi}{5} \omega R^4 h_2 \beta \right] + \left(1 - \frac{2}{R}\right)^{\frac{1}{2}} \frac{R}{c^2} \frac{\partial p_0}{\partial R} \right\} \right] = 0, \quad (4.1.19) \end{aligned}$$

$$\frac{\partial}{\partial R} \left[\left(1 + R^2 \omega^2 \sin^2 \theta\right)^{-\frac{1}{2}} \left\{ \left(\epsilon_0 + \frac{p_0}{c^2}\right) R \left[\frac{1}{R} - \left(1 - \frac{3}{R}\right) R^2 \omega^2 \sin^2 \theta \right] \right\} \right]$$

$$\begin{aligned}
& \lambda \left(1 - \frac{z}{R}\right)^{-L} + \omega \sin^2 \theta \left[\alpha (-C_1 g_1 - C_2 g_2) + \frac{8\pi}{5} \omega R^5 h_1 \beta \right] \\
& + R^2 \left(1 - \frac{z}{R}\right)^{-L} \left\{ \frac{1}{c^2} \frac{\partial p_0}{\partial R} \right\} \\
& - \frac{1}{\sin \theta} \left(1 - \frac{z}{R}\right)^{-L} \frac{\partial}{\partial \theta} \left[(1 + R^2 \omega^2 \sin^2 \theta)^{-L} \left\{ (e_0 + \frac{p_0}{c^2}) R^2 \omega^2 \sin \theta \cos \theta \right. \right. \\
& \left. \left. + \omega \sin^2 \theta \cos \theta \left[\frac{2\alpha}{R} (C_1 f_1 + C_2 f_2) - \frac{4\pi}{5} \omega R^4 h_1 \beta \right] \right. \right. \\
& \left. \left. - \frac{1}{c^2} \sin \theta \frac{\partial p_0}{\partial \theta} \right\} \right] \\
& = 4\pi \beta R^2 \left(1 - \frac{z}{R}\right)^{-L} (1 + R^2 \omega^2 \sin^2 \theta)^{-L}, \tag{4.1.20}
\end{aligned}$$

wherein

$$R = \frac{r}{m}, \quad \omega = \frac{m \Omega}{c}, \quad \alpha = \frac{\mu \epsilon_0}{m^2 c^2}, \quad \beta = \frac{m^4 \epsilon_0^L}{c^L}. \tag{4.1.21}$$

Thus in principle we have the entire system solved self-consistently. But in practice it is formidable to solve these two equations completely for e_0 and p_0 . We limit ourselves to the case of incoherent fluid disk which has $p_0 = 0$ and further treat the disk to be infinitesimally thin and confined to the equatorial plane. In order to bring in the last requirement we introduce a 'height coordinate' $h = r(\pi/2 - \theta) = R m(\frac{\pi}{2} - \theta)$ and further express the 3-densities e_0, α, β in terms of corresponding 2-densities $\bar{e}_0, \bar{\alpha}, \bar{\beta}$ as

$$e_0 = \bar{e}_0(R) \delta(h), \quad \alpha = \bar{\alpha} \delta(h), \quad \beta = \bar{\beta} \delta(h) \tag{4.1.22}$$

ensuring $\bar{\alpha}$ and $\bar{\beta}$ to be independent of R . Putting these in (4.1.20) and integrating the resulting equation with respect to h we get

$$\begin{aligned}
& \frac{d}{dR} \left[(1+R^2\omega^2)^{-\frac{L}{2}} \left\{ \bar{P}_0 R \left[\frac{1}{R} - \left(1 - \frac{3}{R}\right) R^2 \omega^2 \right] \left(1 - \frac{2}{R}\right)^{-\frac{L}{2}} \right. \right. \right. \\
& \quad \left. \left. + \omega \left[\bar{\alpha} (-c_1 g_1 - c_2 g_2) + \frac{8\pi}{5} \omega R^5 h_2 \bar{B} \right] \right\} \right] \\
& = 4\pi \bar{B} R^2 \left(1 - \frac{2}{R}\right)^{-\frac{L}{2}} (1+R^2\omega^2)^{-\frac{L}{2}}, \tag{4.1.23}
\end{aligned}$$

while the equation (4.1.20) becomes identically zero. To solve this equation we expand the factor $(1-2/R)^{-\frac{L}{2}}$ binomially, keeping the terms upto $(2/R)^6$ and obtain the solution:

$$\begin{aligned}
\bar{P}_0 = & \left[4\pi \bar{B} D - \omega (1+R^2\omega^2)^{-\frac{L}{2}} \left\{ \bar{\alpha} (-c_1 g_1 - c_2 g_2) + \frac{8\pi}{5} \omega R^5 h_2 \bar{B} \right\} \right. \\
& \left. + C_3 \right] \frac{1}{R} \left(1 - \frac{2}{R}\right)^{-\frac{L}{2}} (1+R^2\omega^2)^{-\frac{L}{2}} \left\{ \frac{1}{R} - \left(1 - \frac{3}{R}\right) R^2 \omega^2 \right\}^{-1}, \tag{4.1.24}
\end{aligned}$$

wherein

$$\begin{aligned}
D = & (1+R^2\omega^2)^{\frac{3}{2}} \left(R/4\omega^2 - 231/48 R^3 + 43\omega^2 \right) \\
& + (1+R^2\omega^2)^{\frac{L}{2}} \left(5/2 - 35/8 R + 3R/4 - 63/16 R^2 - R/8\omega^2 \right) \\
& + \omega \left[R\omega + (1+R^2\omega^2)^{\frac{L}{2}} \right] (41 - 1/\omega^2) / 8\omega \\
& + \frac{1}{4} \omega \left[\frac{(1+R^2\omega^2)^{\frac{L}{2}} - 1}{(1+R^2\omega^2)^{\frac{L}{2}} + 1} \right] \left(5 + \frac{63}{8} \omega^2 \right) \tag{4.1.25}
\end{aligned}$$

and C_3 is the constant of integration.

From the expression (4.1.24) we find that \bar{P}_0 has singularities at the values of R given by the roots of the equation

(4.1.26)

The second factor of (4.1.26) has a pair of complex conjugate roots and one real root as given by

$$R_{\text{sing}} = 1 + \frac{1}{(2\omega^2)^{1/3}} \left[\left\{ 1 + 2\omega^2 + (1 + 4\omega^2)^{1/2} \right\}^{1/3} + \left\{ 1 + 2\omega^2 - (1 + 4\omega^2)^{1/2} \right\}^{1/3} \right] \quad (4.1.27)$$

Thus for any given value of ω we can evaluate R_{sing} where we have a singularity in addition to the one at $R = 2$. For lower values of ω , R_{sing} lies far out and as ω increases R_{sing} approaches the value 3 asymptotically. Hence we can consider two kinds of disks, (1) $R_b < R_{\text{sing}}$ and (2) $R_a > R_{\text{sing}}$, the disks in the second case are fast rotating compared to those in the first case.

To get the equations for electromagnetic field for the infinitesimally thin disk considered above we also introduce surface charge density $\bar{\epsilon}_0$ by

$$\epsilon_0 = \bar{\epsilon}_0 \delta(h) \quad (4.1.28)$$

and obtain

$$(B_r)_{\theta=\pi/2} = 0,$$

$$X = \frac{m \bar{\epsilon}_0}{c^2} (B_\theta)_{\theta=\pi/2} = \frac{2}{R^3} (-g_1, -g_2) + \frac{8\pi}{5} \omega R^2 h_2 \bar{\beta},$$

$$(E_\theta)_{\theta=\pi/2} = 0,$$

$$Y = \frac{m \bar{\epsilon}_0}{c^2} (E_r)_{\theta=\pi/2} = \frac{4\pi \bar{\beta} D + C_3}{R^2} \quad (4.1.29)$$

Finally using (4.1.29) in (4.1.24) we obtain

$$\bar{P}_0 = \left[Y - \frac{U_0}{c} X \right] R \left(1 - \frac{2}{R} \right)^{\frac{1}{2}} (1 + R^2 \omega^2)^{\frac{1}{2}} \left\{ \frac{1}{R} - \left(1 - \frac{2}{R} \right) R^2 \omega^2 \right\}^{-1} \quad (4.1.30)$$

Case 2. Rigid Rotation

We solve this case exactly on the same lines as for case 1 with $b = \text{constant}$, $u^\theta / u^0 = \Omega / c$, $\Omega = \text{constant}$. We now have $\varphi_0^{(\theta)} = \Omega \sin \theta \left(1 - \frac{2u}{R} \right)^{-\frac{1}{2}}$. The expression for magnetic fields (4.1.15) and (4.1.16) remain unchanged except for the fact that ξ_0 gets replaced by b . The components of the electric field as calculated from momentum equations become

$$\begin{aligned} F_{0(r)(t)} = E_r = & \left(e_0 + \frac{p_0}{c^2} \right) \frac{c^2}{b r} \left(1 - \frac{2u}{R} - \frac{\Omega^2 R^2}{c^2} \sin^2 \theta \right)^{-1} \left(\frac{u}{R} - \frac{\Omega^2 R^2}{c^2} \sin^2 \theta \right) \\ & + \frac{1}{b} \frac{\partial p_0}{\partial r} + \frac{\Omega}{c} \left(1 - \frac{2u}{R} \right)^{-\frac{1}{2}} \frac{\mu g}{R^3} \sin^2 \theta, \end{aligned} \quad (4.1.31)$$

$$\begin{aligned} F_{0(\theta)(t)} = E_\theta = & - \left(e_0 + \frac{p_0}{c^2} \right) \frac{c^2}{b r} \left(1 - \frac{2u}{R} \right)^{-\frac{1}{2}} \left(1 - \frac{2u}{R} - \frac{\Omega^2 R^2}{c^2} \sin^2 \theta \right)^{-1} \\ & \times \frac{\Omega^2 R^2}{c^2} \sin \theta \cos \theta + \left(1 - \frac{2u}{R} \right)^{-\frac{1}{2}} \frac{1}{b r} \frac{\partial p}{\partial \theta} \\ & - \frac{\Omega}{c} \left(1 - \frac{2u}{R} \right)^{-\frac{1}{2}} \frac{2 \mu f}{R^3} \sin \theta \cos \theta \end{aligned} \quad (4.1.32)$$

Substituting these in Maxwell's equations, using

$$\alpha = \frac{\mu b}{m^2 c^2}, \quad \beta = \frac{m^2 b^2}{c^2}, \quad p_0 = 0 \quad (4.1.33)$$

and integrating with respect to h after putting δ function as in the previous case, we get the following expression for

the electromagnetic field components and for \bar{e}_0 ,

$$X = \frac{u\bar{b}}{c^2} (B_\theta)_{\theta=\pi/2} = \frac{\bar{\omega}}{R^3} (-c_1 g_1 - c_2 g_2) + \frac{2\pi}{5} \omega R^2 h_2 \bar{B}, \quad (4.1.34)$$

$$Y = \frac{u\bar{b}}{c^2} (E_r)_{\theta=\pi/2} = \frac{4\pi}{3} \bar{B} R + \frac{c_3}{R^2} \quad (4.1.35)$$

$$\bar{e}_0 = [Y - \frac{v_0}{c} X] R (1 - \frac{2}{R} - R^2 \omega^2) (\frac{1}{R} - R^2 \omega^2)^{-1} \quad (4.1.36)$$

The expression for \bar{e}_0 in this case is exact and we can put the inner edge of the disk very near to the event horizon.

The singularity point in this case is given by

$$R_{\text{sing}} = \omega^{-2/3} \quad (4.1.37)$$

Because of the nature of the velocity function v_0 , in this case we have to confine only to the slowly rotating disks with $R_b < R_{\text{sing}}$. The limitation comes from the consideration that the maximum linear velocity v_0 at R_b should be less than c , the velocity of light.

Boundary conditions

In order to determine the constants appearing in the expressions for magnetic and electric field components we take the fields to be continuous at boundaries R_a and R_b . For magnetic field at $R > R_b$ we take the Ginzburg-Ozernoi field which gives

$$(X)_{R > R_b} = \frac{3}{8} \bar{\omega} \frac{g_1}{R^3} \quad (4.1.38)$$

To obtain another boundary condition for the magnetic field we use the familiar results of the field in the interior of a

circular current loop at $\theta = \pi/2$ plane restricting only to the lowest order terms. In the present case of the disk these fields appear as

$$F_0(\varphi)(r) = B_\theta = -\mu D' \sin \theta g'(r)/m^3,$$

$$F_0(\theta)(\varphi) = B_r = \mu D' \cos \theta f'(r)/m^3, \quad (4.1.39)$$

wherein $D' = 8(R_b - R_a)/(R_b^4 - R_a^4)$ and f' and g' represent the correction due to curvature of spacetime. Substituting these in Maxwell's equations governing magnetic field we get

$$\frac{d}{dr} [r^2 f'] - 2r g' \left(1 - \frac{2m}{r}\right)^{-\frac{1}{2}} = 0 \quad (4.1.40)$$

and

$$\frac{d}{dr} \left[r \left(1 - \frac{2m}{r}\right)^{\frac{1}{2}} g' \right] - f' = 0. \quad (4.1.41)$$

Solutions of (4.1.40) and (4.1.41) yield

$$f' = c_1' \left[\ln \left(1 - \frac{2m}{r}\right) + \frac{2m}{r} \left(1 + \frac{m}{r}\right) \right] + c_2'$$

and

$$g' = \left\{ c_1' \left[\ln \left(1 - \frac{2m}{r}\right) + \frac{m}{r} + \frac{m}{r} \left(1 - \frac{2m}{r}\right)^{-1} \right] + c_2' \right\} \left(1 - \frac{2m}{r}\right)^{\frac{1}{2}}.$$

We choose $c_1' = 0$ in order to avoid singularity at $r = 2m$ and take $c_2' = 1$ to obtain the flat space time limit ($m \rightarrow 0$). With these we get $R < R_a$

$$(X)_{R < R_a} = -\frac{1}{2} D' \left(1 - \frac{2m}{R}\right)^{\frac{1}{2}} \quad (4.1.42)$$

To obtain the boundary conditions for the electric field we use the results of the field due to a circular charged current loop and use only the monopole term

$$\begin{aligned} (E_r)_{r > r_b} &= \frac{q}{r^2} , \\ (E_r)_{r < r_a} &= 0 , \end{aligned} \quad (4.1.43)$$

where q is the net charge of the ring. The monopole field does not get modified due to the curvature of the space time as may be seen by applying the similar procedure as was done by Ginzburg and Ozernoi. For the case of extended disk, above results give

$$\begin{aligned} (Y)_{R > R_b} &= \frac{8\pi A}{R^2(R_b^2 - R_a^2)\omega} , \\ (Y)_{R < R_a} &= 0 , \end{aligned} \quad (4.1.44)$$

where

$$A = \left[\frac{1}{3\omega^2} (1 + R^2\omega^2)^{3/2} \right]_{R_a}^{R_b} , \quad (4.1.45)$$

for the case of differential rotation and

$$A = \left[\frac{1}{2} \left\{ (R-1) \sqrt{R^2 - 2R} - \ln(2\sqrt{R^2 - 2R} + 2R - 2) \right\} \right]_{R_a}^{R_b} , \quad (4.1.46)$$

for the case of rigid rotation. In obtaining the above boundary conditions we have used the following expressions obtained by elementary considerations

$$\mu = \frac{\pi}{c} \frac{r_b^4 - r_a^4}{4} \bar{\epsilon}_0 \Omega,$$

$$q = 2\pi \bar{\epsilon}_0 m^2 A,$$

$$\bar{\alpha} = \frac{\mu \bar{\epsilon}_0}{m^2 c^2}, \quad \text{for differential rotation} \quad (4.1.47)$$

and

$$\mu = \frac{\pi}{c} \frac{r_b^4 - r_a^4}{4} \bar{b} \Omega,$$

$$q = 2\pi \bar{b} m^2 A,$$

$$\bar{\alpha} = \frac{\mu \bar{b}}{m^2 c^2}, \quad \text{for rigid rotation.} \quad (4.1.48)$$

Using these boundary conditions we determine C_1 , C_2 , C_3 and $\bar{\beta}$ and finally the expressions for fields as follows:

Case 1. Differential rotation

$$\bar{\beta} = \frac{A}{2(D_b - D_a)} \frac{m \bar{\epsilon}_0^2}{c^2}, \quad C_3 = - \frac{2\pi A}{(D_b - D_a)} D_a \frac{m \bar{\epsilon}_0^2}{c^2},$$

$$X = \frac{\pi \omega}{4} \frac{m \bar{\epsilon}_0^2}{c^2} \left\{ (R_b^4 - R_a^4) \frac{(-C_1 g_1 - C_2 g_2)}{R^3} + \frac{16}{5} R^2 h_2 \frac{A}{(D_b - D_a)} \right\}, \quad (4.1.49)$$

$$Y = \frac{2\pi A}{(D_b - D_a) R^4} \frac{m \bar{\epsilon}_0^2}{c^2} \quad (4.1.50)$$

Case 2. Rigid rotation

$$\bar{\beta} = \frac{3A}{2(R_b^3 - R_a^3)} \frac{\omega \bar{b}^2}{c^2}, \quad C_3 = -2\pi A \frac{R_a^3}{R_b^3 - R_a^3} \frac{\omega \bar{b}^2}{c^2},$$

$$X = \frac{\pi \omega}{4} \frac{\omega \bar{b}^2}{c^2} \left\{ (R_b^4 - R_a^4) \frac{(-C_1 g_1 - C_2 g_2)}{R^3} + \frac{48}{5} R^2 h_2 \frac{A}{R_b^3 - R_a^3} \right\}, \quad (4.1.51)$$

$$Y = \frac{2\pi A}{R_b^3 - R_a^3} \frac{\omega \bar{b}^2}{c^2} \left[\frac{R^3 - R_a^3}{R^2} \right], \quad (4.1.52)$$

where

$$C_1 = \frac{g_{2b} \left\{ D' R_a^3 \left(1 - \frac{2}{R_a} \right)^{\frac{1}{2}} + F_1 \right\} + g_{2a} \left\{ \frac{3}{8} g_{1b} + F_2 \right\}}{(g_{1a} g_{2b} - g_{1b} g_{2a})}, \quad (4.1.53)$$

$$C_2 = \frac{g_{1b} \left\{ D' R_a^3 \left(1 - \frac{2}{R_a} \right)^{\frac{1}{2}} + F_1 \right\} + g_{1a} \left\{ \frac{3}{8} g_{1b} + F_2 \right\}}{(g_{2a} g_{1b} - g_{2b} g_{1a})}, \quad (4.1.54)$$

$$F_1 = \frac{48}{5} \frac{R_a^5 h_{2a} A}{(D_b - D_a)(R_b^4 - R_a^4)},$$

$$F_2 = -\frac{16}{5} \frac{R_b^5 h_{2b} A}{(D_b - D_a)(R_b^4 - R_a^4)}, \quad (4.1.55)$$

for differential rotation and

$$F_1 = \frac{48}{5} \frac{R_a^5 h_{za} A}{(R_b^3 - R_a^3)(R_b^4 - R_a^4)},$$

$$F_2 = -\frac{48}{5} \frac{R_b^5 h_{zb} A}{(R_b^3 - R_a^3)(R_b^4 - R_a^4)}, \quad (4.1.56)$$

for rigid rotation.

From the expression (4.1.30) for \bar{e}_0 , and from the boundary condition that at inner edge, $Y = 0$ and $X < 0$, we find that for fast rotating disk ($R_A > R_{\text{sing}}$), \bar{e}_0 becomes negative. We therefore exclude the possibility of having fast rotating disks and limit ourselves to the slowly rotating disks ($R_b < R_{\text{sing}}$) only.

Tables 4.1 to 4.4 show \bar{e}_0 , B_0 and E_r profiles for various values of R_a , R_b and ω for the case of differential and rigid rotations. Because of the approximation made in expanding the factor $(1-2/R)^{\frac{1}{2}}$ in evaluating \bar{e}_0 , we have restrained ourselves from going too near to the event horizon. We find that R_a as small as 3.5 is a reasonably good choice for the inner edge.

2. Stability Analysis

We shall now take up the analysis of the stability of such disks as described above under purely radial perturbation. We use normal mode analysis and use the variational

principle as outlined in Chapter 2 to examine the criteria for the onset of instability. The equations governing the perturbations can be obtained from the set of equations

(2.2.42) to (2.2.45) and (2.2.47) to (2.2.54) by putting

$\vartheta_0(\eta)$, $\vartheta_0(\theta)$, p_0 , $F_{0(\varphi)(t)}$ and $F_{0(\eta)(\theta)}$ equal to zero.

Limiting ourselves to the case when $\delta p = 0$, $\delta \vartheta(\theta) = 0$

and $\delta \vartheta(\varphi) = 0$, we obtain

$$\rho_0 \frac{\partial}{\partial t} \delta \vartheta(\eta) + \delta \rho \left[\frac{mc^2}{\eta^2} - \frac{1}{\eta} \left(1 - \frac{2m}{\eta} \right) \vartheta_0^2 \right] = \left(1 - \frac{2m}{\eta} \right)^{\frac{1}{2}} \left(1 - \frac{\vartheta_0^2}{c^2} \right)^{\frac{1}{2}} \times \left[\left\{ F_{0(\eta)(t)} - \frac{\vartheta_0}{c} F_{0(\varphi)(\eta)} \right\} \delta \varepsilon + \varepsilon_0 \left\{ \delta F_{(\eta)(t)} - \frac{\vartheta_0}{c} \delta F_{(\varphi)(\eta)} \right\} \right], \quad (4.2.1)$$

$$- \delta \rho \frac{\vartheta_0^2}{\eta^2} \left(1 - \frac{2m}{\eta} \right)^{\frac{1}{2}} \cos \theta = \left(1 - \frac{2m}{\eta} \right)^{\frac{1}{2}} \left(1 - \frac{\vartheta_0^2}{c^2} \right)^{\frac{1}{2}}$$

$$\times \left[\left\{ F_{0(\theta)(t)} + \frac{\vartheta_0}{c} F_{0(\theta)(\varphi)} \right\} \delta \varepsilon + \varepsilon_0 \left\{ \delta F_{(\theta)(t)} + \frac{\vartheta_0}{c} \delta F_{(\theta)(\varphi)} \right\} \right], \quad (4.2.2)$$

$$\rho_0 \left[\left(1 - \frac{2m}{\eta} \right) \frac{\partial \vartheta_0}{\partial \eta} + \frac{1}{\eta} \left(1 - \frac{3m}{\eta} \right) \vartheta_0 \right] \delta \vartheta(\eta) = \varepsilon_0 \left(1 - \frac{2m}{\eta} \right)^{\frac{1}{2}} \left(1 - \frac{\vartheta_0^2}{c^2} \right)^{\frac{1}{2}}$$

$$\times \left[\delta F_{(\varphi)(t)} \left(1 - \frac{\vartheta_0^2}{c^2} \right) + \left\{ F_{0(\varphi)(\eta)} - \frac{\vartheta_0}{c} F_{0(\eta)(t)} \right\} \frac{\delta \vartheta(\eta)}{c} \right], \quad (4.2.3)$$

$$\rho_0 \left[\frac{\partial}{\partial t} \delta \varepsilon + \left(1 - \frac{2m}{\eta} \right) \delta \vartheta(\eta) \frac{\partial \varepsilon_0}{\partial \eta} \right] = \varepsilon_0 \left[\frac{\partial}{\partial t} \delta \rho + \left(1 - \frac{2m}{\eta} \right) \frac{\partial \rho_0}{\partial \eta} \delta \vartheta(\eta) \right],$$

$$\frac{1}{c} \frac{\partial}{\partial t} \left[\eta \sin \theta \delta F_{(\theta)(\varphi)} \right] + \frac{\partial}{\partial \theta} \left[\sin \theta \left(1 - \frac{2m}{\eta} \right)^{\frac{1}{2}} \delta F_{(\varphi)(t)} \right] = 0, \quad (4.2.4)$$

$$\frac{1}{c} \frac{\partial}{\partial t} \left[\eta \left(1 - \frac{2m}{\eta} \right)^{\frac{1}{2}} \delta F_{(\varphi)(\eta)} \right] - \frac{\partial}{\partial \eta} \left[\eta \left(1 - \frac{2m}{\eta} \right)^{\frac{1}{2}} \delta F_{(\varphi)(t)} \right] = 0, \quad (4.2.5)$$

$$\frac{1}{c} \frac{\partial}{\partial t} \left[\eta \left(1 - \frac{2m}{\eta} \right)^{\frac{1}{2}} \delta F_{(\eta)(\theta)} \right] + \frac{\partial}{\partial \theta} \left[\eta \sin \theta \left(1 - \frac{2m}{\eta} \right)^{\frac{1}{2}} \delta F_{(\theta)(t)} \right] \quad (4.2.6)$$

$$-\frac{\partial}{\partial \theta} \delta F_{(r)(t)} = 0, \quad (4.2.7)$$

$$\frac{\partial}{\partial r} \left[r^2 \sin \theta \delta F_{(\theta)(\varphi)} \right] + \frac{\partial}{\partial \theta} \left[r \sin \theta \left(1 - \frac{2m}{r} \right)^{-\frac{1}{2}} \delta F_{(\varphi)(r)} \right] = 0, \quad (4.2.8)$$

$$-\frac{1}{c} \frac{\partial}{\partial t} \delta F_{(r)(t)} + \frac{1}{\sin \theta} \frac{\partial}{\partial \theta} \left[\frac{\sin \theta}{r} \left(1 - \frac{2m}{r} \right)^{\frac{1}{2}} \delta F_{(r)(\theta)} \right] \\ = 4\pi/c \left(1 - \frac{2m}{r} \right)^{\frac{1}{2}} \left(1 - \frac{v_0^2}{c^2} \right)^{-\frac{1}{2}} \varepsilon_0 \delta \vartheta(r), \quad (4.2.9)$$

$$-\frac{1}{c} \frac{\partial}{\partial t} \delta F_{(\theta)(t)} - \frac{1}{r} \left(1 - \frac{2m}{r} \right)^{\frac{1}{2}} \frac{\partial}{\partial r} \left[r \left(1 - \frac{2m}{r} \right)^{\frac{1}{2}} \delta F_{(r)(\theta)} \right] = 0, \quad (4.2.10)$$

$$-\frac{1}{c} \frac{\partial}{\partial t} \delta F_{(\varphi)(t)} + \frac{1}{r} \left(1 - \frac{2m}{r} \right)^{\frac{1}{2}} \frac{\partial}{\partial r} \left[r \left(1 - \frac{2m}{r} \right)^{\frac{1}{2}} \delta F_{(\varphi)(r)} \right] \\ - \frac{\partial}{\partial \theta} \left[\frac{1}{r} \left(1 - \frac{2m}{r} \right)^{\frac{1}{2}} \delta F_{(\theta)(\varphi)} \right] = \frac{4\pi}{c} \left(1 - \frac{2m}{r} \right)^{\frac{1}{2}} \left(1 - \frac{v_0^2}{c^2} \right)^{-\frac{1}{2}} v_0 \delta \varepsilon, \quad (4.2.11)$$

$$\frac{1}{r} \frac{\partial}{\partial r} \left[r^2 \delta F_{(r)(t)} \right] + \frac{1}{\sin \theta} \frac{\partial}{\partial \theta} \left[\sin \theta \left(1 - \frac{2m}{r} \right)^{-\frac{1}{2}} \delta F_{(\theta)(t)} \right] \\ = 4\pi r \left(1 - \frac{2m}{r} \right)^{-\frac{1}{2}} \left(1 - \frac{v_0^2}{c^2} \right)^{-\frac{1}{2}} \delta \varepsilon \quad (4.2.12)$$

and making use of the δ -functions for ρ_0 , α and β we get the pulsation equation.

Case 1. Differential rotation

In this case we have

$$(\bar{\rho}_0 z - x) \frac{m^2}{c^2} \frac{\partial^2}{\partial t^2} \delta \vartheta(r) - \frac{1}{R} \left(1 - \frac{r}{R} \right)^{\frac{1}{2}} \frac{\partial}{\partial R} \left[\left(1 - \frac{r}{R} \right) \frac{\partial}{\partial R} \left\{ R \left(1 - \frac{r}{R} \right)^{\frac{1}{2}} \right. \right. \\ \left. \left. \times (-\bar{\rho}_0 z + x) \delta \vartheta(r) \right\} \right] = -\frac{4\pi}{R} \omega \beta (1 + R^2 \omega^2)^{-\frac{1}{2}} \left(1 - \frac{r}{R} \right) \\ \times \frac{\partial}{\partial R} \left[R^2 \left(1 - \frac{r}{R} \right)^{\frac{1}{2}} (1 + R^2 \omega^2)^{\frac{1}{2}} \delta \vartheta(r) \right], \quad (4.2.13)$$

wherein

$$Z = 2\omega (1 - 2/R)^{\frac{1}{2}} \quad (4.2.14)$$

Using $\delta \mathcal{L}^{(n)} = \delta \mathcal{L}^2 / \delta t$ where \mathcal{L}^2 is the Lagrangian displacement and integrating with respect to time t , we get pulsation equation. Finally we set

$$\xi^r(r, t) = \xi^r(r) e^{i\sigma t} \quad (4.2.15)$$

and get the characteristic value equation for ξ^r

$$\begin{aligned} \frac{d}{dR} \left[\left(1 - \frac{2}{R}\right) \frac{d}{dR} \{(-\bar{\rho}_0 Z + X) Y\} \right] = & -4\pi\omega \bar{\rho} (1 - R^2 \omega^2)^{-\frac{1}{2}} \left(1 - \frac{2}{R}\right)^{\frac{1}{2}} \\ & \times \frac{d}{dR} \left[R(1 + R^2 \omega^2)^{\frac{1}{2}} Y \right] + \left(1 - \frac{2}{R}\right)^{-1} (-\bar{\rho}_0 Z + X) \frac{\omega^2 \sigma^2}{c^2} Y = 0 \end{aligned} \quad (4.2.16)$$

wherein $Y = R(1 - 2/R)^{\frac{1}{2}} \xi^r(r)$. To bring (4.2.16) into the self-adjoint form we impose the boundary condition $Y = 0$ at the two edges R_a and R_b and integrate it by parts after multiplying by $(-\bar{\rho}_0 Z + X)Y$. The resultant equation is

$$\begin{aligned} \frac{m^2 \sigma^2}{c^2} \int_{R_a}^{R_b} \left(1 - \frac{2}{R}\right)^{-1} (-\bar{\rho}_0 Z + X)^2 Y^2 dR = & \int_{R_a}^{R_b} \left(1 - \frac{2}{R}\right) \left[\frac{d}{dR} \{(-\bar{\rho}_0 Z + X) Y\} \right]^2 dR \\ & + 2\pi\omega \bar{\rho} \int_{R_a}^{R_b} Y^2 \left[(-\bar{\rho}_0 Z + X) \left(1 - \frac{2}{R}\right)^{-\frac{1}{2}} \left\{ 2\left(1 - \frac{2}{R}\right) R^2 \omega^2 (1 + R^2 \omega^2)^{-1} \right. \right. \\ & \left. \left. + 1 - \frac{3}{R} \right\} - R \left(1 - \frac{2}{R}\right)^{\frac{1}{2}} \frac{d}{dR} (-\bar{\rho}_0 Z + X) \right] dR \end{aligned} \quad (4.2.17)$$

which is the variational base corresponding to the characteristic value equation

$$\begin{aligned}
& \frac{d}{dR} \left[\left(1 - \frac{Z}{R}\right) \frac{d}{dR} \{ (-\bar{p}_0 Z + X) Y \} \right] - 2\pi\omega \bar{\beta} \left[\left(1 - \frac{Z}{R}\right)^{-\frac{1}{2}} \left\{ 2\left(1 - \frac{Z}{R}\right) R^2 \omega^2 (1 + R^2 \omega^2)^{-1} \right. \right. \\
& \left. \left. + 1 - \frac{3}{R} \right\} - \frac{R \left(1 - \frac{Z}{R}\right)^{\frac{1}{2}}}{(-\bar{p}_0 Z + X)} \frac{d}{dR} (-\bar{p}_0 Z + X) \right] Y \\
& + \frac{m^2 \sigma^2}{c^2} \left(1 - \frac{Z}{R}\right)^{-1} (-\bar{p}_0 Z + X) Y = 0
\end{aligned} \tag{4.2.18}$$

which is clearly a characteristic value equation of a self-adjoint operator.

Case 2. Rigid rotation

The variational base corresponding to a characteristic value equation for rigid rotation is

$$\begin{aligned}
& \frac{m^2 \sigma^2}{c^2} \int_{R_a}^{R_b} \left(1 - \frac{Z}{R}\right)^{-1} (-\bar{p}_0 Z + X)^2 Y^2 dR = \int_{R_a}^{R_b} \left(1 - \frac{Z}{R}\right) \left[\frac{d}{dR} \{ (-\bar{p}_0 Z + X) Y \} \right]^2 dR \\
& + 2\pi\omega \bar{\beta} \int_{R_a}^{R_b} Y^2 \left[(-\bar{p}_0 Z + X) \left(1 - \frac{Z}{R}\right)^{-\frac{1}{2}} \left(1 - \frac{1}{R}\right) \right. \\
& \left. - R \left(1 - \frac{Z}{R}\right)^{\frac{1}{2}} \frac{d}{dR} (-\bar{p}_0 Z + X) \right] dR,
\end{aligned} \tag{4.2.19}$$

wherein

$$Z = \omega \left(1 - \frac{Z}{R}\right)^{\frac{1}{2}} \left(1 - \frac{Z}{R} - R^2 \omega^2\right)^{\frac{1}{2}} \left(2 - \frac{Z}{R} - R^2 \omega^2\right) \tag{4.2.20}$$

and y satisfies same boundary condition as in case 1.

From the expressions (4.2.17) and (4.2.19) and the expressions for X , Y and \bar{p}_0 , we find that σ^2 is independent of charge density. We then choose R_a , R_b and evaluate

the integrals appearing on the right hand sides of (4.2.17) and (4.2.19) for different choices of ω such that $R_{\text{sing}} > R_b$ using a trial function $Y = (R - R_a)(R_b - R)$ which satisfies the same boundary condition as the true eigenfunction. For all the choices of ω we found that $\sigma^2 > 0$ indicating that the disks are stable.

Results and Discussions

We have considered in this Chapter pressureless thin disks of charged fluid with differential as well as rigid rotation and have found that in all cases the disk is stable under radial pulsations. The disk which is in equilibrium under gravitational, centrifugal and electromagnetic forces seems to adjust its material and field structure such that it can always retain the stability under perturbation. We find that $\bar{\rho}_0$ increases outward while electric field which is directed radially outward, increases in magnitude as R increases. The magnetic field always changes sign as we go from inner edge to outer edge indicating its role as a confining field. It is important to notice that we have several examples of disks which have their inner edge well within $6m$ and are stable under perturbations. This supports our view expressed in Chapter I concerning the significance of general relativistic effects in the study of disk structure.

In this analysis, though $B_r = 0$ along the equatorial plane $\theta = \pi/2$ to which the disk is confined, it should be recognised that B_r field outside the disk (above and below $\theta = \pi/2$ plane) will give rise to vertical forces which, in general, compress the disk from above and below. These do not affect the perturbations in radial direction but could give rise to plasma instabilities like 'pinch' and 'tearing mode' for a general perturbation.

Captions for the Tables

Tables 4.1	}	Profiles of velocity electromagnetic fields and density for differential and rigid rotations.
4.4		

Table 4.1

Differential Rotation

$$R_a = 2.1, \quad R_b = 10.0, \quad \omega = 0.037$$

R	V	Y	X	$c_o/10^2$
3.5	0.13	0.0	-0.99	0.01
3.8	0.14	0.37	-0.83	0.05
4.5	0.16	0.90	-0.65	0.15
5.1	0.19	1.27	-0.52	0.31
5.8	0.21	1.57	-0.41	0.52
6.8	0.24	1.92	-0.26	1.02
7.4	0.27	2.13	-0.15	1.58
8.1	0.29	2.32	-0.04	2.49
8.7	0.31	2.51	0.08	4.27
9.4	0.33	2.68	0.22	9.18
10.0	0.35	2.86	0.36	77.88

Table 4.2

Differential Rotation

$$R_a = 3.5, R_b = 50.0, \omega = 0.003$$

R	$V \times 10^2$	Y	$X \times 10$	$e_b / 10^3$
3.5	0.11	0.0	-0.62	0.56×10^{-6}
8.2	0.26	0.61	-0.42	0.04
12.8	0.41	0.91	-0.41	0.14
17.5	0.56	1.18	-0.38	0.34
22.1	0.71	1.46	-0.34	0.68
31.4	1.01	2.01	-0.23	1.93
36.1	1.17	2.29	-0.15	2.91
40.7	1.32	2.57	-0.07	4.18
45.4	1.47	2.85	0.03	5.78
47.7	1.54	2.99	0.08	6.71
50.0	1.62	3.13	0.13	7.75

Table 4.3

Rigid Rotation

$$R_a = 2.1, R_b = 10.0, \omega = 0.031$$

R	V	Y	X	ℓ_0
2.1	0.30	0.0	-0.34	0.02
2.9	0.16	0.44	-0.43	1.30
3.7	0.17	0.74	-0.46	5.14
4.5	0.19	0.98	-0.44	12.44
5.3	0.21	1.21	-0.38	24.64
6.1	0.23	1.43	-0.31	44.19
6.8	0.25	1.63	-0.21	75.78
7.6	0.28	1.84	-0.10	130.0
8.4	0.30	2.04	0.02	237.5
9.2	0.32	2.23	0.16	537.5
10.0	0.35	2.44	0.30	5567.0

Table 4.4

Rigid Rotation

$$R_a = 2.1, R_b = 50.0, \omega = 0.003$$

R	V	Y	X	ρ_0
2.1	0.003	0.0	-0.19	0.001
6.9	0.02	0.40	-0.35	13.87
11.7	0.04	0.70	-0.35	81.39
16.5	0.05	0.99	-0.34	247.9
21.3	0.06	1.27	-0.30	572.9
26.1	0.08	1.57	-0.26	11.50×10^2
30.8	0.09	1.86	-0.20	21.56×10^2
35.6	0.10	2.14	-0.14	39.96×10^2
40.4	0.12	2.43	-0.06	78.70×10^2
45.2	0.13	2.72	0.02	19.68×10^3
50.0	0.14	3.01	0.12	11.77×10^5

CHAPTER V

STRUCTURE AND STABILITY OF ROTATING THICK DISKS AROUND COMPACT OBJECTS : NEWTONIAN FORMULATION.

In chapter iv we considered pressureless infinitesimally thin disk confined to the equatorial plane of a Schwarzschild black hole. Forces other than the gravitational and centrifugal were the electromagnetic forces generated by the charges residing on the disk. However, if the pressure is not zero, the pressure gradient forces will cause the disks to be thick and its structure off the equatorial plane needs to be considered. In chapter I we have mentioned the work done by various authors on thick accretion disks. Thick accretion disks seem to be physically more plausible and as such we present our studies of thick disk with pressure but with zero charge density. Presently we study the disks in Newtonian formulation (Chakraborty and Prasanna II, 1981) and we shall consider the complete general relativistic discussion in the subsequent chapter.

1. STEADY STATE SOLUTION.

We assume a non-self gravitating perfect fluid disk around a compact object of mass M producing Newtonian gravitational field. The general set of equations governing the dynamics of such disks are obtained from equations (2.2.23) to (2.2.25) and (2.2.27) by putting $\epsilon = 0$, $c \rightarrow \infty$ and are given by the momentum equations

$$\rho \left[\frac{Dv^r}{Dt} + \frac{M G}{r^2} - \frac{(\omega \theta)^2 + (\omega \phi)^2}{r} \right] = - \frac{\partial p}{\partial r}, \quad (5.1.1)$$

$$\rho \left[\frac{Dv^\theta}{Dt} + \frac{v^r v^\theta}{r} - \frac{\cot \theta (v^\phi)^2}{r} \right] = -\frac{1}{r} \frac{\partial p}{\partial \theta} \quad (5.1.2)$$

$$\rho \left[\frac{Dv^\phi}{Dt} + \frac{v^r v^\phi}{r} + \frac{\cot \theta v^\theta v^\phi}{r} \right] = -\frac{1}{r \sin \theta} \frac{\partial p}{\partial \phi} \quad (5.1.3)$$

and the continuity equation,

$$\rho \left[\frac{1}{r^2} \frac{\partial}{\partial r} (r^2 v^r) + \frac{1}{r \sin \theta} \left\{ \frac{\partial}{\partial \theta} (\sin \theta v^\theta) + \frac{\partial v^\phi}{\partial \phi} \right\} \right] + \frac{D\rho}{Dt} = 0 \quad (5.1.4)$$

wherein the rate of change operator in the present case is given by

$$\frac{D}{Dt} = \frac{\partial}{\partial t} + v^r \frac{\partial}{\partial r} + \frac{v^\theta}{r} \frac{\partial}{\partial \theta} + \frac{v^\phi}{r \sin \theta} \frac{\partial}{\partial \phi} \quad (5.1.5)$$

We further assume for making the system determinate, the equation of state as expressed by the adiabatic law (equations 2.2.37 and 2.2.11)

$$\frac{D}{Dt} (p e^{-\gamma}) = 0 \quad (5.1.6)$$

As we assumed in the case of charged fluid disk (chapter iv), here also we shall restrict to the case of pure rotational flow as expressed by $v_o^r = 0$ and $v_o^\theta = 0$ and $v_o^\phi = v_o$. Further we assume the disk to be axisymmetric and therefore the steady state equations are given by:

$$\rho_o \left[\frac{M \omega}{r^2} - \frac{v_o^2}{r} \right] = -\frac{\partial p_o}{\partial r} \quad (5.1.7)$$

$$\rho_o v_o^2 \cot \theta = \frac{\partial p_o}{\partial \theta} \quad (5.1.8)$$

the remaining equations being identically satisfied. While solving the steady state equations for charged fluid disk we choose the velocity distribution and the charge density and then calcu.

lated the remaining steady state variables. In the present problem we find it more convenient to select a density distribution and then to calculate the remaining variables appearing in the steady state equations. In the case when ρ_0 is independent of θ these equations may be solved exactly. Thus considering

$$\rho_0 = \rho_0(r), \quad (5.1.9)$$

equations (5.1.7) and (5.1.8) together give the equation

$$-\frac{1}{r} \frac{\partial}{\partial \theta} (\rho_0 v_\theta^2) + \cot \theta \frac{\partial}{\partial r} (\rho_0 v_r^2) = 0, \quad (5.1.10)$$

whose solution is given by

$$\rho_0 v_\theta^2 = A r^K \sin^K \theta, \quad (5.1.11)$$

A and K being constants. Substituting these in (5.1.7) and (5.1.8) we get

$$\frac{\partial p_0}{\partial r} = A r^{K-1} \sin^K \theta - \frac{M G \rho_0}{r^2}, \quad (5.1.12)$$

$$\frac{\partial p_0}{\partial \theta} = A r^K \cot \theta \sin^K \theta \quad (5.1.13)$$

whose solution may be obtained as:

$$p_0 = \frac{A}{K} r^K \sin^K \theta - M G \int \frac{\rho_0 dr}{r^2} + B \quad (5.1.14)$$

for $K \neq 0$. For the case $k=0$, the pressure is given by

$$p_0 = A \ln(r \sin \theta) - M G \int \frac{\rho_0 dr}{r^2} + B. \quad (5.1.15)$$

Assuming

$$\rho_0 = \rho_c (r/m)^L \quad (5.1.16)$$

wherein $m (= M G / c^2)$, ρ_c and L are constants the expressions

for p_0 are given by

$$p_0 = -\frac{M G_c \rho_c}{m \ell} \frac{r^{\ell-1}}{(\ell-1)} + \frac{A}{K} r^K \sin^K \theta + B, \quad \ell \neq 1, K \neq 0, (5.1.17)$$

$$p_0 = -\frac{M G_c \rho_c}{m \ell} \frac{r^{\ell-1}}{(\ell-1)} + A \ln(r \sin \theta) + B, \quad \ell \neq 1, K=0, (5.1.18)$$

$$p_0 = -\frac{M G_c \rho_c}{m} \ln r + \frac{A}{K} r^K \sin^K \theta + B, \quad \ell=1, K \neq 0, (5.1.19)$$

and

$$p_0 = A \ln(\sin \theta) + \left(A - \frac{M G_c \rho_c}{m}\right) \ln r + B, \quad \ell=1, K=0. (5.1.20)$$

The special case when $k=-2$ and $\ell=0$, corresponds to that of Fishbone and Moncrief. The whole class of solutions obtained above are all physically plausible provided the pressure satisfies the condition $p_0 > 0$ throughout the interior of the disk and $p_0=0$ over the boundary. The constants A and B may be obtained by using the relation $p_0=0$ at r_a and r_b , the inner and outer edges at the plane $\theta = \pi/2$ and from $p_0 > 0$ we can obtain the condition relating k and ℓ . Evaluating the constants thus, we have the pressure given by the expressions

$$\frac{p_0}{c^2} = \frac{\rho_c}{(\ell-1)(b^K - a^K)} \left\{ (b^{\ell-1} - a^{\ell-1}) R^K \sin^K \theta - R^{\ell-1} (b^K - a^K) + b^K a^{\ell-1} - a^K b^{\ell-1} \right\}, \quad \ell \neq 1, K \neq 0, (5.1.21)$$

$$\frac{p_0}{c^2} = \frac{\rho_c}{(\ell-1)(\ln b - \ln a)} \left\{ (b^{\ell-1} - a^{\ell-1}) \ln(R \sin \theta) - R^{\ell-1} (\ln b - \ln a) + a^{\ell-1} \ln b - b^{\ell-1} \ln a \right\}, \quad \ell \neq 1, K=0, (5.1.22)$$

$$\frac{p_0}{c^2} = \frac{\rho_c}{(b^K - a^K)} \left\{ R^K \sin^K \theta (\ln b - \ln a) - (b^K - a^K) \ln R + b^K \ln a - a^K \ln b \right\}, \quad \ell=1, K \neq 0 (5.1.23)$$

and $p_0 = 0$ for $\ell = 1$, $k=0$. In the above R, a, b are dimensionless quantities denoting r/m , r_a/m and r_b/m respectively. In order to get the boundary θ_e of the disk off the equatorial plane we solve these equations $p_0 = 0$ for $\sin \theta_e$ and thus every ' r ' we get θ_e and $(\pi - \theta_e)$, corresponding to the edge of the disk in the meridional plane. Finally using the condition that $p_0 > 0$ throughout the interior of the disk we get the criterion connecting k and ℓ as $K < \ell - 1$. If $K = \ell - 1$ then it follows immediately that $p_0 = 0$, $\theta = \pi/2$ and

$$v_0^2 = \frac{M G_r}{r_2} \quad (5.1.24)$$

showing that the disk is a pressureless thin disk confined to the equatorial plane and having Keplerian motion, a well-known result. Thus the non-zero pressure would definitely require a structure off the equatorial plane. As ℓ and k are then related through $K < \ell - 1$, taking $\ell - 1 = k + n$, n being a positive real number, we can write the velocity function to be

$$v_0^2 = A \left(\frac{M G_r}{R^{n+\ell}} \right) \sin^k \theta \quad (5.1.25)$$

where the constant ' A ' for the three different cases is given by:

$$\begin{aligned} A &= \frac{k}{\ell-1} \left(\frac{b^{\ell-1} - a^{\ell-1}}{b^k - a^k} \right), & k \neq 0, \ell \neq 1, \\ A &= \frac{1}{\ell-1} \left(\frac{b^{\ell-1} - a^{\ell-1}}{\ln b - \ln a} \right), & k = 0, \ell \neq 1, \\ A &= k \left(\frac{\ln b - \ln a}{b^k - a^k} \right), & k \neq 0, \ell = 1. \end{aligned} \quad (5.1.26)$$

2. STABILITY ANALYSIS.

In order to discuss the stability of the configuration we perturb the system and consider the equations governing the axisymmetric perturbations and perform the normal mode analysis restricting the perturbations to linear terms only. The general procedure we use is as given by Chandrasekhar and Friedman (I, II 1972) and as outlined in Chapter II. The complete set of equations governing the perturbations may be obtained from equations (2.2.42) to (2.2.44) and (2.2.46) which in the Newtonian limit are given by

$$\rho_0 \left[\frac{\partial}{\partial t} \delta v^r - \frac{2}{r} v_0 \delta v^\theta \right] + \delta p \left[\frac{M G}{r^2} - \frac{v_0^2}{r} \right] = - \frac{\partial}{\partial r} \delta p, \quad (5.2.1)$$

$$\rho_0 \left[\frac{\partial}{\partial t} \delta v^\theta - \frac{2}{r} \cot \theta v_0 \delta v^\theta \right] + \delta p \frac{v_0^2}{r} \cot \theta = - \frac{1}{r} \frac{\partial}{\partial \theta} \delta p, \quad (5.2.2)$$

$$\frac{\partial}{\partial t} \delta v^\theta + \frac{1}{r} \left(\frac{\partial v_0}{\partial \theta} + v_0 \cot \theta \right) \delta v^\theta + \left(\frac{\partial v_0}{\partial r} + \frac{v_0}{r} \right) \delta v^r = 0, \quad (5.2.3)$$

$$\rho_0 \left[\frac{1}{r^2} \frac{\partial}{\partial r} (r^2 \delta v^r) + \frac{1}{r \sin \theta} \frac{\partial}{\partial \theta} (\sin \theta \delta v^\theta) \right] + \frac{\partial}{\partial t} \delta p + \delta v^r \frac{\partial \rho_0}{\partial r} + \frac{\delta v^\theta}{r} \frac{\partial \rho_0}{\partial \theta} = 0, \quad (5.2.4)$$

whereas the condition of adiabaticity gives

$$\frac{\partial}{\partial t} (\bar{e}_0^r - r \bar{p}_0 \bar{e}_0^{-r-1} \delta p) + \delta v^r \frac{\partial}{\partial r} (\bar{p}_0 \bar{e}_0^{-r}) + \frac{\delta v^\theta}{r} \frac{\partial}{\partial \theta} (\bar{p}_0 \bar{e}_0^{-r}) = 0. \quad (5.2.5)$$

We introduce the Lagrangian displacement ξ^α , ($\alpha = r, \theta$) through the relation

$$\frac{\partial \xi^\alpha}{\partial t} = \delta v^\alpha, \quad \xi^\alpha(r, \theta, t) = \xi^\alpha(r, \theta) e^{i\sigma t} \quad (5.2.6)$$

Denoting the perturbed variables to represent only their spatial parts we obtain after some rearrangement of terms the following

set of equations governing the perturbations:

$$\delta\varphi = -\frac{1}{\bar{\eta}} \left(\frac{\partial\varphi_0}{\partial\theta} + \cot\theta \varphi_0 \right) \bar{\xi}^\theta - \left(\frac{\partial\varphi_0}{\partial\bar{\eta}} + \frac{\varphi_0}{\bar{\eta}} \right) \bar{\xi}^{\bar{\eta}}, \quad (5.2.7)$$

$$\delta\rho = -\rho_0 \left[\frac{1}{\bar{\eta}^2} \frac{\partial}{\partial\bar{\eta}} (\bar{\eta}^2 \bar{\xi}^{\bar{\eta}}) + \frac{1}{\bar{\eta} \sin\theta} \frac{\partial}{\partial\theta} (\sin\theta \bar{\xi}^\theta) \right] - \bar{\xi}^{\bar{\eta}} \frac{\partial\rho_0}{\partial\bar{\eta}} - \frac{\bar{\xi}^\theta}{\bar{\eta}} \frac{\partial\rho_0}{\partial\theta}, \quad (5.2.8)$$

$$\delta p = -\bar{\rho}_0 \left[\frac{1}{\bar{\eta}^2} \frac{\partial}{\partial\bar{\eta}} (\bar{\eta}^2 \bar{\xi}^{\bar{\eta}}) + \frac{1}{\bar{\eta} \sin\theta} \frac{\partial}{\partial\theta} (\sin\theta \bar{\xi}^\theta) \right] - \bar{\xi}^{\bar{\eta}} \frac{\partial p_0}{\partial\bar{\eta}} - \frac{\bar{\xi}^\theta}{\bar{\eta}} \frac{\partial p_0}{\partial\theta}, \quad (5.2.9)$$

$$-\rho_0 \bar{\xi}^{\bar{\eta}} = \frac{2\rho_0 \varphi_0}{\bar{\eta}} \delta\varphi - \left(\frac{M_0}{\bar{\eta}^2} - \frac{\varphi_0^2}{\bar{\eta}} \right) \delta\rho - \frac{\partial}{\partial\bar{\eta}} \delta p, \quad (5.2.10)$$

$$-\rho_0 \bar{\xi}^\theta = \frac{2\rho_0 \varphi_0}{\bar{\eta}} \cot\theta \delta\varphi + \frac{\varphi_0^2}{\bar{\eta}} \cot\theta \delta\rho - \frac{1}{\bar{\eta}} \frac{\partial}{\partial\theta} \delta p. \quad (5.2.11)$$

Equations (5.2.7) to (5.2.9) are the initial value equations obtained after integrating once with respect to time while (5.2.10) and (5.2.11) are the pulsation equations obtained by putting the form (5.2.6) for the time dependence of the Lagrangian displacements. Equations (5.2.10) and (5.2.11) have to be solved as an eigenvalue problem consistently with the equations (5.2.7) to (5.2.9) with proper boundary conditions. Equation (5.2.9) being the condition of adiabaticity, is identical with (using 5.2.8)

$$\frac{\Delta p}{p} = \gamma \frac{\Delta \rho}{\rho}$$

wherein Δp and $\Delta \rho$ are the Lagrangian perturbations in p and ρ . At the edge of the disk we need the boundary condition $\Delta p = 0$, which is satisfied by restricting $\bar{\xi}^\alpha$ and their derivatives to remain finite everywhere.

Following the procedure of Chandrasekhar and Friedman (loc.cit), we multiply the dynamical equations (5.2.10) and (5.2.11) by $\bar{\xi}^{\bar{\eta}}$ and $\bar{\xi}^\theta$ respectively, add them and integrate

with respect to r and θ over the entire region of the disk. Here $\bar{\xi}^r$ and $\bar{\xi}^\theta$ are the 'trial functions' which satisfy the same boundary conditions as the true eigen functions ξ^r and ξ^θ but otherwise completely arbitrary. By performing several integrations by parts and using the steady state relations, we can then bring the resultant equation, to symmetrical form in barred and unbarred displacements, as given by

$$\begin{aligned}
 & \sigma^2 \iint \rho_0 r^2 \sin \theta (\bar{\xi}^r \xi^r + \bar{\xi}^\theta \xi^\theta) dr d\theta \\
 &= \iint \left\{ 2\rho_0 r v_0 \sin \theta \left\{ \left(\frac{\partial v_0}{\partial r} + \frac{v_0}{r} \right) \bar{\xi}^r \xi^r + \frac{\omega r \theta}{r} \left(\frac{\partial v_0}{\partial \theta} + \omega \theta v_0 \right) \bar{\xi}^\theta \xi^\theta \right. \right. \\
 &+ \left. \frac{v_0^2}{r} \omega \theta (\bar{\xi}^\theta \xi^\theta + \bar{\xi}^r \xi^r) \right\} dr d\theta - Mg \iint \frac{\partial \rho_0}{\partial r} \sin \theta \bar{\xi}^r \xi^r dr d\theta \\
 &+ \iint v_0^2 r \sin \theta \left\{ \bar{\xi}^r \xi^r \frac{\partial \rho_0}{\partial r} + \frac{\bar{\xi}^\theta \xi^\theta}{r} \omega \theta \frac{\partial \rho_0}{\partial \theta} \right\} dr d\theta \\
 &- \iint \left\{ r^4 \sin \theta \bar{\xi}^r \xi^r \frac{\partial}{\partial r} \left(\frac{1}{r^2} \frac{\partial \rho_0}{\partial r} \right) + \sin^2 \theta \bar{\xi}^\theta \xi^\theta \frac{\partial}{\partial \theta} \left(\frac{1}{\sin \theta} \frac{\partial \rho_0}{\partial \theta} \right) \right\} dr d\theta \\
 &- \iint \left\{ \rho_0 \frac{\partial}{\partial r} (r^2 \bar{\xi}^r) \frac{\partial}{\partial \theta} (\sin \theta \xi^\theta) + \rho_0 \frac{\partial}{\partial \theta} (\sin \theta \bar{\xi}^\theta) \frac{\partial}{\partial r} (r \xi^r) \right. \\
 &- \rho_0 \frac{\partial}{\partial \theta} (r \bar{\xi}^r) \frac{\partial}{\partial r} (\sin \theta \xi^\theta) - \rho_0 \frac{\partial}{\partial r} (\sin \theta \bar{\xi}^\theta) \frac{\partial}{\partial \theta} (r \xi^r) \\
 &- \left. (\bar{\xi}^\theta \xi^r + \bar{\xi}^r \xi^\theta) \sin \theta \frac{\partial \rho_0}{\partial \theta} \right\} dr d\theta \\
 &+ \iint \left\{ \frac{\rho_0 \sin \theta}{r^2} \frac{\partial}{\partial r} (r^2 \bar{\xi}^r) \frac{\partial}{\partial r} (r^2 \xi^r) \right. \\
 &+ \frac{\rho_0}{r} \left[\frac{\partial}{\partial r} (r^2 \bar{\xi}^r) \frac{\partial}{\partial \theta} (\sin \theta \xi^\theta) + \frac{\partial}{\partial \theta} (\sin \theta \bar{\xi}^\theta) \frac{\partial}{\partial r} (r^2 \xi^r) \right. \\
 &+ \left. \left. \frac{\rho_0}{\sin \theta} \frac{\partial}{\partial \theta} (\sin \theta \bar{\xi}^\theta) \frac{\partial}{\partial \theta} (\sin \theta \xi^\theta) \right\} dr d\theta .
 \end{aligned}$$

As shown by Chandrasekhar and Friedman, the symmetrical form of σ^2 equation implies a variational principle; for identifying $\bar{\xi}^\alpha$ with ξ^α one can write the following equation for σ^2 :

$$\begin{aligned}
 & \sigma^2 \iint \rho_0 r^2 \sin \theta (\xi^2 r^2 + \xi^2 \theta^2) dr d\theta \\
 &= \iint 2\rho_0 v_0 r \sin \theta \left\{ \left(\frac{\partial \theta_0}{\partial r} + \frac{v_0}{r} \right) \xi^2 r^2 + \frac{\cot \theta}{r} \left(\frac{\partial \theta_0}{\partial \theta} + \cot \theta v_0 \right) \xi^2 \theta^2 \right. \\
 &+ \left. \frac{2v_0}{r} \cot \theta \xi^2 r \xi^2 \theta \right\} dr d\theta - M_0 \iint \frac{\partial \rho_0}{\partial r} \sin \theta \xi^2 r^2 dr d\theta \\
 &- \iint \left\{ r^4 \sin \theta \xi^2 r^2 \frac{\partial}{\partial r} \left(\frac{1}{r^2} \frac{\partial p_0}{\partial r} \right) + \sin^2 \theta \xi^2 \theta^2 \frac{\partial}{\partial \theta} \left(\frac{1}{\sin \theta} \frac{\partial p_0}{\partial \theta} \right) \right\} dr d\theta \\
 &+ \iint v_0^2 r \sin \theta \left\{ \xi^2 r^2 \frac{\partial \rho_0}{\partial r} + \frac{\xi^2 \theta^2}{r} \cot \theta \frac{\partial \rho_0}{\partial \theta} \right\} dr d\theta - \iint \left\{ 2p_0 \left[\frac{\partial}{\partial r} (r \xi^2 r) \right. \right. \\
 &\times \left. \left. \frac{\partial}{\partial \theta} (\sin \theta \xi^2 \theta) - \frac{\partial}{\partial \theta} (r \xi^2 r) \frac{\partial}{\partial \theta} (\sin \theta \xi^2 \theta) \right] - 2 \frac{\partial p_0}{\partial \theta} \sin \theta \xi^2 r^2 \xi^2 \theta \right\} dr d\theta \\
 &+ \gamma \iint \left[\left[\frac{p_0}{r^2} \sin \theta \left\{ \frac{\partial}{\partial r} (r^2 \xi^2 r) \right\}^2 + \frac{2p_0}{r} \frac{\partial}{\partial r} (r^2 \xi^2 r) \frac{\partial}{\partial \theta} (\sin \theta \xi^2 \theta) \right. \right. \\
 &\left. \left. + \frac{p_0}{\sin \theta} \left\{ \frac{\partial}{\partial \theta} (\sin \theta \xi^2 \theta) \right\}^2 \right] dr d\theta. \quad (5.2.13)
 \end{aligned}$$

Now if one evaluates (5.2.13) by two trial displacements ξ^α and $\xi^\alpha + \delta \xi^\alpha$ such that the resultant variation in σ^2 is $\delta \sigma^2$, and trace back the calculations that lead to (5.2.12) starting from (5.2.7) - (5.2.11), one gets

$$\begin{aligned}
 & \delta \sigma^2 \iint \rho_0 r^2 \sin \theta (\xi^2 r^2 + \xi^2 \theta^2) dr d\theta \\
 &= \iint -2\delta \xi^2 r^2 \sin \theta \left[\rho_0 \sigma^2 \xi^2 r + \frac{2\rho_0 v_0}{r} \delta \theta \varphi - \left(\frac{M_0}{r^2} - \frac{v_0^2}{r} \right) \delta \rho \right. \\
 &\left. - \frac{\partial}{\partial r} \delta p \right] dr d\theta + \iint -2\delta \xi^2 \theta^2 \sin \theta \left[\rho_0 \sigma^2 \xi^2 \theta \right.
 \end{aligned}$$

$$+ \frac{2\rho_0 v_0}{r} \cot \theta \delta \psi + \frac{v_0^2}{r} \cot \theta \delta \rho - \frac{1}{r} \frac{\partial}{\partial \theta} \delta p \Big] dr d\theta. \quad (5.2.14)$$

It is clear from (5.2.14) that demanding $\delta \sigma^2 = 0$, amounts to solving the original eigenvalue equations (5.2.10) and (5.2.11) along with the initial value equations (5.2.7) to (5.2.9). To meet this requirement we choose trial functions for ξ^r and ξ^θ which satisfy the required boundary condition and which have adjustable parameters α, β, \dots etc. We then extremize σ^2 as obtained by using such ξ^r and ξ^θ in (5.2.13), with respect to the adjustable parameters α, β, \dots etc. Rewriting the equation (5.2.13) in terms of dimensionless quantities R , and $V_0 (= \frac{v_0}{c})$, we get

$$\begin{aligned} & \frac{m^2 \sigma^2}{c^2} \iint \left[\rho_0 R^2 \sin \theta (\xi^r{}^2 + \xi^\theta{}^2) \right] dR d\theta \\ &= \iint \left[2\rho_0 V_0 R \sin \theta \left(\frac{\partial V_0}{\partial R} + \frac{V_0}{R} \right) \xi^r{}^2 - \frac{\partial \rho_0}{\partial R} \sin \theta \xi^r{}^2 - R^4 \sin \theta \frac{\xi^r{}^2}{c^2} \frac{\partial}{\partial R} \left(\frac{1}{R^2} \frac{\partial p_0}{\partial R} \right) \right. \\ & \quad \left. + V_0^2 R \sin \theta \xi^r{}^2 \frac{\partial \rho_0}{\partial R} \right] dR d\theta + \iint \left[2\rho_0 V_0 \cos \theta \left(\frac{\partial V_0}{\partial \theta} + \cot \theta V_0 \right) \xi^\theta{}^2 \right. \\ & \quad \left. - \sin^2 \theta \frac{\xi^\theta{}^2}{c^2} \frac{\partial}{\partial \theta} \left(\frac{1}{\sin \theta} \frac{\partial p_0}{\partial \theta} \right) + \xi^\theta{}^2 V_0^2 \cos \theta \frac{\partial \rho_0}{\partial \theta} \right] dR d\theta + \iint \left[4\rho_0 V_0^2 \cos \theta \xi^r \xi^\theta \right. \\ & \quad \left. - \frac{2p_0}{c^2} \frac{\partial}{\partial R} (R \xi^r) \frac{\partial}{\partial \theta} (\sin \theta \xi^\theta) + \frac{2p_0}{c^2} \frac{\partial}{\partial \theta} (R \xi^r) \frac{\partial}{\partial R} (\sin \theta \xi^\theta) \right. \\ & \quad \left. + \frac{2}{c^2} \frac{\partial p_0}{\partial \theta} \sin \theta \xi^r \xi^\theta \right] dR d\theta + \gamma \iint \left[\frac{p_0}{R^2 c^2} \sin \theta \left\{ \frac{\partial}{\partial R} (R^2 \xi^r) \right\}^2 + \frac{p_0}{\sin \theta c^2} \right. \\ & \quad \left. \times \left\{ \frac{\partial}{\partial \theta} (\sin \theta \xi^\theta) \right\}^2 + \frac{2p_0}{R c^2} \frac{\partial}{\partial R} (R^2 \xi^r) \frac{\partial}{\partial \theta} (\sin \theta \xi^\theta) \right] dR d\theta. \quad (5.2.15) \end{aligned}$$

In order to evaluate σ^2 , we choose two kinds of trial functions (i) with fixed boundary, i.e. the Lagrangian displacements ξ^{α} vanish at the boundary and (ii) expanding or contracting boundary.

(i) Corresponding to the three different types of solutions (5.1.21) - (5.1.23), we choose a function 'q'

$$q = \sin^k \theta - \frac{k}{AR^k} \left(\frac{R^{\ell-1}}{\ell-1} - B \right), \quad \ell \neq 1, k \neq 0, \quad (5.2.15)$$

$$q = \sin \theta - \exp \left\{ -\frac{R^{\ell-1}}{A(\ell-1)} - \frac{B}{A} - \ln R \right\}, \quad \ell \neq 1, k=0, \quad (5.2.17)$$

$$q = \sin^k \theta - \frac{k}{AR^k} (\ln R - B), \quad \ell = 1, k \neq 0, \quad (5.2.18)$$

which vanishes at the boundary and take

$$\xi^r = q + \alpha q^2, \quad \xi^\theta = q + \beta q^2, \quad (5.2.19)$$

wherein α and β are adjustable parameters determined by extremising the expression for σ^L . With this choice of ξ^r and ξ^θ in (5.2.17) we evaluate the critical value of adiabatic index γ_c , for $\sigma^L = 0$, which would give the neutral stability.

(ii) In the case of nonstationary boundary we first consider the case of radial perturbation with $\xi^\theta = 0$. The equations governing such radial perturbation are obtained from the original set of equations (5.2.7) to (5.2.11) as follows:

$$\delta \psi = - \left(\frac{\partial \psi_0}{\partial r} + \frac{\psi_0}{r} \right) \xi^r, \quad (5.2.20)$$

$$\delta \rho = - \frac{\rho_0}{r^2} \frac{\partial}{\partial r} (r^2 \xi^r) - \xi^r \frac{\partial \rho_0}{\partial r}, \quad (5.2.21)$$

$$\delta p = - \frac{\gamma p_0}{r^2} \frac{\partial}{\partial r} (r^2 \xi^r) - \xi^r \frac{\partial p_0}{\partial r}, \quad (5.2.22)$$

$$-\rho_0 \sigma^L \xi^r = \frac{2\rho_0 \psi_0}{r^2} \delta \psi - \left(\frac{M G_0}{r^2} - \frac{\psi_0^L}{r} \right) \delta \rho - \frac{\partial}{\partial r} \delta p, \quad (5.2.23)$$

$$2 \frac{\rho_0 \psi_0}{r} \cot \theta \delta \psi + \frac{\psi_0^L}{r} \cot \theta \delta \rho - \frac{1}{r} \frac{\partial}{\partial \theta} \delta p = 0. \quad (5.2.24)$$

Using initial value equations (5.2.20) to (5.2.22) in (5.2.24) and assuming ξ^2 to be a function of r only we obtain the differential equation

$$(1-r) \frac{d}{dr} (r^2 \xi^2) + 2 r \xi^2 = 0 \quad (5.2.21)$$

for ξ^2 , whose solution is given by

$$\xi^2 = \eta r^{\frac{4-2r}{r-1}} \quad (5.2.26)$$

where η is constant of integration. Using this solution for ξ^2 in (5.2.23) we get

$$\begin{aligned} \rho_0 \sigma^2 \xi^2 = \eta \frac{\rho_c M G}{m^k} & \left\{ \frac{2r(3r-5)}{(r-1)^2} B \right. \\ & + A \sin^k \theta \frac{(3r-5)(kr-k+2r)}{k(r-1)^2} r^k \\ & + \left[\frac{4-2r}{r-1} - \frac{2r}{(r-1)(k-1)} \left(\frac{3r-5}{r-1} \right) \right] r^{k-1} \Big\} r^{\frac{6-4r}{r-1}}, \\ & \quad \ell \neq 1, k=0, \quad (5.2.27) \end{aligned}$$

$$\begin{aligned} \rho_0 \sigma^2 \xi^2 = \eta \frac{\rho_c M G}{m^k} & \left\{ \frac{2r(3r-5)}{(r-1)^2} B \right. \\ & + 2A \ln\left(\frac{r}{m} \sin \theta\right) \frac{(3r-5)}{(r-1)^2} + A \frac{(3r-5)}{r-1} \\ & + \left[\frac{4-2r}{r-1} - \frac{2r}{(r-1)(k-1)} \left(\frac{3r-5}{r-1} \right) \right] r^{k-1} \Big\} r^{\frac{6-4r}{r-1}}, \\ & \quad \ell \neq 1, k=0, \quad (5.2.28) \end{aligned}$$

$$\rho_0 \sigma^2 \xi^2 = \eta \frac{\rho_c M G}{m} \left\{ \frac{2r(3r-5)}{(r-1)^2} B \right.$$

$$+ A \sin k_{\theta} \frac{(3r-5)(kr-k+2r)}{k(r-1)^2} r^k \\ + \left(\frac{4-2r}{r-1} \right) - \left(\frac{4r}{r-1} \right) \frac{2r}{r-1} \left(\frac{3r-5}{r-1} \right) \left\{ r^{\frac{6-4r}{r-1}} \right\},$$

$$\ell = 1, k \neq 0. \quad (5.2.29)$$

For the special case of ordinary gas with $\Gamma = 5/3$ the above equations for σ^2 reduce to a very simple form

$$\sigma^2 = Mg/r^3 \quad (5.2.30)$$

showing that the disks are stable with 'local' frequency being proportional to $r^{-3/2}$ irrespective of the other parameters like ℓ, k, a and b . Incidentally this value of $\Gamma = 5/3$ makes the function ξ^r to be ηr which is exactly the form as used by Bisnovatyi-Kogan and Blinnikov (1972) for analysing the stability of thin gas disks against expansion and contraction. It is interesting to note that the frequency obtained above is also the same for the radial oscillation of a pressureless disk confined to $\theta = \pi/2$ plane and is Keplerian motion with $\vartheta_0 = \sqrt{Mg/r}$.

as may be seen from equations (5.2.20) to (5.2.23) with $\delta\beta = 0$.

To consider the stability with non-stationary boundary and with axisymmetric perturbations we choose

$$\xi^r = R + \alpha q, \quad \xi^{\theta} = R + \beta q \quad (5.2.31)$$

evaluate σ^2 as given by (5.2.15) and calculate r_{c_2} by setting $\sigma^2 = 0$ after extremizing it by adjusting α and β as in the case (i). From the expressions of σ^2 in all the above case we find that σ^2 is independent of the constant C_c which we

take as unity.

Discussion and Conclusions.

As the general solution obtained above refers to a class of solutions with parameters ℓ and k referring to different density and velocity distributions, we have considered a number of cases for various values of ℓ and k for different cases of disk radii. The thickness of the disk vary from case to case depending upon the density and velocity distributions. The general structure of the disks are presented through figures and tables. Figures (5.1) and (5.2) show the upper half of the meridional section (r, θ) plane for two typical cases with (i) $a=4$, $b=20$, $\ell=1$, $k=-1$ and (ii) $a=4$, $b=100$, $\ell=0$, $k=-2$. For these two cases the corresponding profiles of pressure, density and velocity as a function of the equatorial distance are plotted in figures (5.3) and (5.4).

Study of number of cases for the disk structure revealed that the maximum thickness h_m ($h_m = R \cos \theta_m$, θ_m being the minimum value of θ for a given disk) of the disk as well as the shape change with the velocity (n) and density (ℓ) profiles of the disk. For a disk with $a=4$, $b=20$, plots (5.5), (5.6), (5.7) and (5.6) reveal the nature of such changes. As may be seen from the plots (5.5) and (5.6) the maximum thickness increases as ' n ' increases, which is in conformity with the known result that disks with larger angular momentum are thinner than the ones with lesser angular momentum. Also as regard the shape of the disks the maximum thickness occurs

nearer to the inner edge as 'n' increases. Figure (5.7) shows the variation of the maximum thickness with the density distribution for different values of n. As may be seen the maximum thickness raises slowly as ℓ increases, attaining a maximum around $\ell = -2$ to $\ell = 0$ for $n=1$ to 7, and then falls off rapidly as ℓ increases, which is consistent with normal distributions.

As regards the onset of instability, as we remarked above we evaluate the critical adiabatic index γ_c ; by setting $\sigma^2 = 0$ for different values of a, b, n and ℓ . Tables (5.1)-(5.6) show the values of γ_c (we found that $\gamma < \gamma_c$ for the instability) for different ℓ , n, a and b. The tables also show the value of the ratio of the kinetic energy to potential energy ($I\Omega^2/|W|$) for each disk. Normally in the case of self-gravitating fluid sphere if there is rotation then the criterion for stability differs from $\gamma = 4/3$ to $\gamma - 4/3 = -(2/9)I\Omega^2/|W|$ (Lebovitz, 1970) showing an increase in the range of stability. However we find that there is no such simple relation connecting γ_c and the energy ratio for the case of rotating disks. The critical γ however has always been less than 4/3 indicating that all the cases considered here correspond to stable configurations under axisymmetric perturbations.

We have thus found that ordinary perfect fluid ($\gamma = 5/3$) disks rotating around massive objects are stable under radial pulsations with frequency $\sqrt{MG/r^3}$ (Kato and Fukue (1980) and Cox (1981) have also considered the local and quasi radial oscillations of a thin gaseous disk in Schwarzschild back

ground, when $\rho_0 \ll \rho_0 c^2$). In this case the boundary could be expanding or contracting as given by the amplitude function

$\xi^r = \eta r$ on the other hand if the perturbations are axisymmetric the critical γ is much less than $4/3$ thus indicating stability of such disks. From this detailed study, it appears as though that the dynamical configuration of a rotating disk around massive object is similar to that of a self-gravitating fluid sphere.

Captions for Figures and Tables.

Figure 5.1 : Upper half of the meridional section of the disk for $a=4.0, b=20.0, \ell=1, k=-1$. The shaded portion is the section of the central massive object with $R=2$.

Figure 5.2 : Same as figure 5.1 with $a=4.0, b=100, \ell=0, K=-2$.

Figure 5.3 : Profiles of pressure, density and velocity at $\theta=\pi/2$ plane for the disk described in figure 5.1

Figure 5.4 : Profiles of pressure, density and velocity at $\theta=\pi/2$ plane for the disk described in Figure 5.2

Figure 5.5.: Maximum height $h_m = R \cos \theta_m$ as function of n for different values of ℓ for the disk with $a=4.0, b=20.0$.

Figure 5.6: The distance $\hat{R} = R \sin \theta_m$ of the point where the thickness is maximum as function of n for different values of ℓ .

Figure 5.7: Maximum height $h_m = R \cos \theta_m$ as function of ℓ for different values of n .

Figure 5.8: The distance $\hat{R} = R \sin \theta_m$ as function of ℓ for different values of n .

Table 5.1: Ratio of kinetic energy to potential energy

$I \Omega^2 / |W|$ and γ_c for disk with $a=4.0$, $b=100.0$,

$\ell = -3$ and different values of n . γ_{c_1} refers to the case when $\xi^n = q + \alpha q^2$ and $\xi^0 =$

$q + \beta q^2$ while γ_{c_2} refers to the case when

$\xi^n = R + \alpha q$, $\xi^0 = R + \beta q$

Table 5.2 - : Same as table 5.1 with different a, b and ℓ .

5.6 :

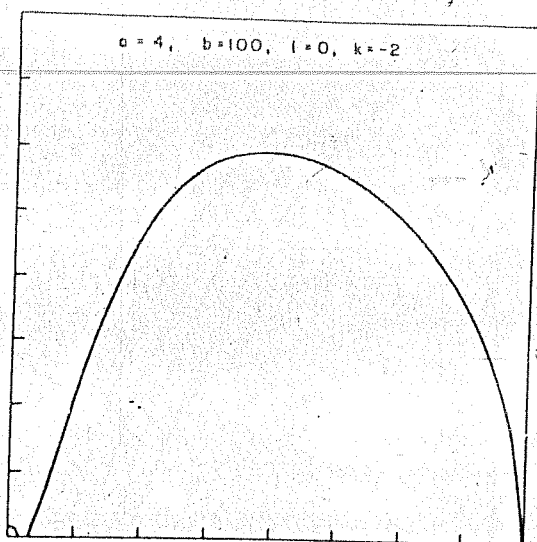


Fig 5.1

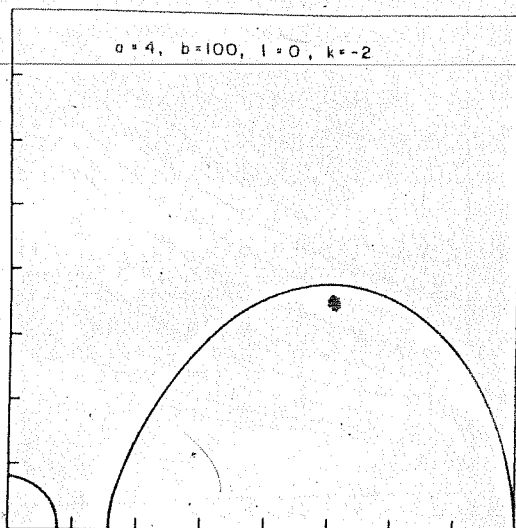


Fig 5.2

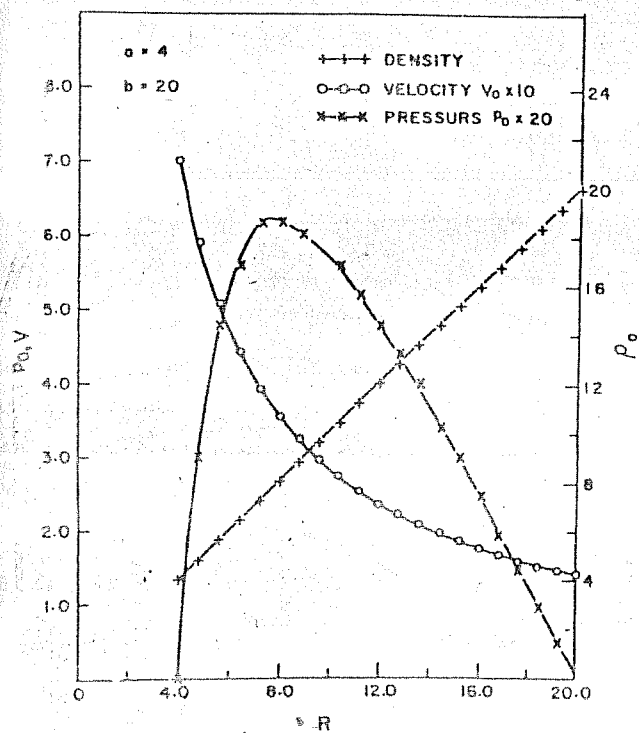


Fig 5.3

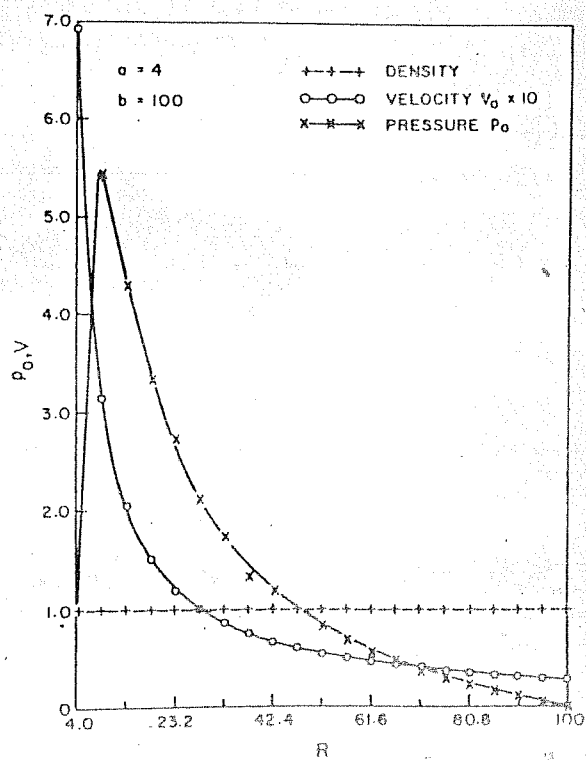


Fig 5.4

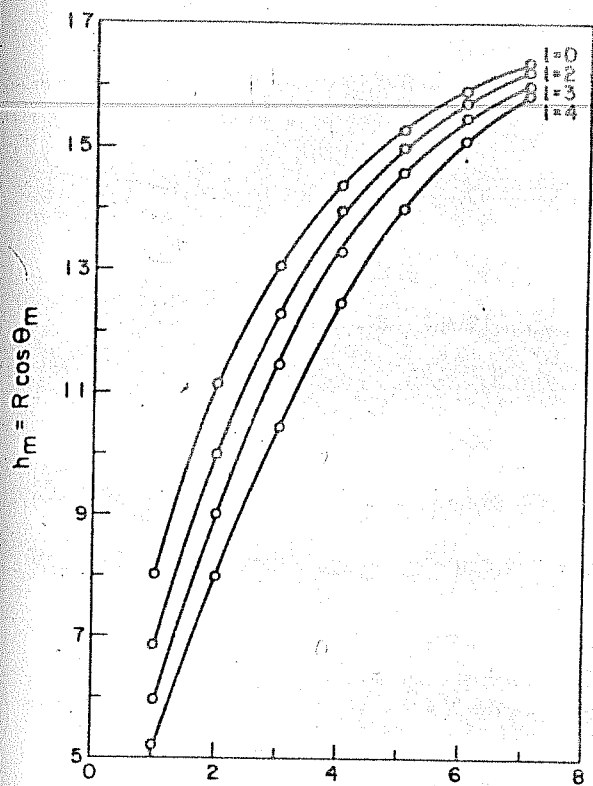


Fig 5.5

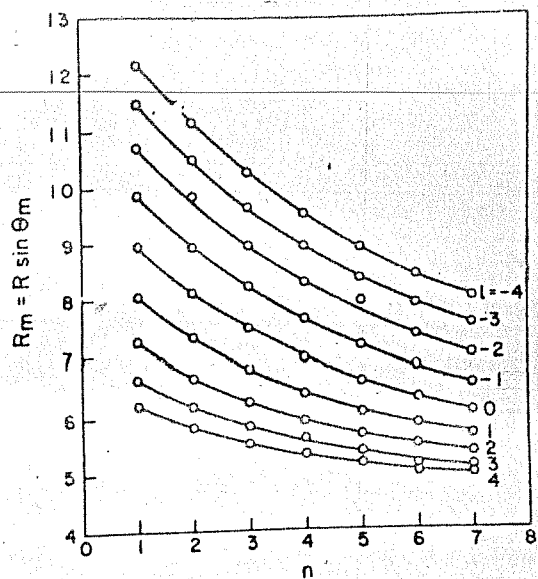


Fig. 5.6

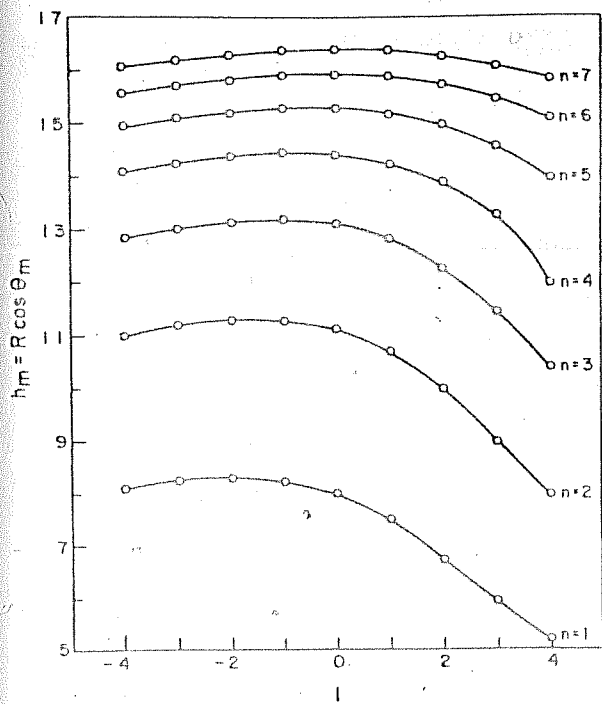


Fig 5.7

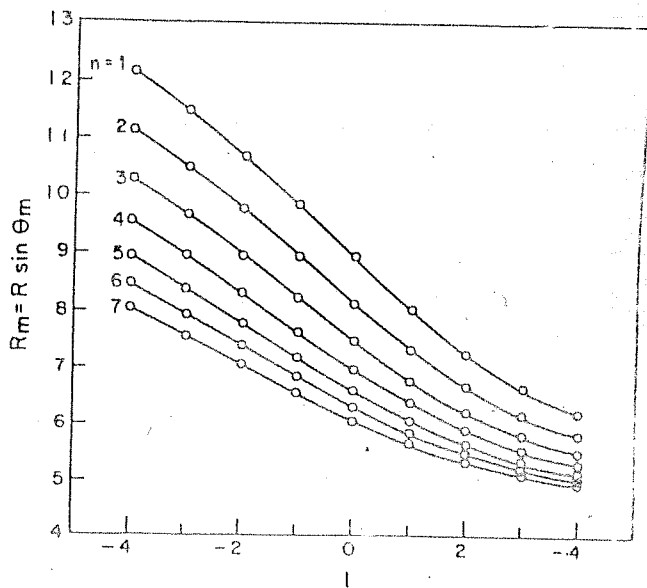


Fig. 5.8

TABLE 5.1

a = 4.0, b = 100.0 $l = 3$

n	$I\Omega^2/ w $	γ_{c_1}	γ_{c_2}
1	0.037	1.07	1.06
2	0.012	1.04	1.17
3	0.005	1.02	1.10
4	0.003	0.96	0.99
5	0.002	0.89	0.90
6	0.001	0.83	0.82

TABLE 5.2

 $a=4.0$, $b=100.0$, $\ell = -2$

n	$I\Omega^2/ w $	γ_{ℓ_1}	γ_{ℓ_2}
1	0.15	1.05	1.10
2	0.050	1.06	1.17
3	0.021	1.02	1.11
4	0.011	0.95	1.04
5	0.006	0.89	0.97
6	0.004	0.83	0.92

TABLE 5.3

$a=4.5$, $b=100.0$, $\ell = -1$

n	$I\Omega^2/ W $	γ_{c_1}	γ_{c_2}
1	0.35	1.00	1.09
2	0.13	1.04	1.17
3	0.054	1.00	1.11
4	0.028	0.94	1.08
5	0.017	0.88	1.04
6	0.011	0.82	0.99

TABLE 5.4

a=4.0, b=100.0

$\ell = 0$

η	$\bar{I} \Omega^2 / W $	γ_{ℓ_1}	γ_{ℓ_2}
1	0.63	0.89	1.04
2	0.24	0.99	1.16
3	0.10	0.97	1.15
4	0.052	0.92	1.11
5	0.031	0.87	1.07
6	0.021	0.81	1.04

TABLE 5.5 $a=4.0, b=100.0, \ell =1$

n	$I\Omega^2/ W $	r_{c_1}	r_{c_2}
1	1.18	0.62	0.93
2	0.49	0.88	1.14
3	0.21	0.92	1.15
4	0.11	0.89	1.13
5	0.066	0.85	1.09
6	0.045	0.80	1.06

TABLE 5.6

$a=20.0$, $b=116.0$, $\ell = 0$

n	$I \Omega^2 / w $	γ_{c_1}	γ_{c_2}
1	1.01	0.47	0.54
2	0.70	0.76	0.94
3	0.49	0.85	1.04
4	0.34	0.86	1.05
5	0.25	0.84	1.04
6	0.19	0.81	1.02

CHAPTER VI

STRUCTURE AND STABILITY OF ROTATING THICK DISKS AROUND COMPACT OBJECT: GENERAL RELATIVISTIC FORMULATION.

In this chapter we present our studies on the complete general relativistic treatment of the structure and stability of thick disks around a Schwarzschild black hole (Chakraborty & Prasanna III, 1981). The same problem in Newtonian formulation was presented in chapter 5. One immediately realises that the Newtonian treatment is inadequate when the inner edge of the disk is situated near the event horizon and one must go over to a general relativistic treatment of the problem. Similar to what we assumed in the case of Newtonian treatment, here also we consider a non-self gravitating perfect fluid disk rotating around a compact object of mass M which is now treated as Schwarzschild black hole.

1. STEADY STATE SOLUTION.

The general set of equations governing the dynamics of the disk can be obtained from equations (2.2.23) to (2.2.25), (2.2.27), (2.2.36) and (2.2.37) by putting $\xi = 0$. We limit ourselves as before to the case of an axisymmetric disk with pure rotational flow in steady state. The equations governing the steady state are then

$$\left(\rho_0 + \frac{p_0}{c^2} \right) \left[\frac{m c^2}{r^2} - \left(1 - \frac{2m}{r} \right) \frac{v_0^2}{r} \right] = - \left(1 - \frac{2m}{r} \right) \left(1 - \frac{v_0^2}{c^2} \right) \partial p_0 / \partial r \quad (6.1.1)$$

and

$$\left(c_0 + \frac{p_0}{c^2}\right) \cot \theta \vartheta_0^2 = \left(1 - \frac{v_0^2}{c^2}\right) \frac{\partial p_0}{\partial \theta}, \quad (6.1.2)$$

other equations are identically satisfied. The above two equations can be solved exactly for a special case of $c_0 = \text{constant}$.

Using this in (6.1.1) and (6.1.2) we obtain

$$\cot \theta \frac{\partial}{\partial r} \vartheta_0^2 - \frac{1}{r} \frac{\partial}{\partial \theta} \vartheta_0^2 + \frac{m}{r^2} \left(1 - \frac{2m}{r}\right) \frac{\partial}{\partial \theta} \vartheta_0^2 = 0, \quad (6.1.3)$$

whose solution is given by

$$\vartheta_0^2 = c^2 A \left(1 - \frac{2m}{r}\right) / r^2 \sin^2 \theta, \quad (6.1.4)$$

A being a constant. Substituting this in (6.1.1) and (6.1.4) we get

$$\left(c_0 + \frac{p_0}{c^2}\right) \left[\frac{mc^2}{r^2} - \frac{Ac^2 \left(1 - \frac{2m}{r}\right)^2}{r^3 \sin^2 \theta} \right] = - \left(1 - \frac{A \left(1 - \frac{2m}{r}\right)}{r^2 \sin^2 \theta}\right) \left(1 - \frac{2m}{r}\right) \frac{\partial p_0}{\partial r}, \quad (6.1.5)$$

$$\left(c_0 + \frac{p_0}{c^2}\right) \cot \theta \frac{A \left(1 - \frac{2m}{r}\right) c^2}{r^2 \sin^2 \theta} = \left(1 - \frac{A \left(1 - \frac{2m}{r}\right)}{r^2 \sin^2 \theta}\right) \frac{\partial p_0}{\partial \theta}, \quad (6.1.6)$$

whose solution may be obtained as

$$\frac{p_0}{c^2} = B \left[\left(1 - \frac{2m}{r}\right)^2 - \frac{A}{r^2 \sin^2 \theta} \right] - c_0 \quad (6.1.7)$$

where B is another constant. Using the boundary condition

$p_0 = 0$ at r_a and r_b , the inner and outer edges at the plane $\theta = \pi/2$ we obtain

$$A = 2m r_b^2 r_a^2 / \{(r_a + r_b)(r_b - 2m)(r_a - 2m)\} \quad (6.1.8)$$

and

and

$$\left(c_0 + \frac{p_0}{c^2}\right) \cos \theta \, \vartheta_0^2 = \left(1 - \frac{v_0^2}{c^2}\right) \frac{\partial p_0}{\partial \theta}, \quad (6.1.2)$$

other equations are identically satisfied. The above two equations can be solved exactly for a special case of $c_0 = \text{constant}$.

Using this in (6.1.1) and (6.1.2) we obtain

$$\cos \theta \frac{\partial}{\partial r} \vartheta_0^2 - \frac{1}{r} \frac{\partial}{\partial \theta} \vartheta_0^2 + \frac{m}{r^2} \left(1 - \frac{2m}{r}\right)^{-1} \frac{\partial}{\partial \theta} \vartheta_0^2 = 0, \quad (6.1.3)$$

whose solution is given by

$$\vartheta_0^2 = c^2 A \left(1 - \frac{2m}{r}\right) / r^2 \sin^2 \theta, \quad (6.1.4)$$

A being a constant. Substituting this in (6.1.1) and (6.1.4) we get

$$\left(c_0 + \frac{p_0}{c^2}\right) \left[\frac{mc^2}{r^2} - \frac{Ac^2 \left(1 - \frac{2m}{r}\right)^2}{r^3 \sin^2 \theta} \right] = - \left(1 - \frac{A \left(1 - \frac{2m}{r}\right)}{r^2 \sin^2 \theta}\right) \left(1 - \frac{2m}{r}\right) \frac{\partial p_0}{\partial r}, \quad (6.1.5)$$

$$\left(c_0 + \frac{p_0}{c^2}\right) \cos \theta \frac{A \left(1 - \frac{2m}{r}\right) c^2}{r^2 \sin^2 \theta} = \left(1 - \frac{A \left(1 - \frac{2m}{r}\right)}{r^2 \sin^2 \theta}\right) \frac{\partial p_0}{\partial \theta}, \quad (6.1.6)$$

whose solution may be obtained as

$$\frac{p_0}{c^2} = B \left[\left(1 - \frac{2m}{r}\right)^{-1} - \frac{A}{r^2 \sin^2 \theta} \right]^{\frac{1}{2}} - c_0 \quad (6.1.7)$$

where B is another constant. Using the boundary condition

$p_0 = 0$ at r_a and r_b , the inner and outer edges at the plane $\theta = \pi/2$ we obtain

$$A = 2m r_b^2 r_a^2 / \{ (r_a + r_b) (r_b - 2m) (r_a - 2m) \} \quad (6.1.8)$$

and

$$B = e_0 \left[\frac{(\eta_b^2 - \eta_a^2)(\eta_b - 2m)(\eta_a - 2m)}{\eta_b^3(\eta_a - 2m) - \eta_a^3(\eta_b - 2m)} \right]^{\frac{1}{2}} \quad (6.1.9)$$

In terms of the dimensionless quantities R , a and b denoting respectively η/m , η_a/m , η_b/m , the steady state solutions read as

$$e_0 = \text{constant},$$

$$\left(\frac{v_0}{c}\right)^2 = \frac{A(1-2/R)}{R^2 \sin^2 \theta},$$

$$\frac{p_0}{c^2} = e_0 \left[B \left\{ \left(1 - \frac{2}{R}\right)^{-1} - \frac{A}{R^2 \sin^2 \theta} \right\}^{\frac{1}{2}} - 1 \right],$$

wherein

$$A = \frac{2a^2 b^2}{(a+b)(a-2)(b-2)},$$

$$B = \left[\frac{(b^2 - a^2)(b-2)(a-2)}{b^3(a-2) - a^3(b-2)} \right]^{\frac{1}{2}} \quad (6.1.10)$$

The solutions obtained above are physically acceptable if $p_0 > 0$ throughout the interior of the disk and if it goes over to zero at the boundary. The former condition leads us to the constraint that the inner edge can not lie within 4 and further

$$b > 2a/(a-4), \text{ if } 4 < a < 6 \quad (6.1.11)$$

There is not restriction on the outer edge if $a \geq 6$. The later condition gives the edge of the disk θ_e (and $\pi - \theta_e$) on the meridional plane as

$$\sin^2 \theta_e = \frac{AB^2}{R^2 \left[B^2 \left(1 - \frac{L}{R} \right)^2 - 1 \right]} \quad (6.1.12)$$

Figures (5.1) and (5.2) show the meridional section of the disk while figures (5.3) and (5.4) show the profiles of velocity and pressure.

2. STABILITY ANALYSIS.

We consider the axisymmetric perturbations of the disk as described above and use the normal mode analysis restricting the perturbations to linear terms only ; the general procedure of the analysis remains the same as used in the Newtonian case. The set of equations governing the perturbation are obtained from equations (2.2.42) to (2.2.44), (2.2.46), (2.2.55) and (2.2.56) by putting $\epsilon_0 = 0$ and $\delta \epsilon = 0$. Defining the Lagrangian displacement ξ^α , ($\alpha = r, \theta$) through

$$\delta \vartheta^\alpha = \frac{\partial \xi^\alpha}{\partial t}, \quad \xi^\alpha(r, \theta, t) = \xi^\alpha(r, \theta) e^{i\sigma t}, \quad (6.2.1)$$

we obtain

$$\left(\rho_0 + \frac{p_0}{c^2} \right) \delta \vartheta^{(\varphi)} = -S_2 \frac{v_0}{c^2} \delta p, \quad (6.2.2)$$

$$\begin{aligned} \delta p = & - \left(\rho_0 + \frac{p_0}{c^2} \right) \sqrt{S_1} \left[\frac{\sqrt{S_1}}{r^2} \frac{\partial}{\partial r} (r^2 \xi^r) + \frac{1}{r \sin \theta} \frac{\partial}{\partial \theta} (\sin \theta \xi^\theta) \right] \\ & + \frac{v_0^2}{c^4} \delta p + \sqrt{S_1} \left\{ \sqrt{S_1} \xi^r \frac{\partial}{\partial r} + \frac{\xi^\theta}{r} \frac{\partial}{\partial \theta} \right\} \left(\frac{p_0}{c^2} \right), \end{aligned} \quad (6.2.3)$$

$$\delta n = -n_0 \sqrt{S_1} \left[\frac{\sqrt{S_1}}{r^2} \frac{\partial}{\partial r} (r^2 \xi^r) + \frac{1}{r \sin \theta} \frac{\partial}{\partial \theta} (\sin \theta \xi^\theta) \right]$$

$$\begin{aligned}
& -\sqrt{s_1} \left[\sqrt{s_1} \xi^2 \frac{\partial n_0}{\partial r} + \frac{\xi^0}{r} \frac{\partial n_0}{\partial \theta} \right] \\
& + \left(e_0 + \frac{p_0}{c^2} \right) \frac{1}{c^2} \left[\delta p + \sqrt{s_1} \left\{ \sqrt{s_1} \xi^2 \frac{\partial p_0}{\partial r} + \frac{\xi^0}{r} \frac{\partial p_0}{\partial \theta} \right\} - s_2 \delta p \right], \quad (6.2.4)
\end{aligned}$$

$$\begin{aligned}
\delta p = & \frac{r p_0}{n_0} \delta n - \sqrt{s_1} \left\{ \sqrt{s_1} \xi^2 \frac{\partial p_0}{\partial r} + \frac{\xi^0}{r} \frac{\partial p_0}{\partial \theta} \right\} \\
& + \frac{r p_0}{n_0} \sqrt{s_1} \left\{ \sqrt{s_1} \xi^2 \frac{\partial n_0}{\partial r} + \frac{\xi^0}{r} \frac{\partial n_0}{\partial \theta} \right\}, \quad (6.2.5)
\end{aligned}$$

$$\begin{aligned}
-(e_0 + \frac{p_0}{c^2}) \sigma^2 \xi^2 = & (e_0 + \frac{p_0}{c^2}) \frac{2}{r} s_1 v_0 \delta \varphi(\varphi) - \left(\delta e + \frac{\delta p}{c^2} \right) \left[\frac{m c^2}{r^2} - \frac{s_1 v_0^2}{r} \right] \\
& - s_1 s_2 \frac{\partial}{\partial r} \delta p + 2 s_1 \frac{v_0}{c^2} \frac{\partial p_0}{\partial r} \delta \varphi(\varphi), \quad (6.2.6)
\end{aligned}$$

$$\begin{aligned}
-(e_0 + \frac{p_0}{c^2}) \sigma^2 \xi^0 = & (e_0 + \frac{p_0}{c^2}) \frac{2}{r} \sqrt{s_1} \cot \theta v_0 \delta \varphi(\varphi) + \left(\delta e + \frac{\delta p}{c^2} \right) \frac{v_0^2}{r^2} \sqrt{s_1} \cot \theta \\
& - \sqrt{s_1} s_2 \frac{1}{r} \frac{\partial}{\partial \theta} \delta p + 2 \sqrt{s_1} \frac{v_0}{c^2} \frac{1}{r} \frac{\partial p_0}{\partial \theta} \delta \varphi(\varphi), \quad (6.2.7)
\end{aligned}$$

wherein

$$s_1 = (1 - 2m/r), \quad s_2 = (1 - v_0^2/c^2) \quad (6.2.8)$$

and all perturbed variables represent only their spatial parts. Equations (6.2.2) to (6.2.5) are the initial value equations while (6.2.6) and (6.2.7) are the pulsation equations. In above, we have dropped out those terms which become zero because of the steady state solutions that we have and also we have integrated the initial value equations with respect to time. Equation (6.2.3) together with (6.2.4) yields

$$\frac{\Delta e}{e_0 + p_0/c^2} = \frac{\Delta n}{n_0}, \quad (6.2.9)$$

while (6.2.5) can be rewritten as

$$\frac{\Delta p}{p_0} = \gamma \frac{\Delta n}{n_0}, \quad (6.2.10)$$

in terms of Lagrangian perturbations. From equations (6.2.3) to (6.2.5) we obtain

$$\begin{aligned} \delta p \left[1 - \frac{\gamma p_0 / c^2}{\rho_0 + p_0 / c^2} \frac{v_0^2}{c^2} \right] = & - \left[1 - \frac{\gamma p_0 / c^2}{\rho_0 + p_0 / c^2} \right] \left(s_1 \xi^{\bar{r}} \frac{\partial p_0}{\partial r} + \sqrt{s_1} \frac{\xi^{\bar{\theta}}}{r} \frac{\partial p_0}{\partial \theta} \right) \\ & - \gamma p_0 \left[\frac{s_1}{r^2} \frac{\partial}{\partial r} (r^2 \xi^{\bar{r}}) + \frac{\sqrt{s_1}}{r \sin \theta} \frac{\partial}{\partial \theta} (\sin \theta \xi^{\bar{\theta}}) \right], \end{aligned} \quad (6.2.11)$$

$$\begin{aligned} \delta p \left[1 - \frac{\gamma p_0 / c^2}{\rho_0 + p_0 / c^2} \frac{v_0^2}{c^2} \right] = & - \left(\rho_0 + \frac{p_0}{c^2} \right) \left[\frac{s_1}{r^2} \frac{\partial}{\partial r} (r^2 \xi^{\bar{r}}) + \frac{\sqrt{s_1}}{r \sin \theta} \frac{\partial}{\partial \theta} (\sin \theta \xi^{\bar{\theta}}) \right] \\ & + \frac{s_1}{c^2} \left(s_1 \xi^{\bar{r}} \frac{\partial p_0}{\partial r} + \sqrt{s_1} \frac{\xi^{\bar{\theta}}}{r} \frac{\partial p_0}{\partial \theta} \right), \end{aligned} \quad (6.2.12)$$

which along with (6.2.2) from alternative expressions for the set of initial value equations.

Our problem is then to solve equations (6.2.6) and (6.2.7) as the eigen-value equations consistently with the initial value equations and the appropriate boundary conditions.

We now define 'trial displacements' $\bar{\xi}^{\bar{r}}$ and $\bar{\xi}^{\bar{\theta}}$ as we did in the earlier study, multiply (6.2.13) by $\bar{\xi}^{\bar{r}}$ and (6.2.14) by $\bar{\xi}^{\bar{\theta}}$, add them and integrate over the range of r and θ . In order to bring the resultant expression in a symmetrical form in barred and unbarred variables, we limit ourselves to the class of perturbations such that $\delta p = 0$ at the boundary of the disk. This in turn requires that both $\xi^{\bar{r}}$ and $\xi^{\bar{\theta}}$ are zero at the boundary of the disk. Performing several integrations by parts and using (6.2.2) and

the steady state equations we finally obtain

$$\begin{aligned}
 & \sigma^2 \iint \frac{1}{s_2} \left(\rho_0 + \frac{p_0}{c^2} \right) (\bar{\xi}^2 \xi^2 + \bar{\xi}^\theta \xi^\theta) r^2 \sin \theta \, dr \, d\theta \\
 &= \iint \left[s_1 \left(\bar{\xi}^2 \frac{\partial}{\partial r} \delta p + \xi^2 \frac{\partial}{\partial r} \delta \bar{p} \right) + \frac{\sqrt{s_1}}{r} \left(\bar{\xi}^\theta \frac{\partial}{\partial \theta} \delta p + \xi^\theta \frac{\partial}{\partial \theta} \delta \bar{p} \right) \right. \\
 &\quad \left. + \frac{2m}{r^2} (\bar{\xi}^2 \delta p + \xi^2 \delta \bar{p}) \right. \\
 &\quad \left. + \frac{v_0^2}{c^4 (\rho_0 + p_0/c^2)} \left(s_1 \bar{\xi}^2 \frac{\partial p_0}{\partial r} + \frac{\sqrt{s_1}}{r} \bar{\xi}^\theta \frac{\partial p_0}{\partial \theta} \right) \left(s_1 \xi^2 \frac{\partial p_0}{\partial r} + \frac{\sqrt{s_1}}{r} \xi^\theta \frac{\partial p_0}{\partial \theta} \right) \right. \\
 &\quad \left. + \frac{r p_0 s_2}{c^2 (\rho_0 + p_0/c^2)^2} \left\{ \delta e \left(s_1 \bar{\xi}^2 \frac{\partial p_0}{\partial r} + \frac{\sqrt{s_1}}{r} \bar{\xi}^\theta \frac{\partial p_0}{\partial \theta} \right) + \delta \bar{e} \left(s_1 \xi^2 \frac{\partial p_0}{\partial r} + \frac{\sqrt{s_1}}{r} \xi^\theta \frac{\partial p_0}{\partial \theta} \right) \right\} \right. \\
 &\quad \left. - \frac{r p_0}{(\rho_0 + p_0/c^2)^2} \left[1 - \frac{r p_0/c^2}{(\rho_0 + p_0/c^2)} \frac{v_0^2}{c^2} \right] \delta e \delta \bar{e} \right] r^2 \sin \theta \, dr \, d\theta, \quad (6.2.13)
 \end{aligned}$$

where $\delta \bar{e}$ and $\delta \bar{p}$ are variations in perturbed density and pressure obtained by using the trial displacement (in place of the true eigen functions ξ^2, ξ^θ) in initial value equations.

As it was shown in the case of Newtonian analysis, this symmetrical expression for σ^2 implies a variational principle: we identify barred variables with the unbarred ones and write

$$\begin{aligned}
 & \sigma^2 \iint \frac{1}{s_2} \left(\rho_0 + \frac{p_0}{c^2} \right) (\xi^2 + \xi^\theta) r^2 \sin \theta \, dr \, d\theta \\
 &= \iint \left[2s_1 \xi^2 \frac{\partial}{\partial r} \delta p + \frac{2\sqrt{s_1}}{r} \xi^\theta \frac{\partial}{\partial \theta} \delta p + \frac{4m}{r^2} \xi^2 \delta p \right. \\
 &\quad \left. + \frac{v_0^2}{c^4 (\rho_0 + p_0/c^2)} \left(s_1 \xi^2 \frac{\partial p_0}{\partial r} + \frac{\sqrt{s_1}}{r} \xi^\theta \frac{\partial p_0}{\partial \theta} \right)^2 \right. \\
 &\quad \left. + \frac{2r p_0 s_2}{c^2 (\rho_0 + p_0/c^2)^2} \delta e \left(s_1 \xi^2 \frac{\partial p_0}{\partial r} + \frac{\sqrt{s_1}}{r} \xi^\theta \frac{\partial p_0}{\partial \theta} \right) \right.
 \end{aligned}$$

$$-\frac{r p_0}{(e_0 + p_0/c^2)^2} \left[1 - \frac{r p_0/c^2}{(e_0 + p_0/c^2)} \frac{v_0^2}{c^2} \right] (\delta p)^2 \Big] r^2 \sin \theta dr d\theta \quad (6.2.14)$$

and calculate σ^2 as given by (6.2.14) by two trial displacements ξ^α and $\xi^\alpha + \delta \xi^\alpha$. If we now demand the resultant variation $\delta \sigma^2$ in σ^2 to be zero, then it amounts to solving the original eigen value equations (6.2.6) and (6.2.7).

As in the case of Newtonian analysis, here also we calculate the critical value of the adiabatic index for neutral stability. Limiting ourselves to the situations wherein $(r p_0/c^2)$ $(v_0^2/c^2)(e_0 + \frac{p_0}{c^2})$ is very small compared to unity such that we can re-write (6.2.11) and (6.2.12) in the form.

$$\delta p = - \left[\left\{ 1 - \frac{r p_0/c^2}{e_0 + p_0/c^2} \right\} \left(s_1 \xi^r \frac{\partial p_0}{\partial r} + \sqrt{s_1} \frac{\xi^\theta}{r} \frac{\partial p_0}{\partial \theta} \right) + r p_0 \left\{ \frac{s_1}{r^2} \frac{\partial}{\partial r} (r^2 \xi^r) + \frac{\sqrt{s_1}}{r \sin \theta} \frac{\partial}{\partial \theta} (\sin \theta \xi^\theta) \right\} \left[1 + \frac{r p_0/c^2}{e_0 + p_0/c^2} \frac{v_0^2}{c^2} \right] \right] \quad (6.2.15)$$

and

$$\delta e = - \left[\left(e_0 + \frac{p_0}{c^2} \right) \left\{ \frac{s_1}{r^2} \frac{\partial}{\partial r} (r^2 \xi^r) + \frac{\sqrt{s_1}}{r \sin \theta} \frac{\partial}{\partial \theta} (\sin \theta \xi^\theta) \right\} - \frac{s_2}{c^2} \left(s_1 \xi^r \frac{\partial p_0}{\partial r} + \sqrt{s_1} \frac{\xi^\theta}{r} \frac{\partial p_0}{\partial \theta} \right) \right] \left[1 + \frac{r p_0/c^2}{e_0 + p_0/c^2} \frac{v_0^2}{c^2} \right] \quad (6.2.16)$$

and using these in (6.2.14) we obtain

$$\begin{aligned} \frac{m^2 \sigma^2}{c^2} &= \iint \frac{1}{s_2} \left(e_0 + \frac{p_0}{c^2} \right) (\xi^r{}^2 + \xi^\theta{}^2) R^2 \sin \theta dR d\theta \\ &= \iint \left[\frac{v_0^2/c^2}{e_0 + p_0/c^2} T_2^2 - 2 s_1 \xi^r \frac{\partial T_2}{\partial r} - \frac{2 \sqrt{s_1}}{R} \xi^\theta \frac{\partial T_2}{\partial \theta} - \frac{4}{R^2} \xi^r T_2 \right] R^2 \sin \theta dR d\theta \\ &\quad + r \iint \left[-2 s_1 \xi^r \frac{\partial}{\partial r} \left(T_1 \frac{p_0}{c^2} \right) + 2 s_1 \xi^r \frac{\partial}{\partial r} (s_2 s_3 T_2) \right] R^2 \sin \theta dR d\theta \end{aligned}$$

$$\begin{aligned}
& + \frac{2\sqrt{S_1}}{R} \frac{\partial}{\partial \theta} \left(T_1 \frac{p_0}{c^2} \right) + \frac{2\sqrt{S_1}}{R} \frac{\partial}{\partial \theta} (S_2 S_3 T_2) \\
& - \frac{4}{R^2} \frac{\partial}{\partial \theta} \left(\frac{p_0}{c^2} T_1 - S_2 S_3 T_2 \right) - 2S_2 S_3 \left\{ T_1 T_2 - S_2 T_2^2 / (p_0 + p_0/c^2) \right\} \\
& - S_3 \left\{ (p_0 + \frac{p_0}{c^2}) T_1^2 + \frac{S_2^2 T_2^2}{(p_0 + p_0/c^2)} - 2S_2 T_1 T_2 \right\} R^2 \sin \theta dr d\theta \\
& + r^2 \left\{ \left[-2S_1 \frac{\partial}{\partial R} (S_5 T_1 \frac{p_0}{c^2}) + 2S_1 \frac{\partial}{\partial R} (S_4^2 T_2) \right. \right. \\
& \quad \left. \left. - \frac{2\sqrt{S_1}}{R} \frac{\partial}{\partial \theta} (S_5 T_1 \frac{p_0}{c^2}) + \frac{2\sqrt{S_1}}{R} \frac{\partial}{\partial \theta} (S_4^2 T_2) \right. \right. \\
& \quad \left. \left. + \frac{4}{R^2} \frac{\partial}{\partial \theta} (S_4^2 T_2 - \frac{p_0}{c^2} T_1 S_5) - 2S_1 S_3 \left\{ S_5 T_1 T_2 - \frac{S_2 S_5}{p_0 + p_0/c^2} T_2^2 \right\} \right. \right. \\
& \quad \left. \left. + S_3 S_5 \left\{ (p_0 + \frac{p_0}{c^2}) T_1^2 + \frac{S_2^2 T_2^2}{(p_0 + p_0/c^2)} - 2S_2 T_1 T_2 \right\} \right. \right. \\
& \quad \left. \left. - S_3 \left\{ 2(p_0 + \frac{p_0}{c^2}) S_5 T_1^2 + \frac{2S_2^2 S_5 T_2^2}{(p_0 + p_0/c^2)} - 4S_5 S_2 T_1 T_2 \right\} \right] R^2 \sin \theta dr d\theta \right. \\
& \left. + r^3 \left\{ \left[-S_3 \left\{ (p_0 + \frac{p_0}{c^2}) S_5^2 T_1^2 + \frac{S_5^2 S_2^2 T_2^2}{(p_0 + p_0/c^2)} - 2S_5^2 S_2 T_1 T_2 \right\} \right. \right. \right. \\
& \quad \left. \left. + S_3 S_5 \left\{ 2(p_0 + \frac{p_0}{c^2}) S_5 T_1^2 + \frac{2S_2^2 S_5 T_2^2}{(p_0 + p_0/c^2)} - 4S_5 S_2 T_1 T_2 \right\} \right] R^2 \sin \theta dr d\theta \right. \\
& \left. + r^4 \left\{ \left[S_3 S_5 \left\{ (p_0 + \frac{p_0}{c^2}) S_5^2 T_1^2 + \frac{S_5^2 S_2^2 T_2^2}{p_0 + p_0/c^2} - 2S_2 S_5^2 T_1 T_2 \right\} \right] R^2 \sin \theta dr d\theta \right. \right. \\
& \quad \left. \left. \right. \right\} (6.2.17)
\end{aligned}$$

wherein

$$S_3 = \frac{p_0/c^2}{p_0 + p_0/c^2}, \quad S_4 = S_3 v_0/c, \quad S_5 = S_4 v_0/c$$

$$T_1 = \frac{S_1}{R^2} \frac{\partial}{\partial R} (R^2 \frac{\partial}{\partial \theta}) + \frac{\sqrt{S_1}}{R \sin \theta} \frac{\partial}{\partial \theta} (\sin \theta \frac{\partial}{\partial \theta})$$

$$T_2 = S_1 \frac{\partial}{\partial R} \left(\frac{p_0}{c^2} \right) + \sqrt{S_1} \frac{\partial}{\partial \theta} \left(\frac{p_0}{c^2} \right). \quad (6.2.18)$$

We choose a function 'q' as

$$q = \sin^2 \theta - \frac{R^2 [B^2 (1 - 2/R) - 1]}{AB^2}, \quad (6.2.19)$$

which is zero at the boundary of the disk and take

$$\xi^r = q + \alpha q^2, \quad \xi^\theta = q + \beta q^2 \quad (6.2.20)$$

wherein α, β are constants determined by extremizing σ^2 as calculated by using these trial displacements in the equation (6.2.17). With such choice of ξ^r and ξ^θ we calculate the critical value γ_c of the adiabatic index for the neutral stability.

Table (6.1) shows the values of γ_c for the onset of instability ($\gamma < \gamma_c$ for instability) for different values of inner edge 'a' and outer edge 'b' for general relativistic as well as for the Newtonian case. It turns out that the coefficients of r^2, r^3 and γ^4 on the right hand side of (6.2.17) are very small as compared to the first two terms and therefore are dropped out while calculating γ_c . The critical γ for the Newtonian case is calculated by taking the limit $C \rightarrow \infty$ of equations (6.2.13), (6.2.11) and (6.2.12).

In this case we obtain

$$\begin{aligned} & \frac{m^2 \sigma^2}{c^2} \iint \rho_0 (\xi^{r^2} + \xi^{\theta^2}) R^2 \sin \theta \, dR \, d\theta \\ &= \iint \left[-2 \xi^r \frac{\partial T_r}{\partial R} - \frac{2 \xi^\theta}{R} \frac{\partial T_r}{\partial \theta} \right] R^2 \sin \theta \, dR \, d\theta \\ &+ r \iint \left[-2 \xi^r \frac{\partial}{\partial R} \left(\frac{\rho_0}{c^2} T_r \right) - \frac{2 \xi^\theta}{R} \frac{\partial}{\partial \theta} \left(\frac{\rho_0}{c^2} T_r \right) - \frac{\rho_0}{c^2} T_r \right] R^2 \sin \theta \, dR \, d\theta, \quad (6.2.21) \end{aligned}$$

wherein

$$T_1 = \frac{1}{R^2} \frac{\partial}{\partial R} (R^2 \xi^R) + \frac{1}{R \sin \theta} \frac{\partial}{\partial \theta} (\sin \theta \xi^\theta),$$

$$T_2 = \xi^R \frac{\partial}{\partial R} \left(\frac{p_0}{c^2} \right) + \frac{\xi^\theta}{R} \frac{\partial}{\partial \theta} \left(\frac{p_0}{c^2} \right) \quad (6.2.22)$$

with steady state solutions (again obtained by taking the limit $c \rightarrow \infty$ of corresponding relativistic solutions) are given by

$$\left(\frac{v_0}{c} \right)^2 = \frac{A}{R^2 \sin^2 \theta},$$

$$\frac{p_0}{c^2} = c_0 \left[\frac{1}{R} - \frac{A}{2R^2 \sin^2 \theta} + B \right],$$

$$A = \frac{2ab}{a+b}, \quad B = -\frac{1}{a+b}. \quad (6.2.23)$$

We note that the σ^2 equation obtained here for Newtonian case has a different form than that reported in Chapter 5. This is because of the different boundary conditions used for ξ^R and ξ^θ . In Chapter 5 we used the condition that $\Delta p = 0$ at the boundary and thereby any finite and continuous ξ^R and ξ^θ is sufficient whereas here we limit ourselves to the case where $\delta p = 0$ at the boundary which implies that both ξ^R and ξ^θ are zero at the boundary.

We find that in case $p_0 = 0$, the disk collapses to $\theta = \pi/2$ plane rotating with velocity

$$v_0 = \left[\frac{m c^2}{\hbar} \left(1 - \frac{2m}{\hbar} \right)^{-1} \right]^{\frac{1}{2}} \quad (6.2.24)$$

as may be seen from equations (6.1.1) and (6.1.2) which is indeed anticipated. Considering further the radial oscillations

of such disks ($\xi^0 = 0, \xi^2 \neq 0$) with $\delta p = 0$ we have

$$\delta \psi(\varphi) = - \left[\left(1 - \frac{2m}{r}\right) \frac{\partial \psi_0}{\partial r} + \frac{1}{r} \left(1 - \frac{3m}{r}\right) \psi_0 \right] \xi^2, \quad (6.2.25)$$

$$\sigma^2 \xi^2 = - \frac{2}{r} \left(1 - \frac{2m}{r}\right) \psi_0 \delta \psi(\varphi), \quad (6.2.26)$$

as the equations governing the radial perturbations appropriate to this case. Combining above we get

$$\sigma^2 = \frac{mc^2}{r^4} (r - 6m), \quad (6.2.27)$$

which shows that such disks are always stable if $r > 6m$.

Results and discussions.

Profiles of the steady state parameters velocity and pressure as a function of radial distance along the equatorial plane for a constant density thick disk rotating around a Schwarzschild black hole, is presented in figures (6.3) and (6.4) while figures (6.1) and (6.2) show the meridional section of such a disk. The corresponding plots in the Newtonian formulation for the same values of the inner and outer radii a and b (for a constant density model) are also shown in these figures, for comparison. We find that for same a and b , Newtonian disk occupies more volume than the relativistic one. It seems that the relativistic disks show a formation of cusp at the inner edge specially when it is near $4m$. For the Newtonian disk pressure at any point is higher while the velocity at any point is lower at the equatorial plane, than for the relativistic disk.

In the case of relativistic disk we find a constraint

that the inner edge can not be inside $4m$. Further if $4 < a < 6$, $b = 2a/(a-4)$. For $a \geq 6$, any $b > a$ gives rise to plausible disks. No such restriction appeared in the Newtonian disks indicating a pure general relativistic origin of the present constraints.

From the values of Υ_c as tabulated in table 6.1 we find that the disks considered represent stable configurations ($\Upsilon_c < 4/3$). In calculating Υ_c through the equation (6.2.7) we have used the approximation that $(U_0/c)(P_0/c)/(P_0 + P_0/c) \ll 1$ which is quite justified from the values of U_0/c and P_0/c as we obtained. There is a qualitative agreement between the Υ_c calculated for relativistic and the corresponding Newtonian disks. In these two cases, although inner and outer radii a and b are the same, the regions occupied by the disks in the two cases are not the same. In general, Newtonian disks are thicker (minimum angular elevation $= \pi - 2\theta_{e_{min}}$). We also find from the numbers that Υ_c depends upon the size of the disk. In the calculations of Υ_c , the effects due to general relativistic corrections and that due to the difference in sizes have contributed simultaneously and therefore the agreement between the general relativistic Υ_c and the Newtonian Υ_c is no better than a qualitative one. It does not seem to be possible to separate the contributions from different effects in the present formulation.

For a pressureless thin disk collapsing to $\theta = \pi/2$ plane we found that it is stable under radial perturbation if the inner edge is beyond $6m$ with local frequency $\sqrt{\frac{mc^2}{24}(2-6m)}$. Now since a pressureless fluid is essentially an aggregate of non-interacting particles, the above conclusion can be regarded as an alternative derivation of the well known result that the last stable circular orbit for Schwarzschild geometry is at $6m$.

The general conclusion that the perfect fluid thick disks of constant density and rotating around a Kerr black hole are generally stable under axi-symmetric perturbations, may have important significance in the study of the models of accretion disks; which one normally uses for explaining radiation from high energy cosmic sources.

Captions for Figures and Tables.

Figures (6.1) : Meridional section of disk in general
 (6.2) : relativistic formulation (solid line)
 and of the corresponding Newtonian disk
 (dashed lines).

Figures (6.3) : Profiles of pressure and velocity for
 (6.4) : relativistic disk (solid line) and of
 Newtonian disk (dashed line)

Table (6.1): Values of γ_c and Θ_{emc} for different
 ent 'a', 'b' .

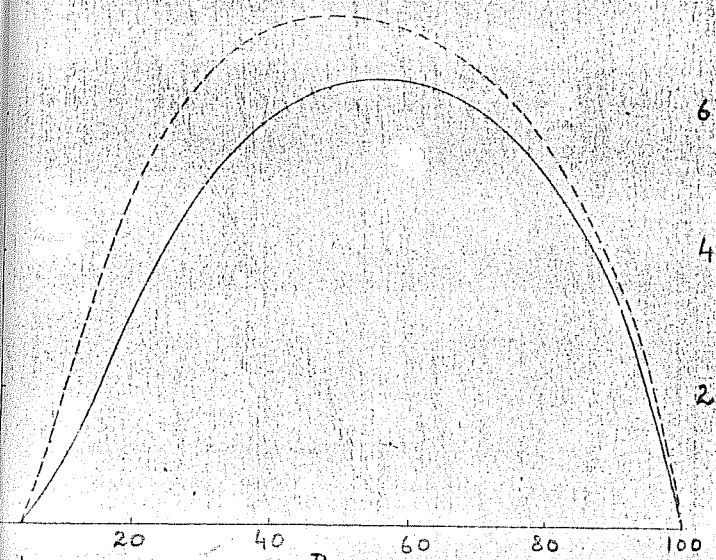


Fig. 6.1

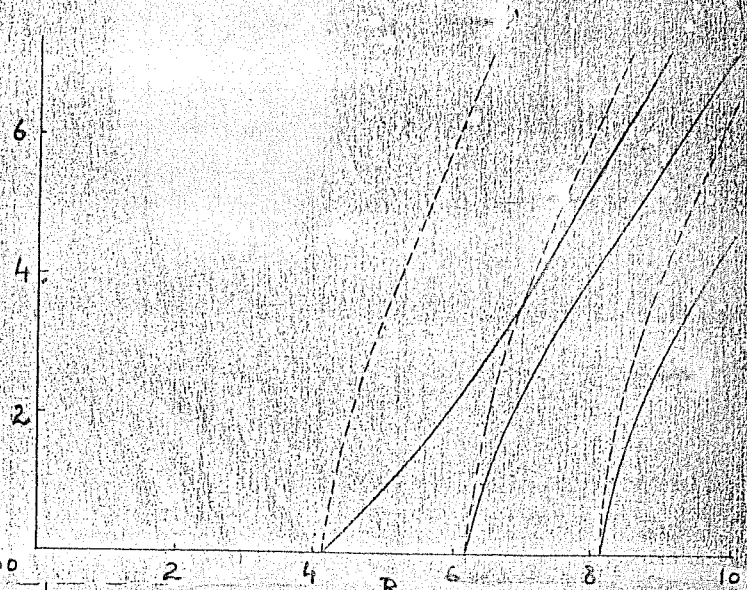


Fig. 6.2

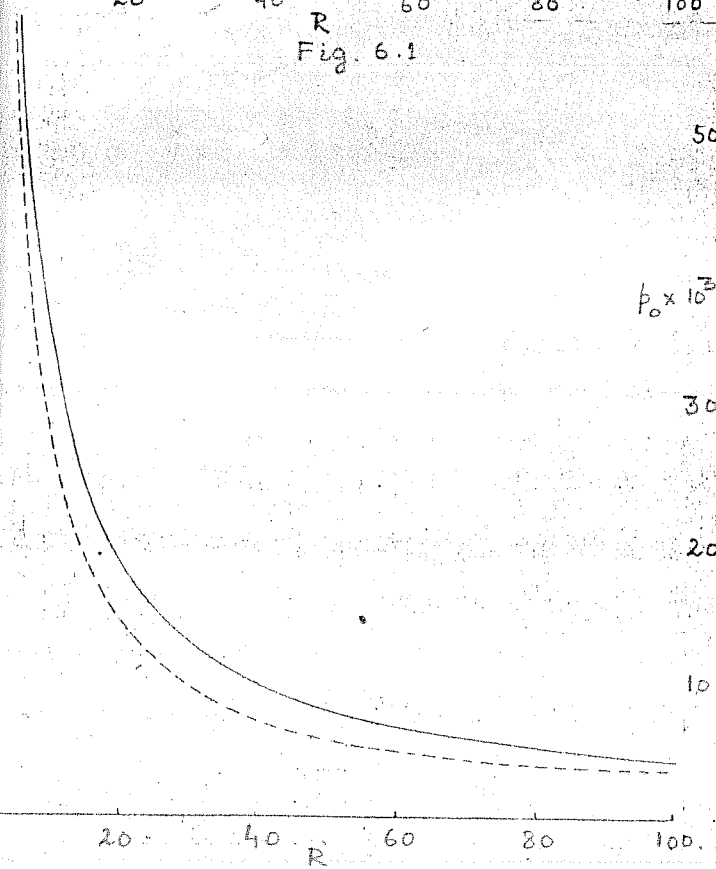


Fig. 6.3

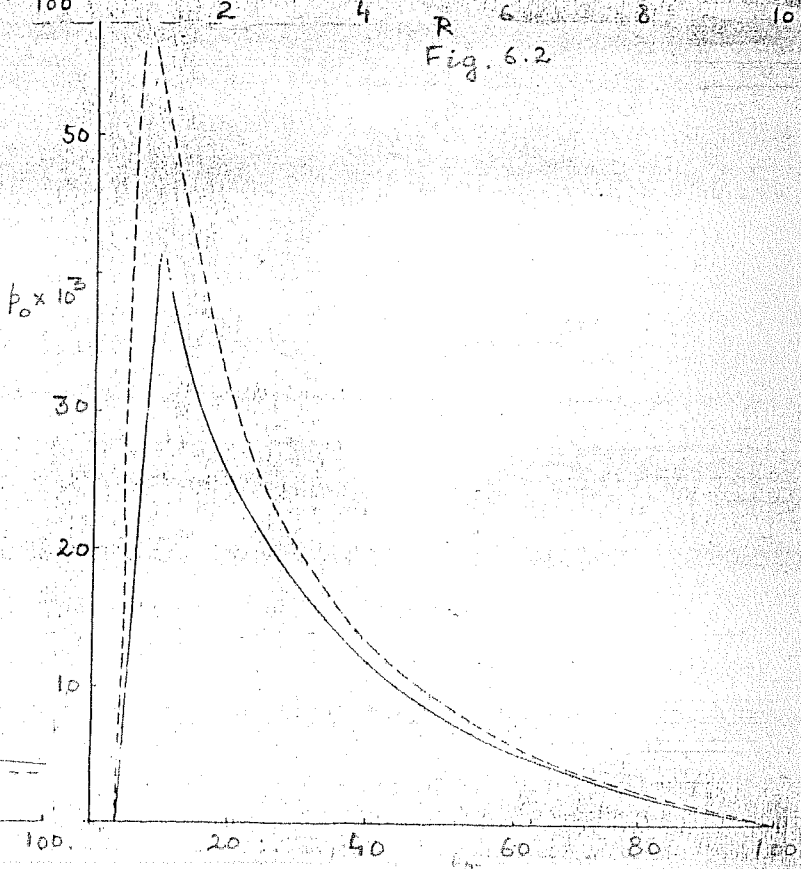


Fig. 6.4

TABLE 6.1

a	b	Gen. rel		Newt.	
		r_c	θ_{cmin}	r_c	θ_{cmin}
8.1	100	0.7488	0.63	0.7107	0.55
7.1	100	0.7758	0.61	0.7420	0.52
6.1	100	0.8007	0.58	0.7732	0.48
5.1	100	0.8214	0.56	0.8043	0.44
4.1	100	0.8320	0.55	0.8356	0.40
4.1	140	0.8850	0.47	0.8726	0.33
4.1	130	0.9155	0.42	0.8936	0.30
4.05	130	0.9155	0.42	0.8946	0.30

REFERENCES:

- Abramowicz M.A., Calvani M. and Nobili L (1980),
 Astrophys. J., 242 , 772
- Abramowicz M., Jaroszynski M and Shikora M (1978),
 Astron and Astrophys., 63 , 221
- Arfken G. (1970) "Mathematical methods for physicists"
 (Academy press N.Y.)
- Bardeen J.M.(1970), Astrophys. J., 162 , 71
- Bardeen J.M.(1973), "Les Houches lectures - blackholes"
 Ed. B.Dewitt & C. Dewitt (New York N.Y.)
- Bardeen J.M., Press W.H. and Teukolsky S.A.(1972),
 Astrophys.J., 178, 347.
- Basko M.M. and Sunyaev R.A.(1976), Mon.Not.R.Astron.
 Soc., 175 , 395
- Bicak I. and Dvorak L.(1977), Czech.J.Phys.B., 27 , 127
- Bondi H.(1952), Mon.Not. R.Astron. Soc. 112 , 195
- Breur R.A.(1975), "Gravitational perturbation Theory,
 and Synchrotron radiation"
 (Springer Verlag)
- Cameron AGW. and Mock M.(1967), Nature, 215 , 464
- Carter B. (1973), "Les Houches lectures-blackholes"
 Ed. B.Dewitt and C.Dewitt (New York N.Y.)
- Chakraborty D.K. and Prasanna A.R. I.(1981), communicated
Pramana, in press
- Chakraborty D.K. and Prasanna A.R.II.(1981), J.Astrophys.
 Astron., ~~in press~~ **2**, 421
- Chakraborty D.K. and Prasanna A.R.III (1981), communicated
J. Astrophys. Astron., in press

Chandrasekhar S. (1964), Astrophys J. 140 , 417

Chandrasekhar S. and Friedman J.L. I (1972), Astrophys J.
175 , 379

Chandrasekhar S. and Friedman J.L. II (1972), Astrophys J.
176 , 745

Chitre DM. and Vishveshwara CV. (1975), Phys. Rev. D, 12, 1538

Cox D.P. and Smith D.W. (1976), Astrophys J., 203, 361.

Cox J.P. (1981), Astrophys J., 247, 1070

Dadhich N. and Witta PJ (1981) Preprint

Doroshkevich A.G. (1965), Astropizika 1 , 255

Eardley D.M. and Lightman A.P. (1975), Astrophys. J., 202, 137.

Fishbone L.G. and Moncrief V (1976), Astrophys. J., 207, 962.

Ginzberg V.L. and Ozernoi IM (1965), Sov. Phys. JETP, 20, 689

Hawking S. and Ellis G.F.R. (1972) "Large scale structure
of space- time "(Cambridge)

Hoshi R. (1977), Prog. Theor. Phys. 58, 1191

Hoshi R. and Shibasaki N. (1977), Prog. Theor. Phys. 58, 1759.

Ichimaru S. (1977), Astrophys J., 214 , 840

Jaroszynski M., Abramowicz M.A. and Paczynski B (1980) Acta.
Astron. 30 , 1

Kato S. and Fukue J. (1980), Publ., Astron., Soc. Jap. 32 , 377

King A.R., Lasota J.P. and Kundt W. (1975), Phys. Rev. D, 12, 3037

Kozłowski M., Jaroszynski M and Abramowicz M (1978),
Astron. and Astrophys. 63 , 209

Lebovitz NR. (1970), Astrophys. J. 160 , 701

Liang EPT. (1977), Astrophys J., 218, 243

- Liang EPT. and Price RH. (1977), *Astrophys J.* 218, 247.
- Lightman A.P.I (1974), *Astrophys J.* 194, 419
- Lightman A.P.II (1974), *Astrophys J.* 194, 429.
- Lightman A.P. and Eardley D.M.(1974), *Astrophys J.letters*
182, L1.
- Lightman A.P., Shapiro S.L. and Rees M.J.(1978), "Physics
and Astrophysics of Black holes "Ed R.
Giacconi and R.Ruffini (North Holland).
- Livio M. and Shaviv G.(1977), *Astron. Astrophys.* 55, 95
- Lynden - Bell D.(1969), *Nature Phys Sci.* 223, 690
- Lynden - Bell D. and Rees M.J. (1971), *Mon.Not.R.Astron.*
Soc. 152, 461
- Mc Cray R. (1977), *Nature*, 243, 94.
- Mestel L (1971), *Nature Phys. Sci.* 223, 149.
- Misner CW., Thorne K.S. and Wheeler J.A.(1973), "Gravi-
tation", (WH.Freeman, San Francisco)
- Novikov ID. and Thorne K.S.(1973) "Les.Houches Lectures-
blackholes".Ed,B.Dewitt and C.Dewitt
(New York N.Y.).
- Novikov I.D. and Zeldovich Y.B.(1966), *Nuovo Cimento*
Suppl. 4, 810, Addendum 2.
- Okuda T.(1980) *Publ.Astron.Soc.Jap.* 32, 127.
- Paczynski B. (1980), *Acta Astronomica* 30.4, 347.
Witta, P.J.
- Paczynski B. and T.IFR. group (1980) preprint.
- Paczynski B. and Witta P.J.(1980), *Astron. and Astrophys*
88, 23.

- Petterson J.A. (1974), Phys. Rev. D., 10 , 3166.
- Petterson J.A. (1975), Phys. Rev. D., 12 , 2213.
- Piran T. (1977), Mon. Not. R. Astron. Soc. 179 , 45.
- Piran T. (1978), Astrophys J., 221 , 652.
- Prasanna A.R. (1980), Rivista Del Nuovo Cimento. 3 , N. 11.
- Prasanna A.R. and Chakraborty D.K. (1980), Pramana, 14 , 113.
- Prasanna A.R. and Chakraborty D.K. (1981), J. Astrophys. Astron., 2 , 1
- Prasanna A.R. and Varma R.K. (1977), Pramana. 8 , 229.
- Prasanna A.R. and Vishveshwara C.V. (1978), Pramana, 11 , 359.
- Prendergast K.H. and Burbidge G.R. (1968) Astrophys. J. letters. 151 , L. 83.
- Pringle J.E. (1973), Nature, 243 , 90.
- Pringle J.E. and Rees M.J. (1972), Astron. and Astrophys., 21 , 1.
- Ruffini R. (1973) "Less Houches lectures-blackholes"
Ed. B. Dewitt and C. Dewitt (New York N.Y.).
- Salpeter E E. (1964), Astrophys. J. 140 , 796.
- Schiff L.I. (1955) "Quantum Mechanics" (Mc Graw Hill) p. 171.
- Shakura N.I. and Sunyaev R.A. (1973), Astron and Astrophys., 24 , 337.
- Shakura N.I. and Sunyaev R.A. (1976), Mon. Not. R. Astron. Soc. 175 , 613.
- Shakura N.I., Sunyaev R.A. and Zilitnkevich SS. (1977), Astron. and Astrophys. 62 , 179.
- Shapiro S.L. (1973), Astrophys. J., 180 , 531.
- Shibazaki N. (1978), Prog. Theor. Phys. 60 , 985.

Shklovsky IS. (1967), Astrophys. J. letters, 148, L1.

Shvaritsman V.F. (1971), Sov. Astron., 15, 377.

Thorne K.S. (1974), Astrophys. J., 191, 507.

Thorne K.S. and Flamming R.A. (1980), Preprint.

Van Den Heuvel (1975), Astrophys. J. letters, 198, L109

Wald R.M. (1974), Phys. Rev. D., 10, 1680.

Zeldovich YB. (1964), Sov. Phys. Doklady., 9, 195.

Zeldovich Y.B. and Novikov I.D. (1971) "Relativistic
Astrophysics-Vol. I "(Chicago
Univ. Press).